(NASA-SP-498) PLANETARY GEOSCIENCES, 1988 N89-26274
(NASA) 113 p CSCL 08G
Unclas
00/42 0219478

Planetary Geosciences–1988

NASA

NASA SP-498

Planetary Geosciences—1988

Edited by

Maria Zuber
Goddard Space Flight Center

Odette James
U.S. Geological Survey

Glenn MacPherson
Smithsonian Institution
Museum of Natural History

Jeff Plescia
Jet Propulsion Laboratory

ORIGINAL CONTAINS
COLOR ILLUSTRATIONS

National Aeronautics and Space Administration
Office of Management
Scientific and Technical Information Division
Washington, DC 1989

Preface

We are in the third decade of one of the most exciting and scientifically important eras in human history—the era of Solar System exploration. Discoveries made as a result of this exploration have had an enormous effect on our understanding of the planets, including the Earth, and the way that we regard our place in the universe.

NASA's Planetary Geosciences Programs (the Planetary Geology and Geophysics Program and the Planetary Materials and Geochemistry Program) provide support and an organizational framework for scientific research into the nature of solid bodies in the Solar System. That research has contributed much to our understanding of these bodies. These research and analysis programs support scientific research aimed at increasing our understanding of the physical, chemical, and dynamic nature of the solid bodies of the Solar System—the Moon, the terrestrial planets, the satellites of the outer planets, the rings, the asteroids, and the comets. Through research supported by these programs, we are expanding our understanding of how the Solar System originated and how it has evolved over time.

This document is intended to provide an overview of some of the more significant scientific findings and discoveries made this year by scientists supported by the Planetary Geosciences Programs. To a large degree, these results and discoveries are the measure of success of the programs.

The scientists responsible for these major scientific discoveries and advances have provided short articles describing their research and its importance in the context of the larger problems of planetary geoscience. These short articles have been edited and incorporated into this document by an editorial board that consists of Maria Zuber (NASA/Goddard Space Flight Center), Odette James (U.S. Geological Survey), Glenn MacPherson (Smithsonian Museum of Natural History), and Jeff Plescia (NASA/Jet Propulsion Laboratory).

Joseph M. Boyce
Discipline Scientist
Planetary Geosciences Programs
Solar System Exploration Division
Office of Space Science and Applications

Contents

Inner Solar System

Outer Solar System

INTENTIONALLY BLANK

Lunar Samples

Meteorites and Cosmic Dust

Lunar Samples

Meteorites and Cosmic Dust

Inner Solar System

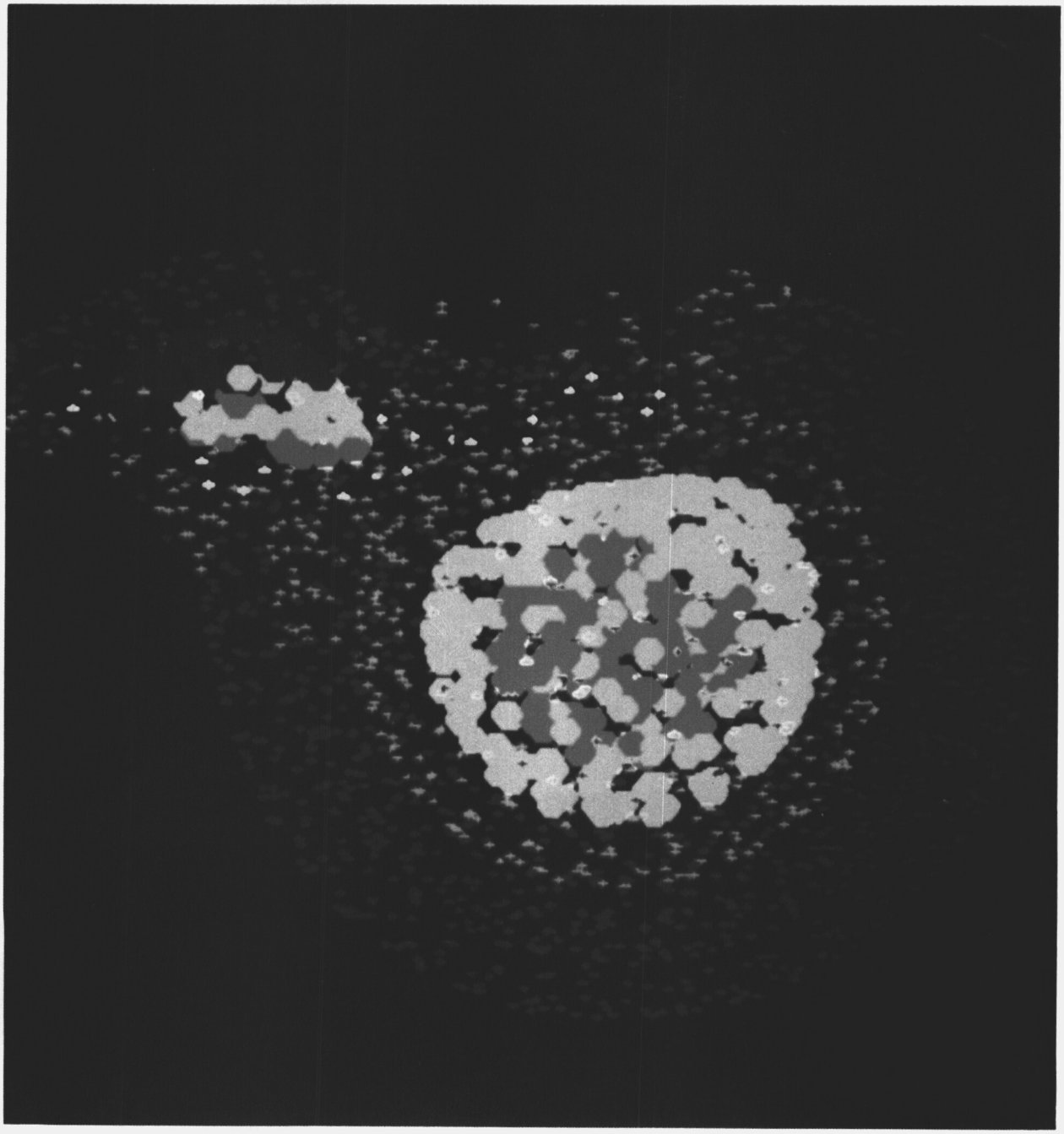

Color Albedo Mapping of Mars

R. M. Batson, Branch of Astrogeology,
U.S. Geological Survey, Flagstaff, AZ 86001

Processing methods have been developed that combine low-resolution, multiple filter, and high-resolution Viking Orbiter images to make controlled photomosaics that show both relief and albedo information.

Color albedo and topographic relief are rarely depicted simultaneously on maps of Mars because the two phenomena are recorded under different viewing conditions and because sufficiently accurate geometric and photometric image controls were unavailable. Albedo markings are dominant under high-Sun (near noon) illumination; they usually are quite broad, so high-resolution images are not mandatory. Images of surface relief, on the other hand, are enhanced by the shading produced by low-Sun (early morning or late afternoon) illumination. The highest possible image resolution is desirable for geologic interpretation. Thus, controlled mapping requires not only the precise registration of images taken through multiple color filters and at different resolutions but also the precise placement of those images on the geodetic grid.

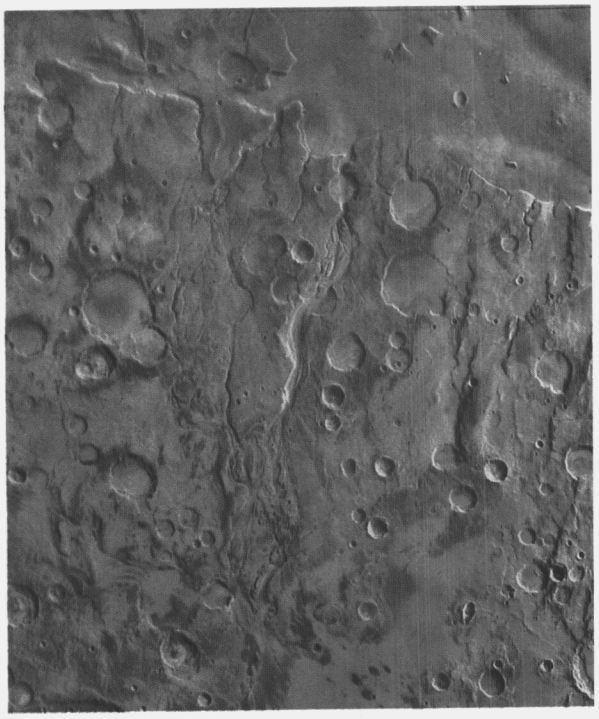

Fig. 1. Controlled photomosaic of part of the Mangala Valles region of Mars.

Several uncontrolled color mosaics have been made with color-filtered images returned by the Viking Orbiter. These mosaics provide spectacular, if qualitative (geometry and photometry were not rigorously controlled), regional views of Mars and have been used as illustrations and cover photographs in many publications. Recently, however, investigators at the U.S. Geological Survey have produced image controls that are accurate enough to compile controlled digital maps with both geodetic and photometric validity.

The feasibility of publishing a planetwide series of color maps of Mars based on this technology is under investigation. Figure 1 is part of a prototype of such a map; it shows the Mangala Valles (MC16NE) region of Mars, which has been proposed as a possible Mars Rover/Sample Return mission landing site. The color mosaic was produced by using a black and white base mosaic (having a resolution of 230 meters/pixel) and then overlaying color albedo mosaic (having a resolution of 1 kilometer per pixel). The figure is a composite of a mosaic. The maps in the new series would also have feature nomenclature and topographic contour lines overprinted on the image mosaics. Additional maps of this kind may be made at even larger scales, where scientific interest warrants.

Color Albedo Mapping of Mars

R. M. Batson, Branch of Astrogeology,
U.S. Geological Survey, Flagstaff, AZ 86001

Processing methods have been developed that combine low-resolution, multiple filter, and high-resolution Viking Orbiter images to make controlled photomosaics that show both relief and albedo information.

Color albedo and topographic relief are rarely depicted simultaneously on maps of Mars because the two phenomena are recorded under different viewing conditions and because sufficiently accurate geometric and photometric image controls were unavailable. Albedo markings are dominant under high-Sun (near noon) illumination; they usually are quite broad, so high-resolution images are not mandatory. Images of surface relief, on the other hand, are enhanced by the shading produced by low-Sun (early morning or late afternoon) illumination. The highest possible image resolution is desirable for geologic interpretation. Thus, controlled mapping requires not only the precise registration of images taken through multiple color filters and at different resolutions but also the precise placement of those images on the geodetic grid.

Fig. 1. Controlled photomosaic of part of the Mangala Valles region of Mars.

Several uncontrolled color mosaics have been made with color-filtered images returned by the Viking Orbiter. These mosaics provide spectacular, if qualitative (geometry and photometry were not rigorously controlled), regional views of Mars and have been used as illustrations and cover photographs in many publications. Recently, however, investigators at the U.S. Geological Survey have produced image controls that are accurate enough to compile controlled digital maps with both geodetic and photometric validity.

The feasibility of publishing a planetwide series of color maps of Mars based on this technology is under investigation. Figure 1 is part of a prototype of such a map; it shows the Mangala Valles (MC16NE) region of Mars, which has been proposed as a possible Mars Rover/Sample Return mission landing site. The color mosaic was produced by using a black and white base mosaic (having a resolution of 230 meters/pixel) and then overlaying color albedo mosaic (having a resolution of 1 kilometer per pixel). The figure is a composite of a mosaic. The maps in the new series would also have feature nomenclature and topographic contour lines overprinted on the image mosaics. Additional maps of this kind may be made at even larger scales, where scientific interest warrants.

Giant Impact Theory of the Origin of the Moon

A. G. W. Cameron, Harvard-Smithsonian Center for Astrophysics, Cambridge, MA 02138

This article summarizes calculations that simulate what may have been the most violent event that has ever occurred to the Earth, its collision with the next largest body that was present in its region of accumulation in the early Solar System. This body was a planet in its own right, an object somewhat more massive than the planet Mars. The collision would have created a disk of molten and gaseous debris in orbit around the protoearth. Dissipation of this disk may have resulted in the formation of the Moon.

Curiosity about the origin of the Moon played an important part in persuading the National Aeronautics and Space Administration to establish the Apollo project that placed men on the surface of the Moon almost 20 years ago. At the time, there were three competing theories of the origin of the Moon:

1. *Capture theory.* The Moon was formed elsewhere in the Solar System and was captured by the Earth.

2. *Formation of the Moon in orbit theory.* The Moon was formed from material that had been captured into orbit around the Earth after the Earth was mostly formed.

3. *Fission theory.* The Earth spun fast enough so that it became deformed and a piece broke off to become the Moon.

As the Apollo project progressed, it became noteworthy that few scientists working on the project were changing their minds about which of these three theories they believed was most likely correct, and each of the theories had its vocal advocates. In the years immediately following the Apollo project, this division of opinion continued to exist. One observer of the scene, a psychologist, concluded that the scientists studying the Moon were extremely dogmatic and largely immune to persuasion by scientific evidence. But the facts were that the scientific evidence did not single out any one of the three theories. Each one of them had several grave difficulties as well as one or more points in its favor.

In the mid-1970s, other ideas began to emerge. William K. Hartmann and D. R. Davis (Planetary Sciences Institute in Tucson, Arizona) pointed out that the Earth, in the course of its accumulation, would undergo some major collisions with other bodies that have a substantial fraction of its mass and that these collisions would produce large vapor clouds that they believed might play a role in the formation of the Moon. A. G. W. Cameron and William R. Ward (Harvard University in Cambridge, Massachusetts) pointed out that a collision with a body having at least the mass of Mars would be needed to give the Earth the present angular momentum of the Earth-Moon system, and they also pointed out that such a collision would produce a large vapor cloud that would leave a substantial amount of material in orbit about the Earth, the dissipation of which could be expected to form the Moon. The "giant impact theory" of the origin of the Moon has emerged from these suggestions.

These ideas attracted relatively little comment in the scientific community during the next few years. However, in 1984, when a scientific conference on the origin of the Moon was organized in Kona, Hawaii, a surprising number of papers were submitted that discussed various aspects of the giant impact theory. At the same meeting, the three classical theories of formation of the Moon were also discussed in depth, and it was clear that all continued to present grave difficulties. The giant impact theory emerged as the "fashionable" theory, but everyone agreed that it was relatively

untested and that it would be appropriate to reserve judgment on it until a lot of testing has been conducted. The next step clearly called for numerical simulations on supercomputers.

This author in collaboration with Willy Benz (Harvard), Wayne L. Slattery at (Los Alamos National Laboratory, Los Alamos, New Mexico), and H. Jay Melosh (University of Arizona, Tucson, Arizona) undertook such simulations. They have used an unconventional technique called smoothed particle hydrodynamics to simulate the planetary collision in three dimensions. With this technique, we have followed a simulated collision (with some set of initial conditions) for many hours of real time, determining the amount of mass that would escape from the Earth-Moon system, the amount of mass that would recollide with the Earth, and the amount of mass that would be left in orbit, as well as the relative amounts of rock and iron that would be in each of these different mass fractions. We have carried out simulations for a variety of different initial conditions and have shown that a "successful" simulation was possible if the impacting body had a mass not very different from 1.2 Mars masses, that the collision occurred with approximately the present angular momentum of the Earth-Moon system, and that the impacting body was initially in an orbit not very different from that of the Earth.

The Moon is a compositionally unique body, having not more than 4% of its mass in the form of an iron core (more likely only 2% of its mass in this form). This contrasts with the Earth, a typical terrestrial planet in bulk composition, which has about one-third of its mass in the form of the iron core. Thus, a simulation could not be regarded as "successful" unless the material left in orbit was iron free or nearly so and was substantially in excess of the mass of the Moon. This uniqueness highly constrains the conditions that must be imposed on the planetary collision scenario. If the Moon had a composition typical of other terrestrial planets, it would be far more difficult to determine the conditions that led to its formation.

The early part of this work was done using Los Alamos Cray X-MP computers. This work established that the giant impact theory was indeed promising and that a collision of slightly more than a Mars mass with the Earth, with the Earth-Moon angular momentum in the collision, would put almost 2 Moon masses of rock into orbit, forming a disk of material that is a necessary precursor to the formation of the Moon from much of this rock. Further development of the hydrodynamics code made it possible to do the calculations on fast small computers that are dedicated to them.

Subsequent calculations have been done at Harvard. The first set of calculations was intended to determine whether the revised hydrodynamics code reproduced previous results (and it did). Subsequent calculations have been directed toward determining whether "successful" outcomes are possible with a wider range of initial conditions than were first used. The results indicate that the impactor must approach the Earth with a velocity (at large distances) of not more than about 5 kilometers. This restricts the orbit of the impactor to lie near that of the Earth. It has also been found that collisions involving larger impactors with more than the Earth-Moon angular momentum can give "successful" outcomes. This initial condition is reasonable because it is known that the Earth-Moon system has lost angular momentum due to solar tides, but the amount is uncertain. These calculations are still in progress and will probably take 1 or 2 years more to complete.

Figures 2–4 show three "snapshots" of a successful collision of the protoearth with an impactor of 1.2 Mars masses. In the figures, iron is represented by relatively large filled outlines and rock is represented by crosses; these symbols tend to be distorted by the finite resolution of the computer screen. Both iron and rock have four levels of internal energy, which are represented by four different colors; both higher temperature and higher pressure contribute to this internal energy. For iron the colors range through dark blue, light blue, dark green, and light green with increasing energy. For rock the color sequence is dark red, orange, brown, and yellow with increasing energy.

In figure 2, the collision is in progress. Note the huge crater taken out of the protoearth at the top

and the deformation of the core. The impactor is destroyed in the process and is spread out to the left. Figure 3 shows the situation a little later. The cloud of debris from the collision has spread out more, and it is gradually falling out. This cloud has formed into a fairly straight rotating bar, and it is easy to see the fallout trail left by the iron from the impactor, which fell in early. The severe damage to the protoearth has spread around a hemisphere. In figure 4, the last stage of the fallout is occurring; the iron from the impactor all falls into the protoearth, but much of the remaining rock in the lower part of the figure goes into orbit to provide a prelunar accretion disk. Note that very little of the protoearth remains unshocked at a lower energy. A layer of very hot iron forms around the core of the protoearth, and a layer of very hot rock forms on top of the protoearth.

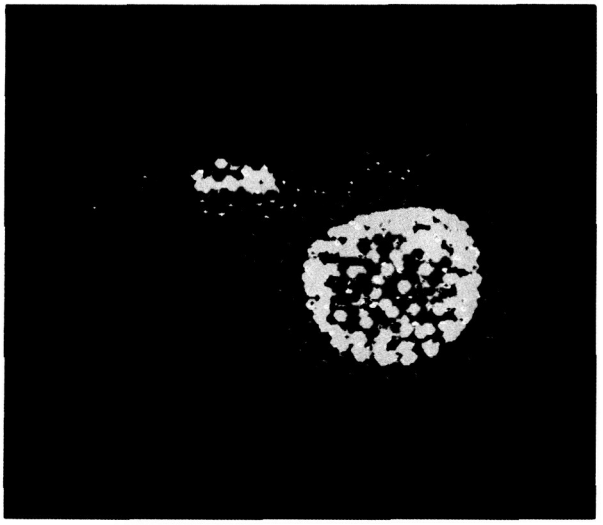

Fig. 2. Initial stages of collision of a Mars-sized body into the protoearth. The impactor is destroyed in the collision.

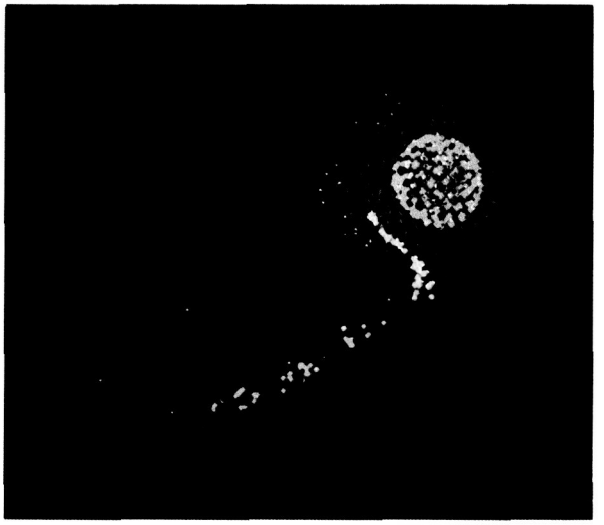

Fig. 3. Intermediate stage of collision. Note fallout of the debris cloud.

Fig. 4. Late stage of collision. All iron (blue-green shades) from impactor falls into the protoearth.

High-Resolution Thermal Imaging of Mars

Philip R. Christensen and Michael C. Malin, Department of Geology, Arizona State University, Tempe, AZ 85287

One of the primary goals of the Viking Mission Infrared Thermal Mapper (IRTM) experiment was to determine the physical properties of martian surface materials. This goal was addressed by measuring the thermal properties of the surface, in particular the thermal inertia. This parameter is sensitive to a wide range of surface properties, including particle size, rock abundance, and the degree of bonding of the surface. Thus, the thermal inertia provides a means for studying the surface characteristics and for investigating surface processes.

In a pioneering work by Frank Palluconi (Jet Propulsion Laboratory) and Hugh Kieffer (U.S. Geological Survey), global thermal inertia determinations were made by fitting measurements of the surface temperature throughout the day to modeled temperature curves. These determinations provide the most accurate measure of the inertia and highlight times of day when the surface does not behave in the simple manner predicted by the thermal models. However, to obtain complete time-of-day coverage from the Viking spacecraft, it was necessary to average the observations over 2° by 2° latitude, longitude bins. Thus, the highest spatial resolution available from this method was 120 kilometers by 120 kilometers at the equator.

The approach used here was to determine inertia using a single predawn observation. This approach has more uncertainty than that used by Palluconi and Kieffer but has the advantage of preserving the original resolution of the data (about 30 km). A single-point value was computed for each IRTM observation (over 7 million) and compared to that obtained by Palluconi and Kieffer, with very good agreement between the two methods.

The data used were obtained during a series of "walks" around the planet, in which the duration of the spacecraft orbit was adjusted so that the equator crossing location was offset on each successive orbit by approximately 20° of longitude. Each complete walk provided nearly complete longitudinal coverage, with some data gaps produced by observing conflicts with other Viking instruments. A series of over 100 Viking 1 and 2 predawn observations from nine separate walks were used to construct a global thermal inertia map from approximately 60°S to 60°N. The spatial resolution of these observations varies but is approximately 30 kilometers, with somewhat higher resolution in the southern hemisphere. Each individual observation was analyzed and evaluated to eliminate any for which the thermal inertia values were affected by uncertainties in instrument calibration, atmospheric dust, or surface frosts. As such, it represents the best global thermal image available for Mars until observations can be obtained by the Mars Observer Thermal Emission Spectrometer (TES) experiment.

The resulting thermal image of Mars is shown in figure 5, shown superimposed on a digital version of the U.S. Geological Survey shaded relief map (scale 1:15,000,000). The most striking feature of this image is the presence of small-scale structures in the surface properties not previously recognized on a global scale. Of particular interest is the distribution of relatively high thermal inertia materials that occur within the volcanic province of Tharsis (−20°S–40°N latitude, 80°–170°W longitude). These high-inertia materials occur at the base of the scarp around Olympus Mons and at the leading edges of several lobes of its surrounding aureole deposits. Detailed analysis indicates that these features are located at the feet of scarps. The regional values of inertia suggest a surface covered by dust particles 20 to 60 micrometers in diameter; the higher inertia regions at the base of the scarps are consistent with a surface of ~70% dust and 30% sand-sized particles.

Several possible mechanisms can be envisioned for the origin of these features. They may represent local, in-place changes to the surface character, such as bonding, or they may represent localized accumulations of relatively coarse materials. The first mechanism appears to be less likely because of the small scale and high degree of correlation with local topography and morphology. A mechanism would be required locally to bond or alter material only in specific regions, while leaving material 50 kilometers away unaffected. The second possibility appears to be more likely, either through local entrapment of a coarse, mobile surface fraction or through the accumulation of coarse talus at the base of the escarpments.

The thermal inertia image also shows other regions with subtle thermal inertia differences that can be associated with surface morphology. The sharp changes in thermal inertia along distinct boundaries in the Lunae Planum region (0°–25°N, 50°–80°W) are of interest for analyzing volcanic terrain. Theses changes in surface properties suggest that a spatially noncontinuous process has acted to produce the present surface. Aeolian mixing of material is not a good candidate in this particular case; differing degrees of bonding of material of possibly different ages is a possible explanation.

Other regions of high-inertia deposits include crater interiors, streaks downwind from topographic obstacles, and rims and walls of large craters. These features are most likely produced by the accumulation of coarse sand that is transported across the surface and trapped.

The data described here provide a new view of varied and heterogeneous martian surfaces and surface processes. Localized processes appear to operate in addition to global-scale processes that have been proposed to produce the continental-scale inertia variations. These observations suggest that Mars will display increased variability in surface characteristics as the resolution of the observations increases. The TES instrument on Mars Observer will provide a complete global image of thermal inertia at resolutions of about 3 kilometers; a factor of 10 better than Viking data. These data should provide an exciting improvement in the knowledge and understanding of the complex nature of martian surface processes and surface evolution.

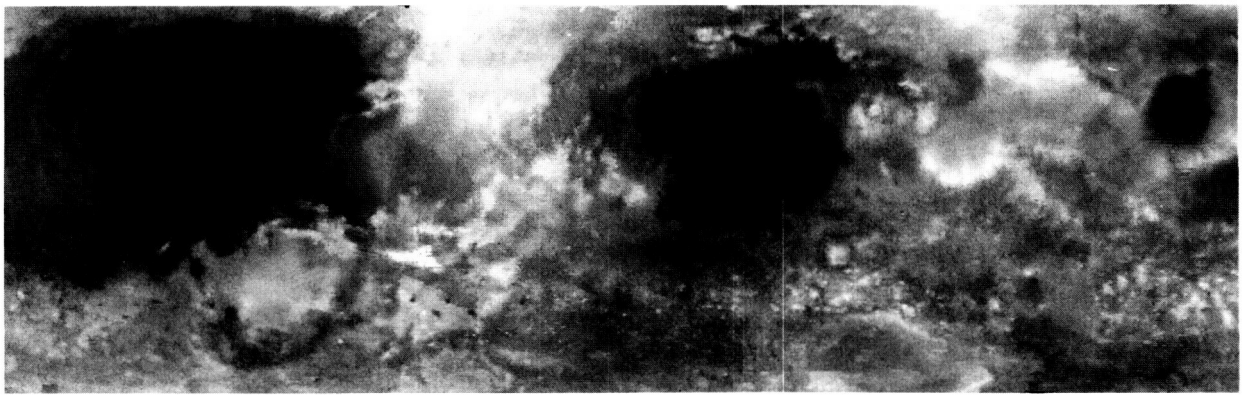

Fig. 5. Global thermal inertia image of Mars. The data have been superimposed on a digital version of the U.S. Geological Survey shaded relief map (scale 1:15,000,000). Areas covered by very fine material appear dark, with increasing particle size shown as increasing brightness on the image. The high degree of correlation between relatively coarse material (bright) and surface features can be seen.

Mapping Lunar Rock Types Using Orbital Chemical Data

Philip A. Davis and Paul D. Spudis, Branch of Astrogeology, U.S. Geological Survey, Flagstaff, AZ 86001

Three main sources of data have been used to interpret the geology of the Moon: photographs, landing-site observations and samples, and orbital chemical data. Photographs have been used extensively to map geologic units and to determine their relative ages. Rock and soil samples returned from six U.S. Apollo and three Soviet Luna missions have been used to determine the mineralogy, chemistry, and absolute ages of materials at nine sites. The absolute sample ages have been combined with relative ages determined from counts of the frequencies of impact craters of various sizes to establish an absolute chronology for geologic units. The chemical, mineralogical, and chronological information has added greatly to our knowledge of the origin and evolution of the Moon, and thus of the Earth.

Chemical data for about 20% of the lunar surface were provided by two of the orbiting Apollo spacecraft. These data exist as maps of the elemental concentrations of iron, titanium, aluminum, magnesium, and thorium. One of the main advantages of the orbital chemical maps is that they show elemental concentrations for areas that were not sampled by the Apollo or Luna missions, most importantly the farside of the Moon. In addition, they allow discrimination of areas of contrasting chemical composition. On four of the maps, it is possible to distinguish between the dark basalt (lava flows) of the maria and the light anorthosite (an aluminum-rich rock consisting essentially of white feldspar) of the highlands. (These dark and light areas are also easily distinguished on the frontside of the Moon by telescope.) Some of the light feldspar-rich highlands also contain magnesium-rich minerals, which make up rocks referred to as the magnesium suite. The thorium map shows several areas that are high in natural radioactivity because of the presence of a rock type known as KREEP, which was so named because of its high concentrations of potassium (K), rare-earth elements (REE), and phosphorus (P). For many years, scientists working on either sample or orbital chemical data addressed geologic problems of the Moon from one or the other of these data bases. However, in an attempt to learn more about the global geology of the lunar surface, we developed a method that uses both the sample and the orbital chemical data to map the distribution of known rock types on the Moon. Our integrated analysis used only those chemical maps produced from the gamma-ray spectrometer (i.e., the iron, titanium, and thorium maps) because these maps have twice the areal coverage of the X-ray spectrometer that produced the aluminum and magnesium maps.

The basis of our method is a ternary (triangular) diagram that is subdivided into equally spaced segments along each of its three sides (fig. 6, lower left). The segments are assigned distinct colors that cover the range of the visible spectrum, and the apex segments are assigned the three primary colors. The triangle in the center of the diagram represents equal proportions of the three apexes and is assigned the color gray. The apexes are defined by the KREEP and magnesium suite rocks (labeled MG), mare basalts (labeled MB), and anorthosite (labeled FAN) and thus represent the average iron and the thorium to titanium ratio compositions of the three common rock types on the Moon. The iron and thorium to titanium composition of every quarter-degree area (picture element [pixel]) within the orbital chemical maps is used to determine its location within the ternary diagram. The color corresponding to this ternary position is then placed within a classification map at the position of the pixel in the original chemical maps (fig. 6, upper right and left).

The resulting classification map shows spatial transitions among rock types, allows direct deter-

mination of the relative proportions of each end-member rock composition in a pixel, and increases the geologic interpretability of these data over that of the individual elemental maps. Our map of lunar rock types shows the following features. (1) The highlands contain large areas of relatively pure anorthosite. (2) The average composition of the upper crust is that of anorthositic gabbro, which supports the hypothesis that the crust of the Moon formed in an early, global magma ocean. (3) KREEP and magnesium suite rocks are a minor fraction of the upper lunar crust. (4) Within the farside highlands, areas of KREEP and magnesium suite rocks coincide mostly with areas of crustal thinning, which are probably areas of KREEP basalt extrusions or localized excavations of magnesium suite rocks or KREEP-rich rocks. (5) Portions of the east limb and farside highlands have considerable amounts of the mare basalt component, whose occurrences coincide with mapped concentrations of light plains that display dark halo craters. This observation supports the hypothesis that mare volcanism occurred within this highland region before the end of the final heavy meteorite bombardment nearly 4 billion years ago.

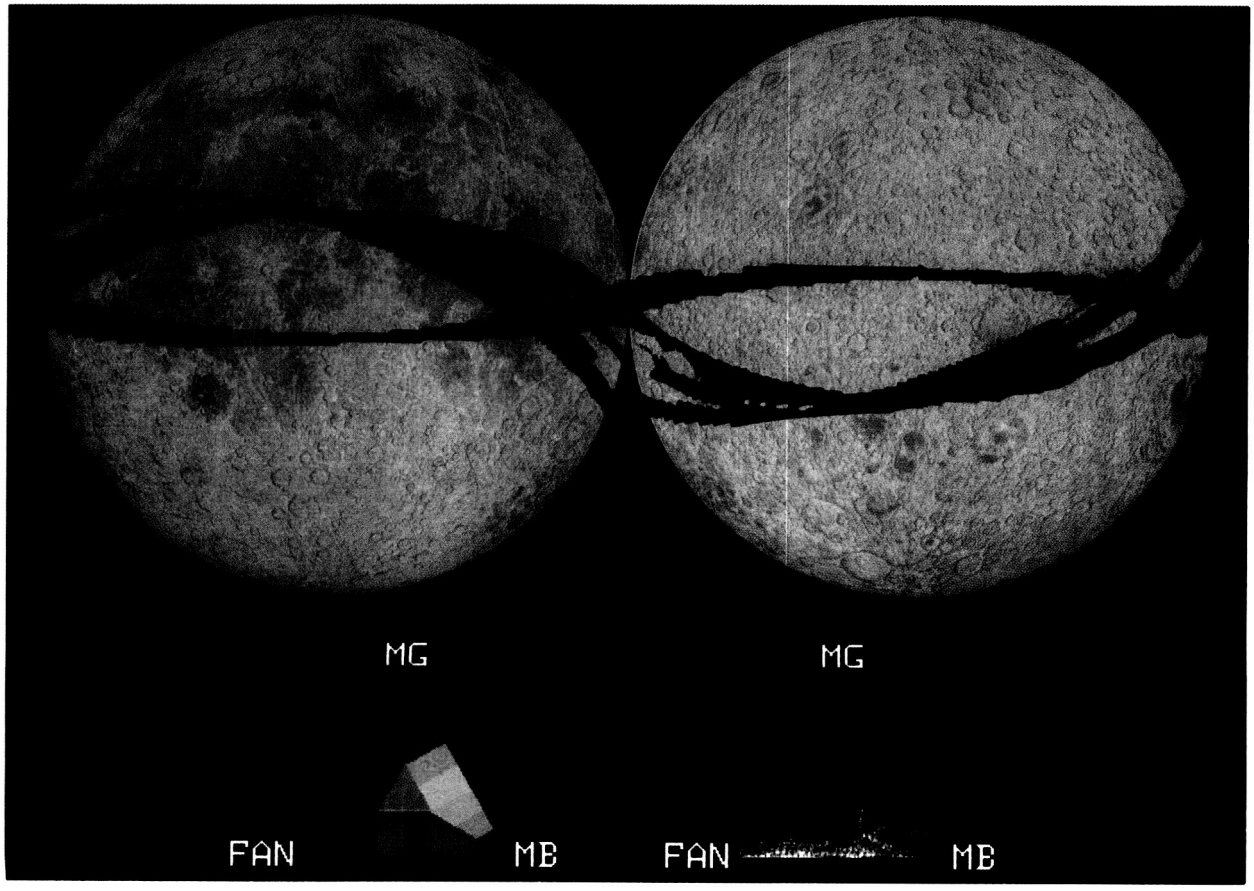

Fig. 6. Lunar orbital geochemical data showing relation between iron (Fe), thorium (Th), and titanium (Ti). Top, rock-unit classification map of frontside (left) and backside (right) of the Moon. Relative end-member compositions for each unit can be determined from ternary reference diagram (lower left). Letters at apexes of the ternary reference diagrams designate KREEP and magnesium suite rocks (MG), mare basalts (MB) and anorthosites (FAN). The diagram on the lower right is a picture element (pixel) frequency scattergram; the color indicates the number of pixels shown in the maps of the Moon corresponding to a given composition. Pixel frequencies are: magenta ≤ 25 pixels; blue, 50 pixels; cyan, 75 pixels; yellow, 125 pixels; dark red, 150 pixels; bright red, 175 pixels; and white ≥ 200 pixels.

Water and Ice in the Soil of Mars

Fraser P. Fanale and Aaron P. Zent,
Planetary Geosciences Division, Hawaii Institute of Geophysics, University of Hawaii, Honolulu, HI 96822

Mars has an atmosphere and is the only planet other than Earth known to exhibit polar caps (e.g., fig. 7) and clear evidence of having had liquid water on its surface and a warmer, wetter climate early in its history. In addition, there exists a reasonable possibility of the present localized occurrence of liquid water and brine. Mars experiences not only major seasonal climate variations but also long-term quasiperiodic climate changes. The forces that drive the latter are similar in origin, period, and thermal effect to those that produce climate change on the Earth.

How much water has degassed into the martian atmosphere, regolith (loosely consolidated material at the surface), and polar caps? And, how much is still there? The latest estimates are based on the assumption that certain classes of meteorites, the Shergottites, Nakhilites, and Chassignites (SNCs), are derived from Mars. On this basis and on the basis of geochemical studies of the Earth and meteorites, C. Dreibus and Heinrich Wanke (Max Planck Institute, Germany) have concluded that Mars is more volatile-rich, in bulk, than the Earth is, a conclusion consistent with the well-established general trend of increasing volatile abundance with increasing distance from the Sun. An important aspect of the Dreibus and Wanke scenario is that Mars, unlike the Earth, accreted homogeneously; hence, almost all of the accreted water on Mars could have been destroyed by interaction (oxidation) with metallic iron. The escape of the freed hydrogen into space would simultaneously have dragged off most of the other degassed volatiles as well. Efficient operation of this process would have led to a present Mars having only about one-tenth the water that is immediately visible in the north polar cap.

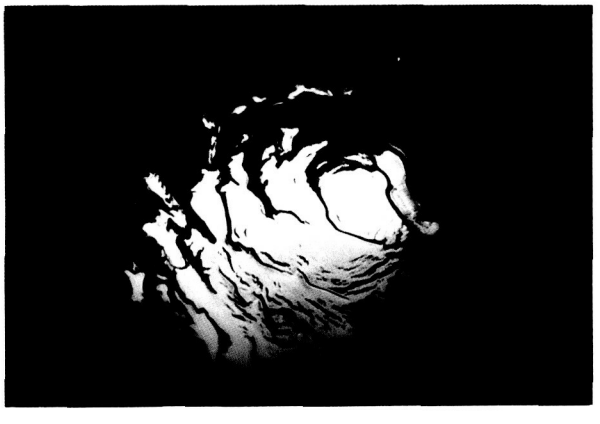

Fig. 7. South polar cap of Mars as imaged by the Viking Orbiter.

In qualitative support of the operation of this loss process studies of the rare gases and other volatiles by Robert Pepin (University of Minnesota) and Donald Hunten (University of Arizona) have suggested that rare gases in the martian atmosphere have been subjected to severe and regular elemental and isotopic fractionation that could be explained by depletion of atmospheric gas due to drag of escaping hydrogen. Furthermore, according to John Lewis and Hampton Watkins of the University of Arizona and Thomas Ahrens of the California Institute of Technology, large impacts could have caused an additional net loss of atmosphere by accelerating it away from the planet.

A different approach to this problem offered by Michael Carr and Gerald Schaber (U.S. Geological Survey) results in an entirely different conclusion. They noted that Mars exhibits many landforms that are associated with the presence of ground ice on Earth, only at a much larger scale, indicating the presence of extensive ground ice on Mars. Carr has also noted that the volume of water needed to cut the large outflow channels that drain into the Chryse Basin would correspond to a global layer at least 350 meters deep.

What should one conclude from these observations? On the one hand, the geochemical evidence for the martian bulk water endowment, theoretical models for homogeneous accretion, and the evidence from studies of rare gases in

SNC meteorites argue for very little water at present on Mars. On the other hand, the ground-ice-related morphologies, the large outflow channels, and the valley networks suggest a water volume equal to a global layer at least 50–100 meters thick. These data suggest the presence of significant quantities of water late in martian history. Considering the evidence and arguments and the validity of the assumptions involved, it must be concluded that at the end of any 'hydrogen sweeping' episode and any late heavy meteor bombardment, Mars retained a volume of water (which it still retains) corresponding to a global layer at least 100 meters thick stored in its regolith.

How are those water molecules distributed today? And, in what state are they? A model of the distribution of water has been proposed by Fraser Fanale, James Salvail, Susan Postawko, and Aaron Zent (University of Hawaii). The model (fig. 8) depicts a cross-section of a possible distribution of water and ice in the martian regolith. Their model was based on quantitative consideration of long-term orbital and climatic variations, atmosphere-regolith interactions, and geophysical aspects. However, there are major factors, such as the local or regional volcanic introduction of new water or the redistribution of the regolith by major impacts, that the model does not consider. Also, the soil porosity can be estimated only within wide limits. Therefore, this model should only be used as a general global reference model to which morphological observations can be compared.

How well does the model compare with the observations? Michael Carr and Steven Squyres (Cornell University) have found that "softened terrain," which appears to be indicative of the presence of ground ice, is restricted to latitudes north and south of 30°, in agreement with predictions of the model. However, James Zimbelman (National Air and Space Museum, Smithsonian Institution) has suggested that the softening may actually be due to mantling of the surface by debris. Data that suggest the presence of water outside polar areas have been presented by Baerbel Lucchitta (U.S. Geological Survey), who noted large fluidized flows in the equatorial region that occurred fairly late in martian history, and Stephen Clifford (State University of New York), who has pointed out that several craters as small as 2 kilometers in diameter in equatorial areas have fluidized ejecta (which may be indicative of near-surface volatiles). These observations may require reexamination of the model. Perhaps ice does occur near the surface in a few selected equatorial areas.

The distribution of water in the very shallow martian regolith is difficult to assess. With the current data, it is possible to produce only a statistical view of global water distribution, without too much emphasis on detail. ("Distribution" is the location of the "frost table"—a term borrowed from terrestrial cold region geology, indicating the upper surface of the ice-rich frozen ground.)

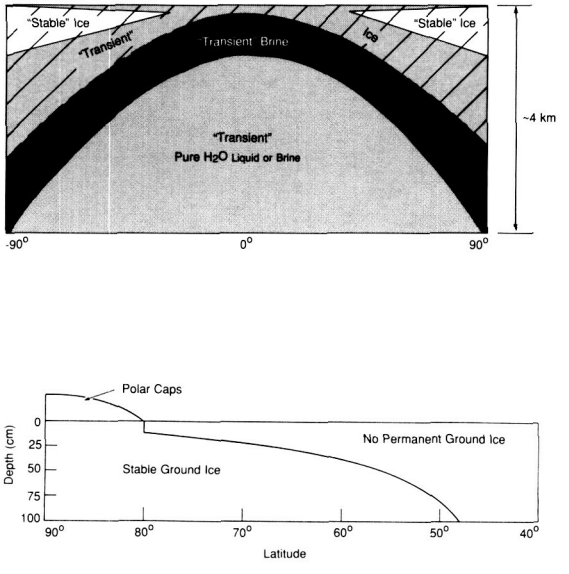

Fig. 8. Cross-sections of a possible distribution of ice on Mars: (top) global distribution showing zones of stable ice and liquid water as a function of latitude and depth; (bottom) detailed cross-section showing the depth to stable ground ice as a function of latitude.

The distribution of water is probably controlled by the process of vapor diffusion. In most regions on Mars it is too cold for liquid water to flow beneath the surface. Water molecules diffuse through the soil between the atmosphere (which acts as one boundary on the soil column) and the frost table (which acts as the other). The boundary condition, which is the water vapor density at the frost table, is determined by the temperature of the frost table. If the temperature of the ice changes, the boundary condition changes with it and the direction in which water vapor is diffusing (to or from the atmosphere) may also change. The fact that the frost table must exchange water molecules with the pore spaces directly above it allows the frost table to migrate vertically.

The distribution of ground ice changes slowly on Mars. Temperatures on Mars are so low that the pore spaces in the regolith cannot hold more than a very small amount of water vapor, and even that small amount must diffuse through the martian soil, which may have very low porosity. Fraser Fanale and Bruce Jakosky (University of Colorado) have determined that a water molecule spends up to 100 times longer adsorbed onto pore walls than it does diffusing through pore volume. In total, the exchange rate of water between the atmosphere and the regolith is very low. It may take as long as 10,000 years for 1 gram of water to migrate through 1 centimeter of regolith. During such protracted periods of time, the critical boundary conditions, the atmospheric water abundance, and the temperature of the frost table are known to change.

Crofton Farmer (California Institute of Technology) and P. E. Doms (University of California at Los Angeles) used Viking observations to calculate the equilibrium position of the frost table as it migrated through a full martian year. However, the Viking data may not be entirely representative of even this portion of the obliquity cycle. Bruce Jakosky and Edwin Barker (University of Texas) pointed out that during 1969, the atmospheric water content of the Southern Hemisphere was three times higher than normal. They suggested that the carbon dioxide cover of the southern polar cap may completely sublimate in some summers, allowing underlying water access to the atmosphere. Brian Toon and co-workers (NASA, Ames Research Center) looked at the problem from a broader (long-term) perspective and found that as the obliquity decreases, the equilibrium position of the frost table moves to greater depth and higher latitudes and vice versa. Zent, Fanale, and co-workers (University of Hawaii) included seasonal and long-term boundary condition variations in their model, along with the kinetics of water migration through the regolith, and produced a mean frost table configuration that is similar to that of Farmer and Doms.

The mean depth to the ice-rich layer is probably a meter or less poleward of roughly 45° latitude. Poleward of 70° or 80°, the frost table is likely to be within centimeters of the surface. Estimates of the capacity of the atmosphere-cap-regolith system to exchange water indicate that the frost table at latitudes >45° may migrate vertically by no more than 10–20 centimeters, approaching the surface at high obliquity and receding at low obliquity. David Paige (University of California at Los Angeles) has modeled Viking thermal observations and concluded that the frost table lies about 15 centimeters deep near 80°S latitude. There may, of course, be deviations from this regime for any number of reasons; the thermal and diffusivity properties of the regolith could vary, and deposition and erosion of the regolith could occur.

The presence of liquid water in the martian surface is problematic. There is no fundamental reason that shallow ground waters are forbidden; they merely require the simultaneous presence of water molecules and sufficient energy to convert them to liquid. However, Fraser Fanale and Roger Clark (University of Hawaii) showed that the high temperatures necessary to produce melt raise the vapor pressure at the frost table, resulting in a vapor phase transfer of water from the regolith to the atmosphere and thence to the polar cap; therefore, high temperatures and the presence of water tend to be mutually exclusive.

The Rate of Volcanism on Venus

Bruce Fegley, Jr., Department of Earth, Atmospheric, and Planetary Sciences, Massachusetts Institute of Technology, Cambridge, MA 02139

Venus is totally covered by sulfuric acid (H_2SO_4) clouds that are formed by the sunlight-powered conversion of gaseous sulfur dioxide (SO_2) into H_2SO_4 cloud particles. In turn, this cloud formation process is part of a larger set of chemical reactions involving the clouds, sulfur gases such as SO_2, and chemically reactive minerals on the hot (approximately 460°C [860°F]) venusian surface. These reactions are continually cycling sulfur between Venus, sulfur gases in the atmosphere, and the clouds. Chemical analyses, conducted by the U.S. Pioneer Venus spacecraft and by several of the Soviet Venera and Vega spacecraft, have detected sulfur in each of these three reservoirs.

The chemical analyses of the surface and atmosphere of Venus, conducted on the spacecraft, in combination with calculations by U.S. and Soviet scientists, show that chemical reactions between SO_2, which is the dominant sulfur gas in the atmosphere of Venus, and calcium minerals on the surface of Venus are continually removing SO_2 from the atmosphere by formation of sulfur minerals such as anhydrite ($CaSO_4$). These gas-solid reactions between the atmosphere and the surface of Venus are thus a net sink for sulfur. Maintenance of the global H_2SO_4 clouds, which would disappear if $CaSO_4$ formation removed all SO_2 from the atmosphere of Venus, therefore, requires a sulfur source of the same size as the sulfur sink. The required sulfur source is active volcanism. However, the global H_2SO_4 clouds, which are a result of the volcanic eruption of sulfur-bearing gases (and hot, reactive sulfur-bearing magmas), also prevent the direct observation of the rate of volcanism on Venus. Thus, this rate must be deduced from the rate at which $CaSO_4$ formation on the Venus surface removes SO_2 from the atmosphere.

The present work is the first experimental measurement of the rate of $CaSO_4$ formation (and thus SO_2 depletion) on Venus and also provides the first estimate of the present-day rate of volcanism on Venus. These experiments use the mineral calcite ($CaCO_3$), which is predicted to be an important sink for incorporation of SO_2 into venusian crustal minerals via the following reaction:

$$CaCO_3 \text{ (calcite)} + SO_2 \text{ (gas)} = CaSO_4 \text{ (anhydrite)} + CO \text{ (gas)} \quad (1)$$

Reaction 1 was studied experimentally by heating $CaCO_3$ samples in a SO_2-bearing gas stream at three different temperatures. Experiments were conducted at atmospheric pressure with a $SO_2 - CO_2$ gas mixture containing 1% SO_2. This mixture was chosen so that the number of SO_2 molecules per unit volume was about the same as that on the surface of Venus, where the atmospheric pressure is about 100 times larger but the SO_2 concentration is about 100 times smaller than in the laboratory. Standard techniques were used to monitor and control temperature and gas flow during the experiments. The rate of reaction 1 was determined by three independent methods: (1) measuring the weight gain at the end of reaction, (2) using the scanning electron microscope (SEM) to measure the porosity and thickness of the reacted surface layers on the samples, and (3) chemical analyses of samples for sulfate.

SEM photographs (figs. 9 and 10), X-ray diffraction data, and chemical analyses show that $CaCO_3$ samples heated in $SO_2 - CO_2$ gas streams for periods ranging from hours to weeks develop coatings of $CaSO_4$, the thermodynamically stable product of reaction 1. The SEM examination of many samples shows that all the exposed surfaces of the $CaCO_3$ samples become coated with layers of $CaSO_4$ (fig. 10). The thickness of the $CaCO_3$ layers increases with longer reaction times and is an indicator of the rate of reaction. Kinetic data obtained from the thickness (and porosity) of the $CaSO_4$ layers agree with the two other indepen-

dent sets of kinetic data obtained from the measured weight gains and chemical analyses. The reaction rates measured at the three experimental temperatures are extrapolated downward to the venusian surface temperature using standard methods.

If we assume that the experimentally determined rate of $CaSO_4$ formation via reaction 1 is representative of the SO_2 reaction rate with calcium-bearing minerals on the surface of Venus, the laboratory data can be used to estimate the SO_2 removal rate from the venusian atmosphere. By using the extrapolated laboratory data, the Soviet Venera 13 and 14 chemical analyses for calcium on the surface of Venus and by taking the altitude (and thus temperature) dependence of the rate into account by using the U.S. Pioneer Venus radar altimetry data, the SO_2 removal rate from the venusian atmosphere is calculated to be approximately 40 million metric tons of SO_2 per year over the entire surface of Venus. The SO_2 concentration in the venusian atmosphere as measured by the U.S. Pioneer Venus and Soviet Venera 11 and 12 spacecraft corresponds to a total atmospheric SO_2 inventory of about 100,000 billion metric tons. Thus, the calculated SO_2 removal rate will remove all SO_2 from the venusian atmosphere in 2.5 million years. The volcanism rate required to resupply sulfur gases to the atmosphere (either directly or by rapid atmospheric reaction with the hot, sulfur-bearing magma) depends on the sulfur content of the erupted gas and magma. This rate is conveniently expressed as the sulfur to silicon (S/Si) ratio. Three plausible cases have been considered: (1) an S/Si ratio equal to that in venusian surface samples analyzed by the Soviet Venera 13 and 14

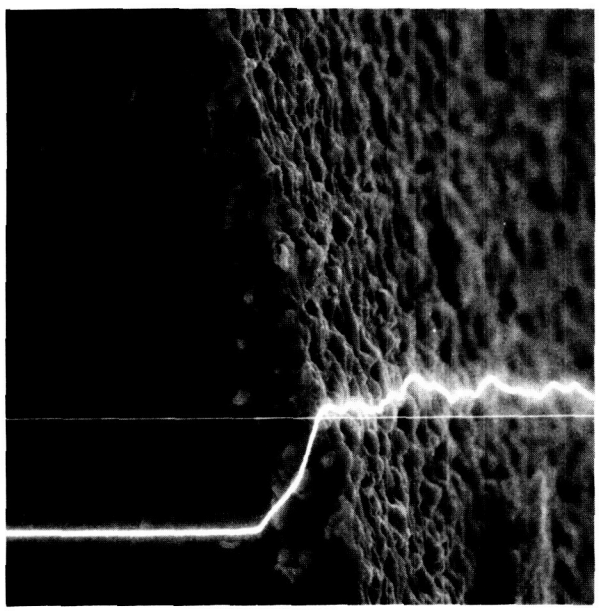

Fig. 9. Scanning electron microscope photomicrograph of the fracture surface of a reacted calcite ($CaCO_3$) sample. The scale bar is 50 micrometers (0.002 in.) long. The horizontal white line on the photograph shows the position of an X-ray line scan for sulfur. The wavy white line shows that sulfur X-rays are produced only at the reacted surface, where grains of the mineral anhydrite ($CaSO_4$) are formed as a result of the gas-solid reaction.

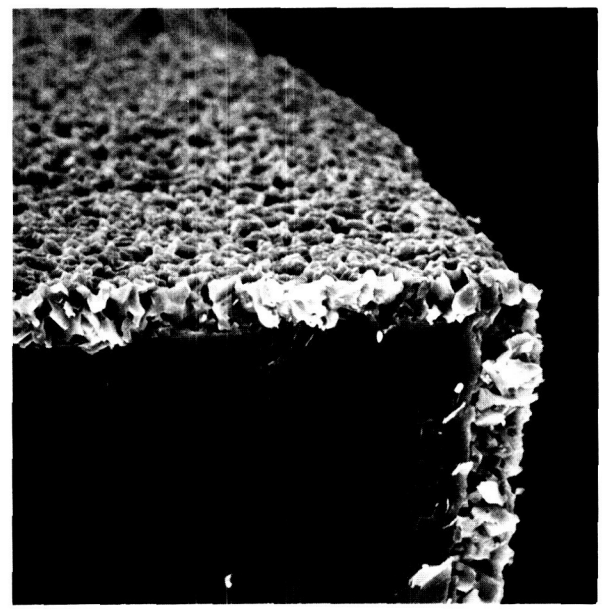

Fig. 10. Scanning electron microscope photomicrograph of the fracture surface of a reacted calcite ($CaCO_3$) sample. The scale bar is 100 micrometers (0.004 in.) long. All external surfaces of the $CaCO_3$ are covered with a layer of anhydrite ($CaSO_4$) grains. This layer gradually becomes thicker as the gas-solid reaction continues.

spacecraft, (2) an S/Si ratio equal to that in the Earth's crust, and (3) an S/Si ratio equal to that in meteorites (ordinary chondrites), generally believed to have compositions close to those of the Earth and Venus. The corresponding rates of volcanism, in terms of cubic kilometers of magma erupted per year, are illustrated in figure 11 (one kilometer = 0.625 miles). The estimated rates range from about 0.2 cubic kilometers/year to about 8 cubic kilometers/year, with the Venera 13 and 14 data giving a rate of about 1 cubic kilometer/year, and are comparable to but slightly smaller than the observed terrestrial rate of about 20 cubic kilometers/year, which is dominated by magmas erupted at mid-ocean ridges. Figure 11 also illustrates an independent upper limit to the rate of volcanism on Venus derived by other scientists from an analysis of the crater densities from meteorite impact (craters per square kilometer of the surface) observed in the Venera 15 and 16 radar images. This upper limit of about 2 cubic kilometers per year strictly applies only to the area of Venus observed by the Venera 15 and 16 radar and is a value averaged over several hundred million years. Nevertheless, the agreement between the two independent estimates is remarkable, and if correct, it means that Venus (on the average) is less volcanically active than the Earth is.

In summary, the maintenance of the global H_2SO_4 clouds on Venus requires active volcanism to replenish the atmospheric SO_2, which is continually being removed from the atmosphere by reaction with calcium minerals on the surface of Venus. Laboratory measurements of the rate of one such reaction, between SO_2 and $CaCO_3$ to form $CaSO_4$, have been taken for the first time. If the rate of this reaction is representative of the SO_2 reaction rate at the venusian surface, all SO_2 in the venusian atmosphere (and thus the H_2SO_4 clouds) will be removed in 2.5 million years unless the lost SO_2 is replenished. The required rate of volcanism ranges from 0.2 to approximately 8 cubic kilometers of magma erupted per year, depending on the sulfur content of the erupted material. If this material has the same composition as the venusian surface at the Venera 13 and 14 landing sites, the required rate of volcanism is about 1 cubic kilometer/year. An independent geophysical estimate based on Venera 15 and 16 radar images and applicable over several hundred million years is less than 2 cubic kilometers/year. Both estimates suggest that Venus is less volcanically active than the Earth is, but only by a small factor.

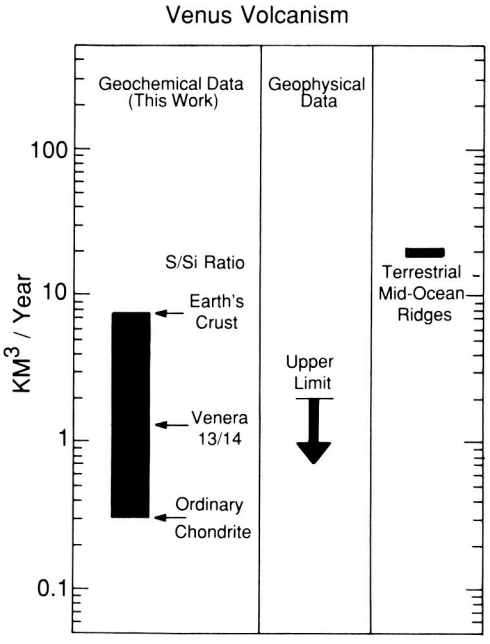

Fig. 11. Two independent estimates of the rate of volcanism on Venus are compared with the rate of volcanism on Earth. All rates are given in cubic kilometers of magma erupted per year. The geophysical rate determined by other scientists is based on impact crater densities (craters per square kilometer of the surface) in the Venera 15 and 16 radar images. The geochemical rate is based on the present laboratory study of the rate of sulfur dioxide (SO_2) reaction with venusian crustal minerals. Different assumptions about the chemical composition (sulfur to silicon [S/Si] ratio) of erupted material on Venus lead to different rates of volcanism. The Venera 13 and 14 chemical analyses of the venusian surface yield a rate of volcanism of about 1 cubic kilometer of magma per year, or about 20 times less than that on Earth.

Weathering on Venus as Inferred from Experiments Using the Venus Simulator Facility

Ronald Greeley and John Marshall, Department of Geology, Arizona State University, Tempe, AZ 85287

The surface of Venus is a searing 460°C (870°F), and it has an extremely dense carbon dioxide atmosphere, which exerts a surface pressure of 95 bar (95 atmospheres)—a pressure equivalent to that of the sea floor at a depth of 970 meters (3180 feet). Spacecraft have measured wind speeds at the surface that are capable of moving sand and small pebbles. The composition of the atmosphere is primarily carbon dioxide and contains small amounts of sulfur dioxide, carbon monoxide, hydrogen sulfide, hydrochloric acid, and water, all of which appear to vary in quantity according to altitude. These atmospheric constituents are thought to react with surface materials to form weathering products. The chemical breakdown of surface materials is one of the major processes that controls the amount and type of debris on the surface of Venus and may influence the composition of the atmosphere through feedback processes. Venus does not have as wide a variety of geomorphic agents as Earth does; the surface is not eroded by running water, waves, or glaciers. Consequently, physical and chemical weathering processes related to the atmosphere are the dominant modifying processes and must be investigated to understand the evolution of the venusian surface.

The Venus Simulator Facility (VSF) (fig. 12) includes an experimental apparatus that allows venusian conditions to be duplicated in the laboratory. It is designed so that important parameters such as temperature, pressure, and atmospheric composition can be varied independently to assess their effects in the general process of weathering on Venus. The VSF is composed of two integrated systems. The first system is a large (80-cm-diameter), internally heated steel pressure vessel (figs. 12 and 13a) used to conduct experiments dealing with physical processes. It duplicates the behavior of windblown material (sand and pebbles) on Venus by propelling particles against sample rock surfaces at temperatures, pressures, and particle speeds appropriate for the planet. Figure 12 shows a video camera used to record the process through a quartz window at the end of the vessel. These tests allow inferences to be made about the evolution of particles on Venus and about the effect of these particles on rock surfaces during transportation by the wind.

The second system of the VSF is a much smaller (15-cm-diameter), externally heated pressure vessel made of Hastelloy—a thermally and chemically resistant nickel alloy. This vessel (fig. 13b) is used to conduct experiments dealing with the chemical reactions between minerals and gaseous components of the venusian atmosphere. For some tests, it is operated under the same conditions as those on Venus, while for others it is operated at much higher temperatures and pressures to accelerate chemical reactions to realistic time scales. It is connected to a gas mixing system and a gas analysis unit (a gas chromatograph, see fig. 12) that measures changes in composition as reactions take place in the vessel. Results from these experiments enable conclusions to be drawn about the nature and the rate of chemical weathering on Venus, the gases extracted from the venusian atmosphere, and gases that may be released from surface materials into the atmosphere.

Samples of rocks and minerals that have been run in VSF experiments are analyzed using techniques such as scanning and transmission electron microscopy, profilometry, Auger electron spectroscopy, X-ray diffraction, and mass spectrometry. These tests permit changes in chemical and physical properties to be assessed.

On Earth, rocks are often eroded by sandblasting from windblown particles. Experiments with the VSF suggest that in many cases, the opposite may be true for Venus. Although the edges of particles are damaged by impact (as on Earth),

extremely fine debris from this damage is "plastered" onto the surfaces of rock. Figure 14 shows a typical example of this accretionary material adhering to a test sample. An extensive series of tests has shown that this accretion occurs at all temperatures above 240°C (460°F) for basaltic materials (rocks typical of the composition of the surface of Venus) and is therefore likely to occur over the complete range of conditions encountered on Venus. Tests also indicate that accretion develops more readily when windblown particles and impacted rock surfaces are composed of the same material, which leads to the conclusion that accretion occurs similar to the engineering phenomenon of "cold-welding." The development of accretionary layers on rock surfaces has important implications for Venus. Windblown material may leave a chemical trail as it moves through a region, thus altering the chemical and physical character of exposed rock surfaces. Moreover, if the tiny fragments worn from the particles have a tendency to stick to rock surfaces, they will not be so readily liberated into the venusian environment as windblown dust.

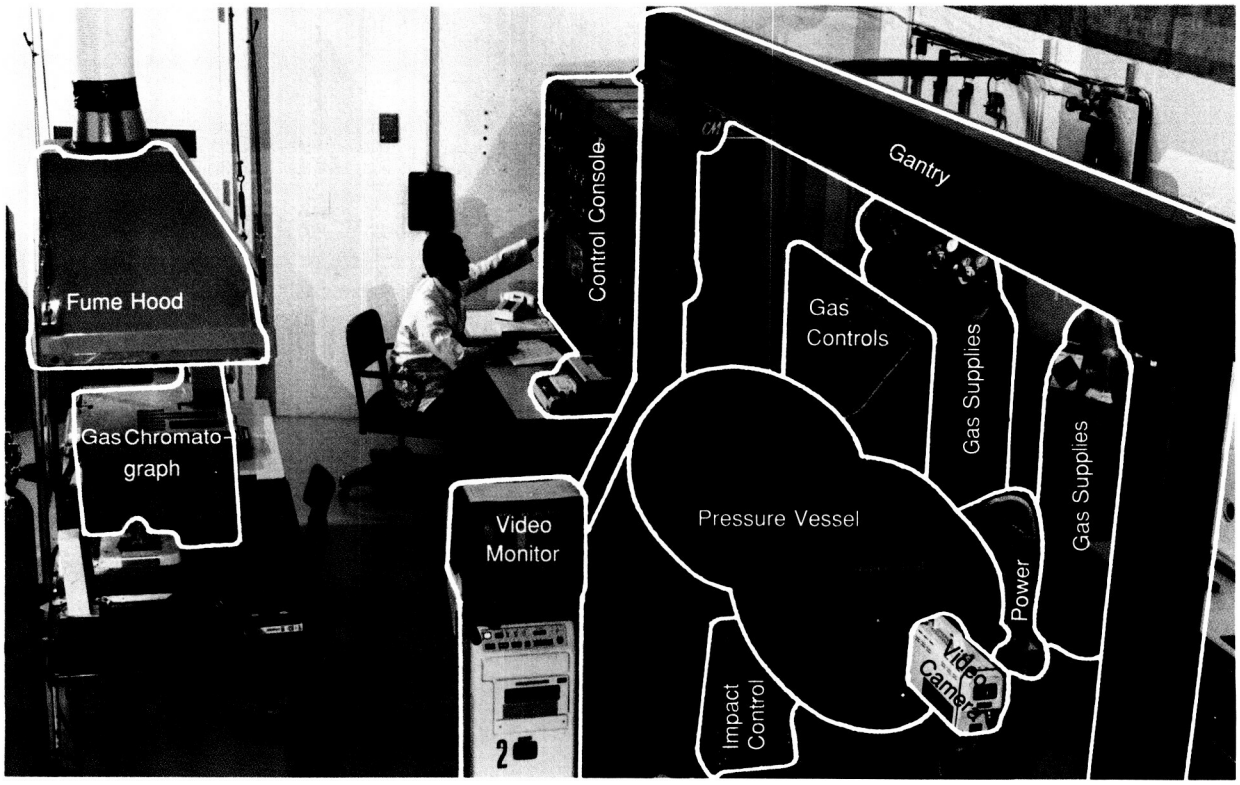

Fig. 12. The Venus Simulator Facility, showing the pressure vessel used to propel particles against rock surfaces and a video camera used to record the experiments. The smaller pressure vessel used for experiments dealing with chemical reactions is not shown in this view, but the associated gas chromatograph is visible on the left.

In summary, these and other experiments show that windblown materials may interact with rock surfaces through a wide variety of processes. It would have been extremely difficult to predict the occurrence of accretion on Venus without the VSF experiments. Future work with the VSF will address the molecular-level physical and chemical processes involved in cold-welding minerals, as well as the effects of particle speed, particle size and shape, experiment durations, and other important factors. Experiments to assess chemical reactions between minerals and gases will increase the understanding of mineral stability on Venus.

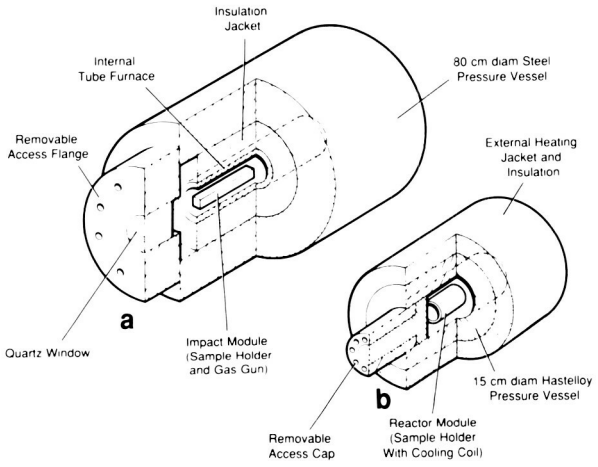

Fig. 13. Venus Simulator Facility pressure vessels. a), *Large vessel used for simulating the effects of windblown particles striking rock surfaces. The test samples are held in the impact module (a small gas gun) that is inserted into the tube furnace from the end of the vessel. The furnace is pressurized with heated carbon dioxide gas. The test is observed through a quartz window.* b), *Small vessel used to study chemical reactions between minerals and atmospheric gases. The vessel is connected to a gas mixing system and a gas chromatograph.*

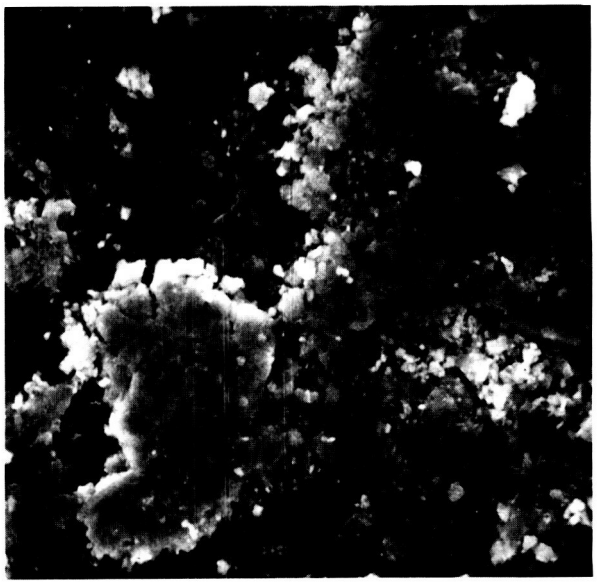

Fig. 14. Accretionary material (lighter areas) on a basaltic rock surface (dark background). The material was derived from erosion of an impacting basalt particle that struck the rock 100,000 times. Small pieces of deformed material are cold-welded to the surface during every impact. Distance across the photograph is about 40 micrometers.

The Freyja Montes–North Polar Plains Boundary of Ishtar Terra on Venus: Evidence for Large-Scale Convergence and Crustal Imbrication

James W. Head, Department of Geological Sciences, Brown University, Providence, RI 02912

The linear mountain belts of Ishtar Terra area on Venus (Akna, Freyja, and Maxwell Montes) have long been recognized as landforms distinct from those typical of the smaller terrestrial planetary bodies (Mercury and Mars) and the Moon. The mountain belts are the loci of compressional deformation features that represent localized zones of regional crustal shortening (orogenic belts). Although all the belts are apparently linked to the formation and evolution of Ishtar Terra, a continent-sized plateau and highland region in the Northern Hemisphere of Venus, each of the mountain ranges has a distinct tectonic relationship with its surroundings. The objective of this study is to characterize a distinct zone of deformation between Freyja Montes and the North Polar Plains, which lies about 500 kilometers to the north of and 6.5 kilometers below the crest of Freyja Montes.

A series of tectonic and geologic units have been mapped extending from the northern part of Lakshmi Planum north to the North Polar Plains (fig. 15). The banded terrain is composed of a series of long parallel ridges and swales spaced 10–20 kilometers apart and occupies a zone about 150 kilometers wide that extends from the crest of Freyja Montes down toward Lakshmi Planum. The features are interpreted to be primary anticlinal (convex) and synclinal (concave) structures oriented parallel to the long axis of the mountain range. The linear grooved terrain is composed of narrow linear grooves and ridges that are 2–10 kilometers across; individual features often extend in straight lines for 50–100 kilometers. This unit occurs in bands 20–45 kilometers wide and 200–600 kilometers long, running parallel to the strike of Freyja Montes and dividing the domed and ridged terrain on the back slope of Freyja Montes into 20- to 50-kilometer-wide segments. On the basis of these characteristics, the linear grooved terrain is interpreted to represent a series of major fault zones that have segmented the domed and ridged terrain. The two plains units (smooth plains and mottled plains) are regionally flat, show signs of flow-front-like features, and often embay other units; they are interpreted to be of volcanic origin. The northern boundary scarp is a 1- to 2.5-kilometer-high linear scarp less than 30 kilometers wide and more than 500 kilometers long. This feature is a major structural boundary that separates the North Polar Plains and Ishtar Terra.

The characteristics and distribution of map units and topography (fig. 15) indicate the following. (1) The northern boundary zone of Ishtar Terra at Freyja Montes is topographically distinct and highly asymmetric. Lakshmi Planum slopes upward toward Freyja Montes; Freyja Montes is asymmetrical, with the steep slope toward Lakshmi Planum and the shallow slope extending down toward the North Polar Plains. (2) The northern boundary scarp is a major tectonic structure bounding the region. (3) The units indicate two fundamental processes. One process is tectonism, which produces distributed deformation in the banded, domed and ridged terrains and localized deformation in the linear grooved terrain and at the northern boundary scarp. The nature and orientation of the structures indicate primarily compressional deformation oriented generally north-south. The other process is volcanism, which produces plains that appear to precede deformation in some cases (mottled plains) and to be either contemporaneous with or to postdate deformation (smooth plains) in others.

On the basis of the geology and topography, Freyja Montes is interpreted to represent the site of

a

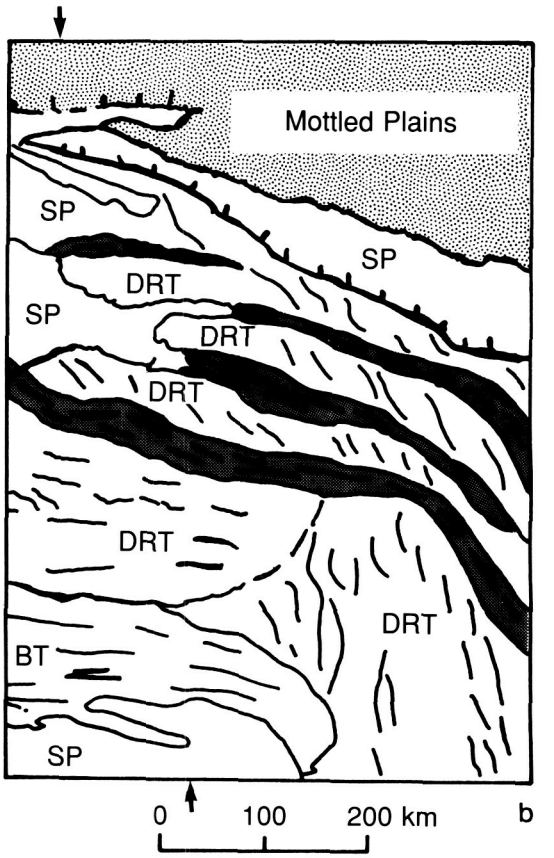

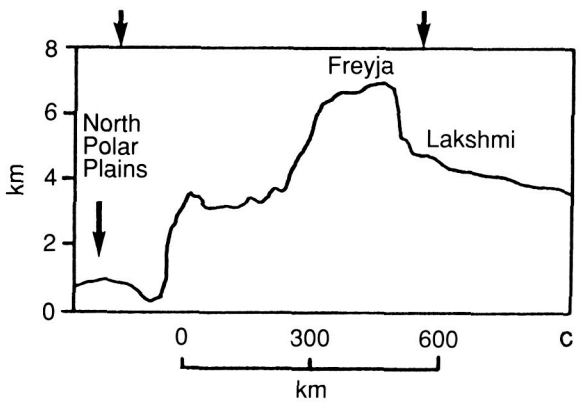

Fig. 15. a), *Venera 15 and 16 image of the Freyja Montes region of Ishtar Terra.* b), *Geologic and tectonic sketch map of the region shown in part* a. *Basal scarp is hatchured; SP = smooth plains, DRT = domed and ridged terrain, and BT = banded terrain, dark pattern within DRT is linear grooved terrain. Arrows show location of profile in part* c. c), *Topographic profile across the region. Arrows on profile indicate edge of map in part* b. *Vertical exaggeration is 75:1.*

large-scale crustal convergence and imbrication caused by the underthrusting of the North Polar Plains beneath Ishtar Terra. The process is visualized in the following ways (fig. 16). (1) North-south compressional deformation causes flexure, buckling, and underthrusting of the crust with the faults dipping toward the south. Evidence that this process operates today is the distinct northern boundary scarp, the slight topographic rise approximately 50 kilometers north of the scarp, and the linear nature of the embaying smooth plains between the scarp and the rise, suggesting flooding of a flexural trough. (2) Continuing convergence causes crustal thickening and uplift, and a new zone of underthrusting is established. The earlier fault zone is incorporated into the mountain range (linear grooved terrain) between the intervening areally deformed blocks (domed and ridged terrains). Volcanic embayment of some of the fault zones suggests that deformation on them may be minimal

once they are incorporated into the mountains. (3) The continuing process of convergence produces large-scale crustal thickening, uplift, and the formation of the asymmetrical front of Freyja Montes.

The elements described here are similar to many terrestrial mountain belts at convergent plate boundary zones. The general structure and stratigraphic relationships indicate that very large-scale horizontal crustal shortening is taking place in this part of Venus. This situation is similar to many plate tectonic convergent environments on the Earth but is different than the tectonic structures of the smaller one-plate planetary bodies (Mercury and Mars) and the Moon. Further exploration of Venus by the Magellan mission will reveal additional evidence of the tectonic structure and its similarities to and differences from the Earth.

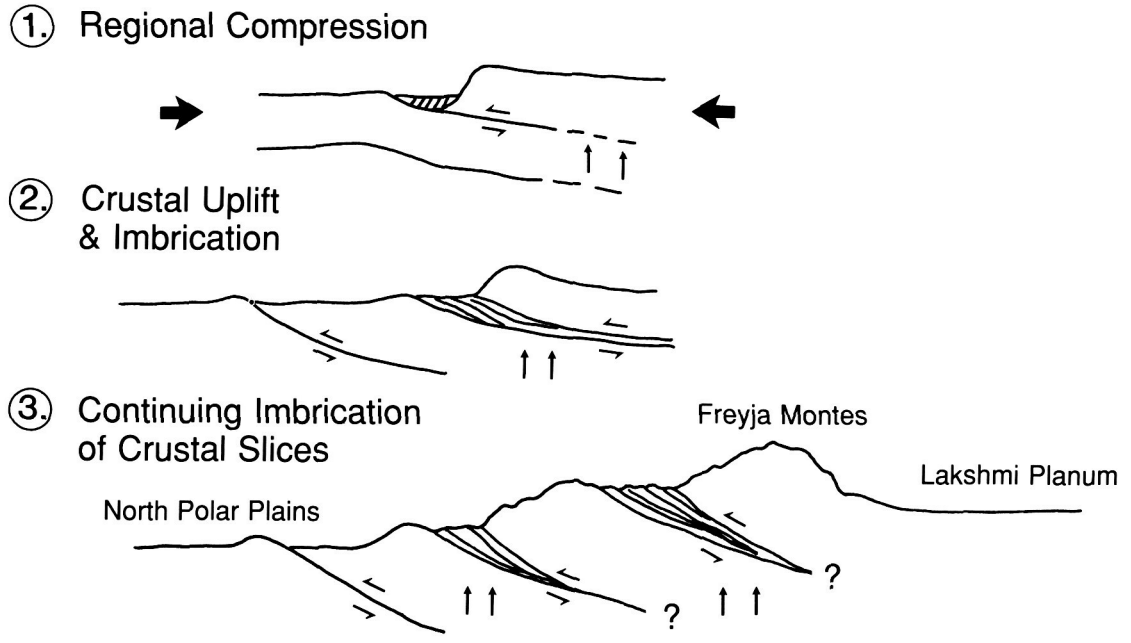

Fig. 16. Interpretive cross-sections showing inferred sequence of events in the formation and evolution of the Freyja Montes region.

Movement of Gases Between Atmospheres and Magma Oceans During the Growth of Venus, Earth, and Mars

John R. Holloway, Departments of Chemistry and Geology, Arizona State University, Tempe, AZ 85287

The purpose of this research is to determine how the abundant volatile elements carbon, hydrogen, oxygen, and nitrogen are incorporated into planetary interiors and atmospheres during the formation of planets. The most abundant forms of these elements on Earth today are the molecules H_2O (water) and CO_2 (carbon dioxide gas), the mineral calcite ($CaCO_3$), and molecular nitrogen (N_2), and oxygen (O_2). These elements ultimately form carbonate sedimentary rocks, the oceans and atmosphere on Earth, and the Earth-like planets Venus and Mars. In addition, these molecules, especially H_2O and CO_2, critically affect the kinds of igneous rocks formed on planets, the violence of volcanic eruptions, and the formation of ore deposits. The model developed in this research offers one explanation for the present elemental abundances on Earth and predicts their original abundances on Venus and Mars.

According to current theory, planets grow by the collection of baseball- to Moon-sized objects termed planetesimals. These planetesimals contain small amounts of carbon, hydrogen, and nitrogen and large amounts of oxygen and several other elements. Experiments by other investigators show that when a planet has grown to about 40% of the present size of the Earth, all of the carbon, hydrogen, and nitrogen are volatilized when planetesimals impact the planet surface. Calculations in the present study show that chemical reactions form new atmospheric gas molecules. A planet 50% the size of the Earth will form a thick atmosphere from these atmospheric gas molecules with planetary surface pressure at least 100 times greater than that of the Earth. This thick atmosphere causes a super-greenhouse effect, and resulting temperatures will melt a thick layer of the outer part of the planet, creating a magma "ocean."

Molecules from the thick atmosphere will dissolve in the molten magma ocean until the final stages of planet growth (fig. 17). In this last stage, the primitive atmosphere will be blown away by the impact of a giant (Mars-sized) planetesimal, an intense solar wind, or both. Loss of the thick insulating atmosphere will cause the planet to cool, and as the magma ocean crystallizes, the dissolved H_2O, CO_2, and NH_3 (ammonia) will escape to form a secondary atmosphere (fig. 18).

A major consequence of this model is that hydrogen and carbon in the impacting planetesimals are separated in the magma ocean stage. Hydrogen is incorporated into the magma ocean as H_2O, whereas carbon is released into the atmosphere as carbon monoxide (CO) and meth-

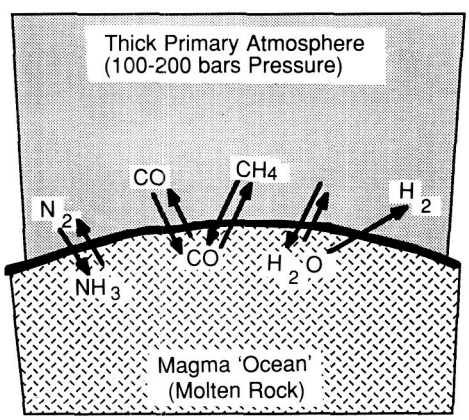

Fig. 17. Exchange of volatile molecules between a thick atmosphere and a magma ocean. The temperature is about 1200°C and the surface pressure is 100–200 bars (100–200 atmospheres). Carbon monoxide (CO) and ammonia (NH_3) are highly insoluble in the magma 'ocean', whereas water (H_2O) is highly soluble.

ane (CH_4). The loss of the primitive atmosphere results in enrichment of the planet in water in comparison with the reduced molecules CO and CH_4 in the atmosphere. The gases that escape from the solidifying magma "ocean" to form the secondary atmosphere are thus comparatively oxidized. Venus and Earth are similar in size, but Mars is only about half as large. Because of this size difference, the magma ocean lasts for about 95% of the formation period of Venus and Earth but only about 67% of that of Mars. This difference should cause the carbon to hydrogen ratio of Mars to be much greater than that of Venus and Earth. A more complete understanding of these evolutionary processes requires information on the crystallization relations of the interior of planets as a function of the volatile content of the magma. The author's research group is currently investigating the crystallization of martian magmas for comparison with Earth.

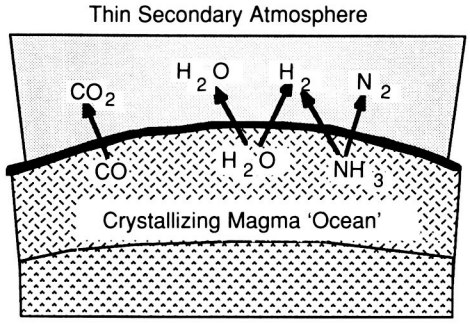

Fig. 18. Loss of volatiles from the magma 'ocean' after the primary atmosphere has been blown away and the magma 'ocean' cools and crystallizes. A magma 'ocean' initially 500 kilometers thick would supply about one ocean of water on Earth and enough carbon dioxide (CO_2) and nitrogen to form limestones and the atmosphere observed on Earth.

Thermal Contraction, Differentiation, and the Stress History of the Moon

R. L. Kirk, Branch of Astrogeology, U.S. Geological Survey, 2255 N. Gemini Drive, Flagstaff, AZ 86001

D. J. Stevenson, California Institute of Technology, Pasadena, CA 91125

The surface of the Moon, although well decorated with impact craters, appears remarkably bland to one interested in tectonics. It displays neither the planetwide network of thrust faults (as does the surface of Mercury) that would indicate a past era of global contraction nor the extensive graben valleys (like those of Mars) that would indicate global expansion over time. Yet, as Sean Solomon of the Massachusetts Institute of Technology first pointed out over a decade ago, the absence of such tectonic features is at least as interesting as their presence would be. He showed that faults *would* have formed if the lunar radius had increased or decreased by as little as 1 kilometer over the last 3.8 billion years. By modeling the production and transfer of heat in the Moon over time and by keeping track of the thermal expansion and contraction of the various layers, Solomon translated the constraint on the lunar radius into one on the initial state. His interpretation is illustrated in the top of figure 19: if the initial state were mostly hot (or mostly cold), the subsequent history of the Moon would involve cooling and contraction (or conversely, warming by radioactive decay and expansion) throughout and the large net volume change would fracture the crust. Faulting can only be avoided by combining a hot outer layer (the early magma ocean indicated by geochemical data) with a cold inner region in such proportions that the cooling of the one just compensates for the warming of the other.

Of course, Solomon's radius constraint is only one of many tests that a successful model of the origin of the Moon must pass, and at the time he

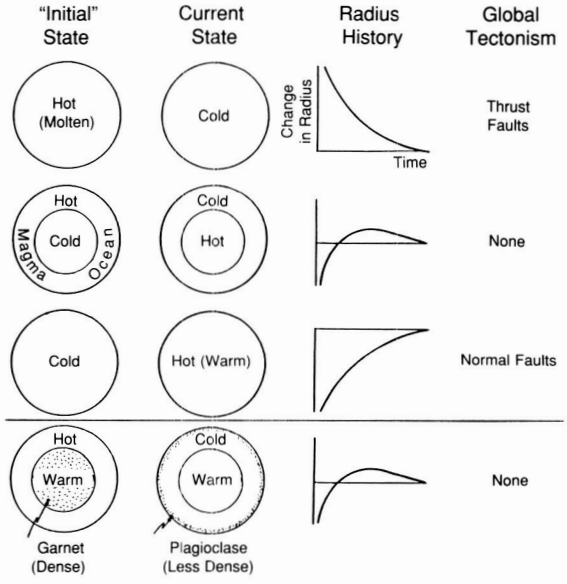

Fig. 19. Top, *traditional interpretation of the lack of global faulting on the Moon, originated by Sean Solomon (Massachusetts Institute of Technology). The early Moon could not have been molten or even nearly molten throughout because it would have cooled and contracted enough to cause thrust faulting at the surface. Additionally, the Moon could not have formed cold because the decay of radioactive elements would cause enough warming and expansion to result in normal faulting. Only a narrow range of initial states is allowed, in which cooling of a magma ocean at the surface offsets the warming of the interior.* Bottom, *including the expansion due to basaltic melt formation broadens the range of possible initial states for the Moon. Cooling of the magma ocean is partly offset by the melting of garnet and its recrystallization to form plagioclase feldspar rather than by warming a cold lunar interior. Such a partially molten, partially warm early Moon might well have formed after a giant impact on the Earth.*

propounded it, it seemed that every hypothesis of lunar origin failed in one or more areas. In the last few years, however, a new class of models has received enthusiastic attention in the planetary community. These giant impact models, in which the material for the Moon is blasted out of the Earth's mantle by the impact of a Mars-sized protoplanet, have not been fully tested, but so far they are not inconsistent with what we know of lunar chemistry and celestial mechanics. (See the article by A. G. W. Cameron in this volume.) Unfortunately, the violence of a giant impact would melt or vaporize most of the material that would make up the Moon; however, Solomon's model seems to rule out such a hot start.

We therefore decided to re-examine Solomon's model, including an effect that he neglected: thermal contraction is not the only manner in which an evolving Moon can change its volume. Differentiation, that is, the formation and migration of magma within a planet, can lead to a substantial, permanent expansion. We wondered if this expansion might be enough to offset thermal contraction if the Moon was formed hot by a giant impact.

The reason for a volume change accompanying basaltic magmatism is straightforward. Magma forms by melting of the minerals in the mantle: olivine, pyroxenes, and (at sufficient depth) garnet. But if the magma can migrate upward to a sufficiently shallow depth, it will crystallize to form olivine, pyroxenes, and plagioclase feldspar. The net effect is thus to destroy garnet (one of the densest of common minerals) and to create feldspar (one of the least dense), thereby lowering the average density of the planet. To determine whether this effect could have been important in the history of the Moon, we had to answer such questions as, how large is the volume change for rocks of lunar composition? How much room is there to accumulate feldspar near the surface? Will the garnet-to-plagioclase conversion be short-circuited? (That is, will the magma bury a substantial amount of pre-existing feldspar deep enough to convert it back to garnet?) On the basis of the availability of energy, how much melt will actually form at depths great enough to destroy garnet, and when? What initial states for the Moon lead to a radius change of less than 1 kilometer, and could such states result from a giant impact?

We estimated the amount of expansion by calculating the density of the lunar mantle from published models of its composition and the densities of the constituent minerals. We also calculated the densities of basalts of lunar composition and, finally, the densities of the mineral assemblages remaining when as much basalt as possible has been extracted from each mantle composition. From these densities, we calculated that complete extraction of basalt from a chunk of mantle would result in a net expansion of 3% or more. To obtain a similar expansion thermally, one would have to heat the mantle material by nearly 1000 K.

Encouraged by the magnitude of the expansion, we next investigated a simple model of the thermal evolution of the Moon. Our model is similar to Solomon's original model but includes the volume change due to differentiation. Like Solomon, we started the model just after the freezing of the lunar magma ocean (which occurs very rapidly); the outermost layers of the Moon are just below the melting point and the remainder farther below. We found a range of acceptable initial conditions (leading to less than ± 1 kilometer radius change) similar to that found by Solomon, with a cold interior that warms up but never melts. We also found a new class of acceptable solutions, shown schematically in the bottom of figure 19, in which the interior starts out hotter and eventually partly melts. Melting occurs at the right depths—below about 500 kilometers, the shallowest depth at which garnet is stable—and the right times to contribute a nonthermal expansion that offsets thermal contraction. Our hottest such model has a magma ocean 400 kilometers deep and the rest of the Moon near 1200 K.

In our model, about one-tenth of the Moon eventually melts, producing roughly 100 times the amount of basalt estimated to have been erupted onto the lunar surface to form the maria (the dark areas visible on the nearside of the Moon). This large amount of unobserved basalt is the most controversial aspect of our model, but we find it

quite plausible that most of the magma intrudes at the base of the lunar crust, which consists largely of feldspar and is even less dense than the basaltic melt. At any rate, the volume of melt produced is not so large as to cause short-circuiting of the expansion process. There is ample room for both the crust and the required volume of basalt in the outermost 180 kilometers of the Moon (the region in which feldspar is stable). Material below the crust will be buried deeper, but it will have formed from the part of the magma ocean that did not make up the crust, and hence it contains little or no feldspar to be converted to garnet.

Could the initial state of our model—by volume about half magma ocean, half hot but solid—have resulted from a giant impact? There is some reason to believe so. David Stevenson and Chris Thompson (California Institute of Technology) have constructed models suggesting that the melt splashed into Earth orbit by a giant impact would spin out into a thin disk, part of which would break up into 100–1000 "moonlets." These small bodies would have ample time for their surfaces to cool and to solidify before being swept up to form the Moon. On the other hand, supercomputer calculations by Willy Benz (Los Alamos National Laboratory) and his co-workers suggest that the impact melt might coalesce directly (in less than 1 hour) to form the Moon; there would be no time for any of the material to solidify. Much more work will be needed before we can determine which of these outcomes is most plausible and whether the promise of the giant impact hypothesis to meet all the criteria for a valid theory of lunar origin will be fulfilled.

Origin of the Fundamental Dichotomy in the Crust of Mars

George E. McGill, Department of Geology and Geography, University of Massachusetts, Amherst, MA 01003

Even a casual glance at either a geologic or a physiographic map of Mars is adequate to demonstrate that the planet is divided into two unequal parts. About two-thirds of Mars makes up what is called the "southern cratered highlands"; it stands relatively high, and its surface is generally heavily cratered. The abundance of craters, especially of large ones, leads to the inference that the surface of the southern cratered highlands is very old, on the basis of a comparison with the lunar surface where generally similar heavily cratered surfaces are about 4 billion years old or older. The remaining third of Mars is the "northern lowland plains," an area averaging about 3 kilometers (2 miles) lower elevation than the southern highlands. The northern plains are much less heavily cratered than the southern highlands and thus the surface materials are believed to be much younger. In most places, the boundary between the southern highlands and the northern lowlands is abrupt, and commonly this boundary is a complex scarp. Although strong gravity anomalies are associated with local features of the northern plains (fig. 20), there is no anomaly clearly related to the northern lowlands as a whole (fig. 21).

The twofold division visible on the surface almost certainly relates to a fundamental dichotomy in the crustal structure of Mars. This dichotomy is equivalent in importance to the continental crust versus the oceanic crust dichotomy on Earth, where the separation into two types of crust is maintained by plate tectonics. There is no evidence to suggest that similar processes are active on Mars; consequently, determining the origin of the martian crustal dichotomy is one of the major unanswered questions of martian geologic history.

Two main hypotheses have been proposed to explain the crustal dichotomy: (1) excavation of the northern lowlands by a giant impact creating a basin 7700 kilometers (4775 miles) in diameter, referred to as the "Borealis Basin" or (2) subsidence due to large-scale internal processes eroding the crust from below. Both hypotheses explain the 3-kilometer elevation difference as the result of crustal thinning; impact thins the crust by removing the upper part, and subcrustal erosion thins the crust by removing the lower part.

The northern lowlands of Mars contain positive gravity anomalies (mascons) and buried topography (figs. 20 and 22) associated with several impact basins more than 1600 kilometers

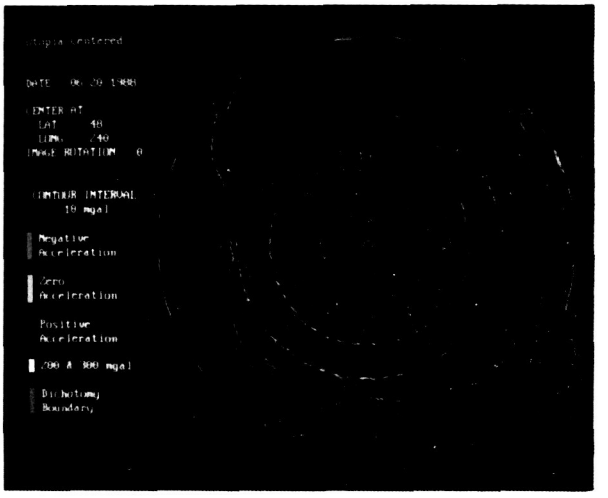

Fig. 20. Gravity anomalies in the Utopia northern lowlands. Dashed circles are estimated positions of two rings of the buried Utopia Basin. Closed red gravity contours within the inner circle indicate a positive gravity anomaly (mascon) associated with this basin. The smaller mascon southwest of Utopia Basin, enclosed within an area of generally low gravity (blue contours), is associated with the Isidis Basin. The intense positive anomaly southeast of Utopia Basin coincides with Elysium Mons, a large, relatively young volcanic pile.

(1000 miles) in diameter. These basins are among the oldest mappable geological features on Mars. Their very existence requires that the Borealis Basin be even older. Thus, if the dichotomy was caused by such a giant impact, the event must have occurred during the first few hundred million years of Solar System history.

In contrast to the giant impact hypothesis are hypotheses explaining the dichotomy as the result of internal processes, such as convective overturn of the mantle, perhaps related to the formation of a dense metallic core very early in martian history. The convective flow is envisioned to have eroded the crust of Mars from below. Gravitational balance is then restored by subsidence of the surface.

These hypotheses imply that the crustal dichotomy was created very early in martian history. However, recent geological and geophysical studies suggest the possibility that the crustal dichotomy was created much later than was formerly believed, during the "middle years" of martian history (2 billion years after the origin of the Solar System). Current studies include detailed analyses of the gravity field in the immediate vicinity of the dichotomy boundary and research on the distribution, topography, and ages of old surfaces buried beneath younger northern lowland plains materials. The initial results of the gravity analyses suggest that there may be a weak negative anomaly coinciding with the highland-lowland boundary even though there is no obvious positive anomaly associated with the central part of the northern lowlands (fig. 21). The geological studies involve inferring the histories of crustal surfaces now partially or even completely buried by young northern lowland plains deposits. These studies point to greater than average tectonic and geomorphic activity about 2 billion years after the presumed ancient time of origin of the crustal dichotomy. Thus, it seems possible that the dichotomy may relate to some as yet not understood internal event that occurred about halfway through the recorded geological history.

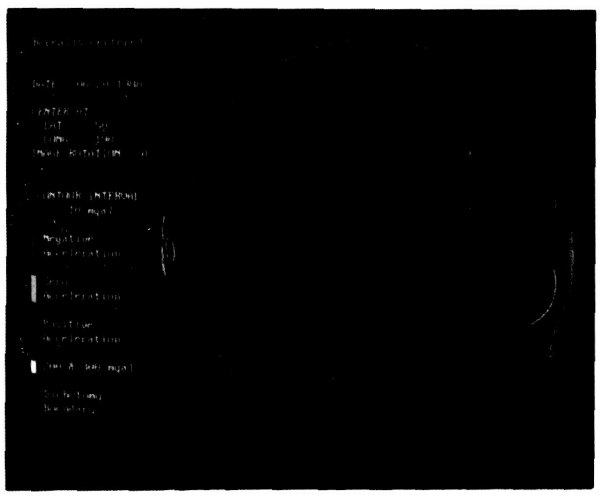

Fig. 21. Gravity anomalies in the Borealis lowlands. The large positive anomalies along the eastern edge of the figure are associated with the relatively young volcanoes of the Olympus Mons and Tharsis regions. The ornamented circle at the center of the figure is the proposed center of the Borealis Basin. There is no mascon at this location.

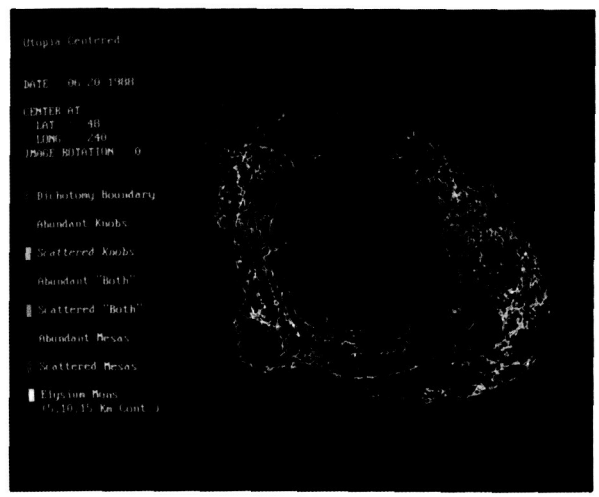

Fig. 22. Distribution of "knobs" and "mesas" in the Utopia Planitia area of the northern plains. These are remnants of the now buried ancient cratered surface. Where these landforms are abundant, the buried ancient surface is close to the present surface; where they are absent, the ancient surface is more deeply buried. The absence of knobs and mesas in the center of the figure defines the central depression of the buried Utopia Basin. This figure centers on the same latitude and longitude as figure 20. Data are from Viking Orbiter images.

Unequivocal, diagnostic evidence capable of proving or disproving either an internal or a giant impact origin for the martian crustal dichotomy has yet to be identified. However, it is common for such evidence to be very difficult to find or to recognize when dealing with fundamental, global-scale planetary characteristics. Present efforts are yielding useful results; the hypotheses are simultaneously being tested against geophysical data and constrained by the geological history of the dichotomy boundary region, using Viking Orbiter data. Better data would help, especially greatly improved elevation control such as is anticipated from the altimeter on the Mars Observer mission. Adequate knowledge of absolute elevations on Mars will permit a major advance in the ability to infer the structure of the martian crust from gravity studies. Absolute elevations will also significantly enhance the ability to interpret structural history by yielding quantitative slope information and the absolute elevation differences between surfaces, especially noncontiguous ones.

Did the Greenhouse Effect Kill the Dinosaurs?

John D. O'Keefe and Thomas J. Ahrens, Seismological Laboratory, California Institute of Technology, Pasadena, CA 91125

This article reports experimental and theoretical evidence that carbon dioxide (CO_2) released by a meteor or comet that struck the Earth 65 million years ago could have doomed many species of plants and animals by dramatically raising the temperature worldwide.

A significant mystery in the evolution of life on Earth has been the massive and rapid extinction of plants and animals, including the dinosaurs, which occurred about 65 million years ago. This event is preserved in the geologic record at the boundary between the Cretaceous and Tertiary periods (the K–T boundary). At many sites throughout the world, the K–T boundary is characterized by a thin layer of clay that contains an abnormally high level of the element iridium. Given that meteorites also exhibit high iridium concentrations and that this unusual chemical signature could have been globally dispersed by meteoritic material ejected into the atmosphere during an impact, many researchers have suggested that a comet or massive meteor may have struck the Earth 65 million years ago. It has further been hypothesized that this impact may have been responsible for the mass extinction.

Most previous studies of the proposed impact event have concentrated on the so-called "nuclear winter scenario," which holds that dust and smoke filled the atmosphere of the Earth after the impact. The dust and smoke blocked much of the sunlight, thereby lowering the temperature at the surface and in the oceans and driving many species out of existence. These studies have always been controversial because others have argued that the dust could not have made the Earth cold enough for long enough periods of time to cause the specific pattern of mass extinction observed in the fossil record.

The present study concentrates on the effects of the gases liberated when a large body strikes the Earth. If this body strikes at a place that contains carbonate-rich sedimentary rocks, large amounts of carbon dioxide (CO_2) would be injected into the atmosphere. Such carbonate-rich sedimentary rocks are found in shallow ocean beds and on dry land that once was under shallow seas. They are absent from the deepest part of the ocean.

To simulate the impact into a carbonate-rich layer, a series of experiments was performed at the Helen & Roland Lindhurst Laboratory of Experimental Geophysics at the California Institute of Technology. These experiments simulated impacts of projectiles at speeds of 4–6 km/s (9,000–13,500 miles/hour) into calcite (limestone) targets. The resultant amount of CO_2 released as a function of pressure (impact speed) was measured. These experimental data were then combined with theoretical calculations to simulate meteors or comets of various sizes striking the Earth on carbonate-rich sedimentary layers of various thicknesses.

Results showed that if a comet with a radius of 50 kilometers (30 miles) were to strike the Earth in an area covered by about a 4-kilometer-thick (2.5-mile-thick) carbonate layer, there would be an immediate 100-fold increase in the amount of CO_2 in the atmosphere. O'Keefe and Ahrens further assume that the rock which has lost the CO_2 remains isolated and thus does not rapidly combine with CO_2. The increase in atmospheric CO_2 from the impact would lead to an increase in the average temperature by about 20°C (36°F) within only 10 days because of the greenhouse effect. (In the greenhouse effect, CO_2 in the atmosphere prevents the heat of the Sun from escaping from the Earth into space, so the Earth heats up; the more CO_2 in the atmosphere, the more heating.) Even in the case of a smaller impact on a thinner carbonate layer, say, a meteor with a radius of 20

kilometers (12.5 miles) landing on a 1-kilometer-thick (0.6-miles-thick) carbonate layer, worldwide temperatures would increase by a still significant 5°C (9°F). The increased CO_2 levels would persist for about 10,000 years.

One can compare these temperature increases to those that many scientists believe will result from a century of fossil fuel burning. Some studies indicate that the greenhouse effect may cause a gradual 2°–3°C (3.6°–5.4°F) increase in the average temperature by the next century. Even such a modest temperature increase may be sufficient to melt a portion of the polar ice caps and to flood coastal cities. An almost instantaneous increase of between 5° and 20°C (9° and 36°F) would have unimaginably dire consequences for all life on Earth.

Marine ecology, for example, would be completely disrupted because higher temperatures in the upper ocean would result in lower concentrations of dissolved CO_2. Without dissolved CO_2, planktons cannot construct their shells. Since planktons are at the base of the major food chain of the oceans, many marine species would be expected to become extinct. This event is exactly what is found in the fossil record. The higher temperature would also disrupt land-based food chains, which might explain the relatively rapid disappearance of the dinosaurs. However, it is noteworthy that this scenario does not lead to an immediate disappearance of many species. This evidence agrees with the recent data indicating that the Cretaceous-Tertiary extinctions, while rapid in a geologic sense, did not happen instantaneously.

Experimental Studies of Vaporization and Magnetic Fields in the Impact Process

Peter H. Schultz and David A. Crawford, Department of Geological Sciences, Brown University, Providence, RI 02912

When an impact occurs on a planetary surface, most of the kinetic energy of the impacting body is transferred (partitioned) into movement that forms a crater, primarily through the excavation of target material. In addition, a fraction of the energy is lost in heating and vaporizing both the projectile and the target. In this study, we report results of experiments on the role of vaporization in the impact process that led to the detection of magnetic fields which we believe were spontaneously generated by the impact.

Over the past two decades, the mechanics of crater formation has been experimentally studied using the Ames Research Center Vertical Gun. Insight into the physics of the impact process is gained by performing experiments under controlled conditions and then systematically changing the controlling variables. For example, shock waves created by an impact pulverize a solid target into a strengthless sandlike state before material is ejected to form a crater. Experiments typically simulate shock-pulverized targets by using loose sand under a variety of impact conditions (projectile size, density, and impact velocity) and environments (atmosphere and gravity).

Studying the effects of impact melting and vaporization requires quite a different simulation. While sand provides a convenient medium for tracing the flow of shocked material created by the impact, its melting and vaporization temperatures are too high for investigations in most laboratories, where impact velocities can achieve 6 kilometers per second (3.1 miles per second). Instead, easily volatized materials have been used to explore phenomena both qualitatively and quantitatively that should occur at much higher impact velocities (15–30 kilometers per second [9.4–18.8 miles per second]) more typical of collisions on the planets. Dry ice (frozen carbon dioxide), ice, and carbonates are convenient and easily obtained. Surprisingly, very little vaporization was observed for vertical (90°) impacts. The Ames Vertical Gun, however, was cleverly designed to permit impact angles in 15° increments from the horizontal to the vertical. When the same experiment was performed at 15°, the intensity of the impact flash was so great that it produced a self-portrait on film with a 35,000 frames per second rate (fig. 23). Moreover, mea-

Fig. 23. Impact of a .25-inch (.635 centimeters) aluminum projectile into dry ice at a velocity of 5.4 kilometers per second (3.375 miles per second). The impact angle is 15° from horizontal. Note the self-luminous vapor cloud. The first frame in the sequence is at the bottom of the figure. Every second frame in a 35,000 frames per second sequence is shown.

surements of the expanding vapor cloud revealed that it contained nearly 50% of the original impactor energy. The ionization inferred from the brilliant cloud prompted measurements to hunt for possible magnetic fields generated during the event.

Spontaneous magnetic fields generated by an impact have long been suspected theoretically (fig. 24), but confirmation in the laboratory has been difficult because previous experiments used naturally occurring rocks (basalts and granites) that required exceedingly high impact velocities for sufficient vaporization and ionization. Observed electromagnetic signals generated during the event could be explained more easily by interactions between the plasma and the ambient terrestrial field than by a magnetic field intrinsic to the impact. Yet, a remnant field of 2500 gammas (10% of the terrestrial field) was found in a very young (less than 1 million years old) impact melt sampled from the floor of a 3-meter (10 feet) diameter crater on the Moon, where the present ambient magnetic field is known to be exceedingly low. In addition, the Soviet Lunokhod-2 rover detected magnetic anomalies associated with 50- to 400-meters (165–1312 feet) diameter craters as it traversed the lunar surface. Theory predicted that a magnetic field should be generated by an impact, and lunar samples confirmed that such fields may be preserved. Previous laboratory experiments, however, failed to confirm the process, and the use of the easily vaporized targets permitted this possibility to be explored.

Simple laboratory measurements of the self-luminous vapor cloud were made with wound copper coils of different sizes acting as radio detectors with different frequency responses. Three types of electromagnetic signals were discovered as the detectors were placed in various locations and orientations: first, a very short-lived (0.3 milliseconds) vertically directed field of about 100 gammas; second, a longer lived (1.5 milliseconds) and larger (2500-gamma) toroidal field; and third, a very long-lived field (20 milliseconds) associated with the expanding luminous vapor cloud. How could a field generated by the impact be distinguished from simple amplification of the preexisting terrestrial field? This ambiguity was resolved by changing the magnetic field environment in two ways. First, a magnetic field much higher than the terrestrial field was applied in the vicinity of the impact and changed in orientation for the same impact conditions. Second, the impact region was shielded from the terrestrial magnetic field (a reduction from 30,000 to 500 gammas). This approach confirmed that an impact-generated plasma indeed compressed the ambient field and was most likely responsible for the long-lived signals. More importantly, neither the short-lived vertical field nor the longer lived toroidal field changed as the magnetic field environment changed. The toroidal field had a maximum strength of 2500 gammas even when the terrestrial field was reduced to only 500 gammas.

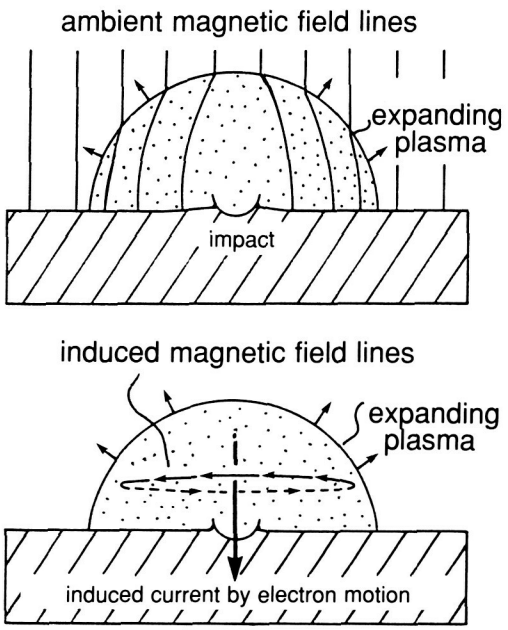

Fig. 24. (top) Distortion and compression of a preexisting magnetic field by an expanding plasma generated during impact. Laboratory experiments confirm this phenomenon. (bottom) Magnetic field produced by an impact-generated plasma with two characteristic temperatures: the electrons and the ions and neutrals. Because electrons initially have a higher temperature and travel faster, an electric current is induced. The resulting magnetic field is generated even without an ambient field and was observed in experiments at the Ames Vertical Gun range.

The vertical and toroidal fields are believed to be spontaneously generated during impact. They arise during the first millisecond after impact because the lighter electrons in the plasma leave at a velocity higher than the heavier ions. The relative motion of the electrons and ions produces a magnetic field shaped like a torus centered on the impact point. The growing toroidal field perturbs the trajectories of the relatively light electrons, thereby producing the other weaker and shorter lived vertical field. The observed intensity of the stronger toroidal field was about the same as the remnant field found in the impact melt sampled from the small lunar crater.

The laboratory experiments hold great promise for helping to understand processes associated with impact vaporization in general and the puzzling young magnetic anomalies observed on the Moon in particular. They may also provide new insight for interpreting processes occurring during late stages of Solar System formation when collisional velocities increased to nearly the same scale and when easily volatized materials were likely impactors or targets. Further experiments will help to explore the phenomena and possible applications.

The Geologic History of Mercury

Paul D. Spudis, Branch of Astrogeology, U.S. Geological Survey, Flagstaff, AZ 86001

One of the primary tools that geologists use to interpret and reconstruct the history of planetary surfaces is photography. This reconstruction includes the recognition of geologic units and their relative age relations to make geologic maps. For planets that are great distances from the Earth, photography can only be obtained from spacecraft. The only such mission to Mercury, Mariner 10, flew by the planet on three separate occasions over a decade ago. This mission returned photographs that covered about 40% of the mercurian surface or a little less than one hemisphere. A cursory examination of the Mariner 10 photographs shows Mercury to be a cratered, Moon-like body. However, a more in-depth examination of the data shows some interesting differences between Mercury and the Moon. A program to make geologic maps of the area of Mercury covered by the data from Mariner 10 has been completed; moreover, a recently compiled synoptic, global geologic map gives new insight into the unique geologic evolution of the planet closest to the Sun.

The surface units of Mercury are divided into categories that reflect both the nature of materials and their relative ages. Material units include crater materials (the products of impact by asteroids and comets), basin materials (much larger scale versions of crater materials), and plains materials (those of a controversial origin). The relative ages of these units are determined by superposition and overlap relations; a crater on top of plains material postdates the plains, whereas one that is filled with plains material predates the plains. With this simple methodology, it is possible to classify all the geologic units on a planet in terms of their relative ages.

The history of Mercury is subdivided into five time periods that are defined by the events that formed recognizable material units. These subdivisions are the pre-Tolstojan (oldest), Tolstojan, Calorian, Mansurian, and Kuiperian (youngest) Periods (fig. 25).

The pre-Tolstojan Period on Mercury witnessed the formation of the planet; the global differentiation that produced a crust, mantle, and core; and the formation of heavily cratered, rugged highlands. The new mapping of Mercury has revealed that many large, ancient, multiring basins formed on the planet during this period; they are very difficult to detect because they have been largely covered by a younger, extensive, rough-textured unit called the intercrater plains. The intercrater plains are of global extent, appear to cover large regions of ancient, heavily cratered

Fig. 25. "Snapshot" views of the geology of Mercury at three separate times in its history. The left view shows the surface of Mercury near the end of the pre-Tolstojan Period, about 4 billion years ago; the widespread highland intercrater plains (brown) have largely obliterated the ancient cratered terrain. The middle view shows Mercury about 3.9 billion years ago, immediately after the impact that formed the giant Caloris Basin (upper left). The view on the right shows the current geology of Mercury; except for widespread smooth plains emplaced about 3.8 billion years ago (pink), the surface of Mercury is largely unchanged from its state immediately after the Caloris Basin impact.

terrain, and were apparently emplaced within a narrow time frame.

The next period, the Tolstojan, began with the large impact that formed the Tolstoj Basin (510 kilometers in diameter). This impact basin, in contrast to the ancient ones previously mentioned, still displays a lineated ejecta blanket of material thrown out of the basin cavity. Numerous craters of the Tolstojan Period have been recognized, but as the high-impact flux of the early bombardment declined, increasingly fewer craters were formed. The impact that formed the giant Caloris Basin (1340 kilometers in diameter) marked the beginning of the Calorian Period; this basin, which dominates one hemisphere of Mercury, was the last major impact basin to form on that planet. The impact was so great that seismic waves generated by it formed an unusual hilly terrain at the point on the planet opposite the Caloris Basin.

The widespread (approximately 40% of the imaged hemisphere) smooth plains of Mercury were emplaced during the early Calorian Period. A major debate has focused on their origin. These plains, like the dark lunar maria, cover vast regions of the mercurian surface. Unlike the lunar maria, which we know (from Apollo sample results) to be of volcanic origin, the smooth plains of Mercury are relatively bright and show little contrast with the average brightness of the rough cratered terrain. This relation has led some workers to question the volcanic origin of the mercurian smooth plains, suggesting instead that they are a part of the Caloris Basin ejecta blanket. The new global mapping of Mercury, however, indicates not only that the smooth plains are distributed all over the imaged hemisphere of Mercury (in contrast to early interpretations that suggested an intimate association with the Caloris Basin) but also that the smooth plains are significantly younger than the Caloris Basin ejecta, as determined from the number of craters per unit area. Thus, a volcanic origin for the smooth plains of Mercury is indicated; these plains were probably emplaced as vast sheets of basaltic flood lavas, their brightness a reflection of an iron and titanium content generally lower than that of the lunar mare basalts.

Since the flood lavas of the smooth plains were emplaced, only an occasional impact crater has formed on Mercury. The last two periods of mercurian history are the Mansurian, which includes craters only slightly degraded, and the Kuiperian, which includes only the freshest, rayed craters on the planet and extends to the present day.

Because there are no rock samples from Mercury, we cannot determine directly the absolute ages of these events in mercurian history. However, the Apollo lunar samples permit us to determine the ages of comparable events on the Moon; this understanding of lunar geologic history permits us to estimate the absolute ages of mercurian surface units. Mercury probably formed at the same time as the other planets of our Solar System, about 4.5 billion years ago. The early differentiation of Mercury probably occurred soon afterward; the lunar analogy suggests that the mercurian pre-Tolstojan Period lasted from 4.5 to approximately 4 billion years ago. The time between the Tolstoj Basin impact and the Caloris Basin impact (the Tolstojan Period) was probably very short; the end of the heavy bombardment on the Moon occurred about 3.9 billion years ago, the likely age of the Caloris Basin. On the Moon, flooding by basaltic lavas then continued for the next billion years (3.9–3 billion years ago); density data from the impact crater for the mercurian smooth plains show a much more restricted time interval of emplacement. The best estimate is that mercurian volcanism ceased about 3.8 billion years ago. Only an occasional impact crater has formed since that time, suggesting that Mercury completed most of its surface evolution about the same time that life emerged on Earth. Thus, Mercury is a fossilized planet and its history helps to shed light on the earliest events in planetary geologic history.

Outer Solar System

Shapes and Internal Structures of Satellites

Stanley F. Dermott and Peter C. Thomas,
Center for Radiophysics and Space Research,
Cornell University, Ithaca, NY 14853

The masses and radii of all the planets in the Solar System, including Pluto, are now known with sufficient accuracy that we have useful measures of their mean densities. Thus, we know that the terrestrial planets have densities consistent with those of rock-iron mixtures, whereas the major planets must contain large complements of light gases. To go beyond these statements to determine the internal structures of the planets (i.e., how mass is radially distributed in the interiors), we require more information than the mean densities alone can provide. For the Earth and Moon, seismic information has enabled us to construct detailed models of their interiors. We are now confident, for example, not only of the size and density of the Earth's liquid iron core but also of the radius and density of its solid inner core. Seismic information is unavailable for Mercury, Venus, and Mars; very little is known with confidence about the interiors of these bodies, and we can only speculate that their internal structures are similar to those of the Earth.

The outer planets have deep fluid mantles and, apart from possible small solid cores, may be fluid throughout. Rotational forces have deformed these bodies into oblate (flattened) spheroids. Because the bodies are in hydrostatic equilibrium (in which inward gravitational attraction everywhere balances outward pressure), their moments of inertia and other constraints on their internal structures (i.e., high-order gravitational moments) can be determined. Their observed flattenings or, equivalently, the departures of their gravitational fields from spherical symmetry are pertinent to determining internal structures of planetary bodies. We have shown that one of these techniques can be usefully applied to some of the satellites of Saturn and Uranus, and our work has led to the first determination of a possible internal structure for a satellite in the outer Solar System, that of the saturnian satellite Mimas.

The overall large-scale shape of the physical surface of a planetary body can be determined by direct imaging. We have demonstrated this accurately by using limb profiles from the six best Voyager images of Mimas to determine its three-dimensional shape. Correction of image distortions allows coordinates on the limbs to be located with an accuracy of approximately one-half picture element: about 0.5 kilometers (0.3 miles) for the two best images and between 1 and 2 kilometers (0.6 and 1.2 miles) for the other images. Because Mimas is distorted by both rotational and tidal forces, the expected equilibrium shape is that of a triaxial ellipsoid, which is a body whose three mutually perpendicular axes are of different lengths. Ellipses fit to the limbs show that the shape of the satellite is indeed ellipsoidal. One of the images is shown in figure 26, while deviations from both the best-fit ellipsoid and the mean sphere for three of the best images are shown in figure 27. Mimas is the smallest satellite in the Solar System whose shape is well represented by a triaxial ellipsoid.

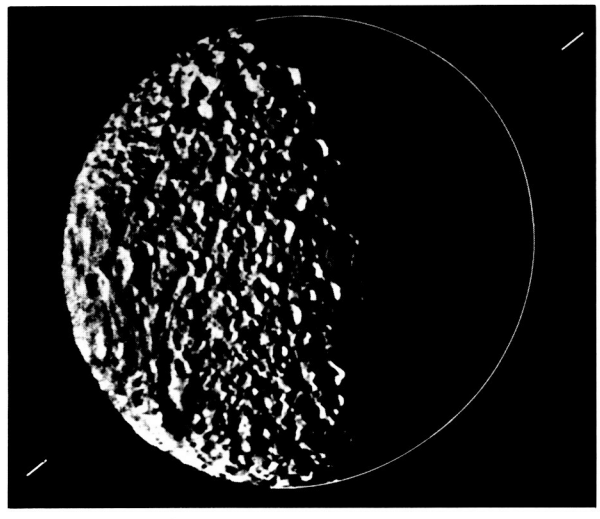

Fig. 26. The best Voyager image of Mimas. Taken from a range of 122,000 kilometers (76,250 miles), it has a resolution of 1.1 kilometers per picture element. The projected ellipse fitted to the limb was determined from the best-fit triaxial ellipsoid. The major axis of this ellipse is oriented, as predicted, about 1° away from the direction to Saturn.

The ratio of the differences of the principal axes of the best-fit ellipsoid, $(b-c)/(a-c)$, is 0.27 ± 0.04 and consistent with the predicted ratio for a synchronous satellite in hydrostatic equilibrium. (A synchronous satellite is one in which the period of rotation equals the period of revolution.) Using the satellite mass determined by celestial mechanics and a theory for the ellipsoidal figure of equilibrium, we deduce that the satellite has a mean radius $<R>$ of 198.8 ± 0.6 kilometers (124.3 ± 0.4 miles) and a mean density of 1.137 ± 0.018 g/cm^3 (0.041 ± 0.001 pounds per cubic inch) and that the difference between the long and the short axes, $a-c$, is 16.9 ± 0.7 kilometers (10.6 ± 0.4 miles). From the known mass and our measured mean radius, we calculate that the expected value of $a-c$ for a comparable, but homogeneous, satellite in hydrostatic equilibrium is 20.3 ± 0.3 kilometers (12.7 ± 0.2 miles), significantly greater than the observed value. We conclude from this that the satellite is not homogeneous and may be differentiated.

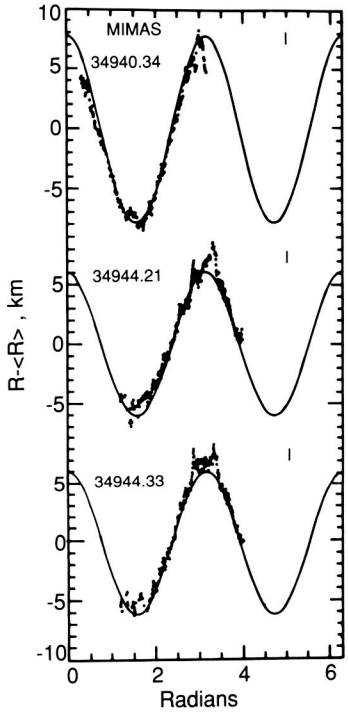

Fig. 27. Limb coordinates from the three best images of Mimas plotted as distances from a circle of radius $<R>$ compared to the predicted limb positions of the best-fit ellipsoid of 210.3, 197.3, and 192.5 kilometers (131.4, 123.3, and 120.3 miles). Given the axes of the best-fit ellipsoid, we are able to predict both the amplitude and the phase of the solid curve. The scale bars denote the sizes of a picture element in each image.

This result is in many ways very surprising, and caution is needed in its interpretation. The satellite may have an overall shape consistent with that of a relaxed body in hydrostatic equilibrium, yet the surface of the satellite is saturated with craters that appear quite rigid and show no signs of relaxation. If we assume that the satellite is a differentiated body, we calculate that it has a rocky core of radius 87 ± 10 kilometers (54 ± 6 miles) and that the material outside the core has a mean density of 0.96 ± 0.08 g/cm^3 (0.035 ± 0.003 pounds per cubic inch), consistent with that of uncompressed but moderately contaminated water-ice. If the matrix of the mantle material is water-ice, the silicate mass fraction of Mimas is 0.27 ± 0.04, which indicates that the satellite is markedly deficient in rock in comparison with solar composition. An alternative interpretation of our data is that the material of Mimas has a solar composition of ice and rock and is undifferentiated but is highly porous down to a depth determined by the crushing strength of cold ice. However, this interpretation requires that the surface porosity of the satellite be very high, between 20% and 60%.

Our major conclusion, that Mimas is probably a differentiated satellite, raises a number of cosmogonically important questions. How and when did the satellite differentiate? When did the satellite adopt the observed shape? And, what was the orbital radius of the satellite at that time? What are the implications of the observed lack of silicate rock? Is it possible that the satellite is not fully relaxed but retains a fossil shape consistent with a different dynamical state? All of these questions are likely to spark lively debates. Further input to these questions will come from careful measurements of the shapes of other satellites. In the near future, we hope to obtain useful data on the shapes of the saturnian satellites Enceladus and Tethys and the uranian satellites Miranda and Ariel.

Crystal Structure and Density of Helium to 233 kilobars

H. K. Mao, Y. Wu, A. P. Jephcoat, R. J. Hemley, and P. M. Bell, Geophysical Laboratory, Carnegie Institution of Washington, Washington, DC 20008

W. A. Bassett, Department of Geological Sciences, Cornell University, Ithaca, NY 14853.

For years, the interiors of the giant, gaseous planets of our Solar System have been shrouded in obscurity. Theories about the interior structures of these bodies always possessed a speculative quality because accurate experiments that create planetary interior conditions in the laboratory were not possible. Since the giant planets are mostly made up of hydrogen (~70%) and helium (~30%), understanding the behavior of these elements at planetary interior temperatures and pressures [from 200 kilobars (1 kilobar = 1000 times atmospheric pressure) and 2200°C (3,992°F) in Uranus and Neptune to 40,000 kilobars and 15,000°C (27,032°F) in Jupiter] is key to the construction of compositional evolutionary models. Important information includes the equations of state and phase diagrams of hydrogen and helium. Equations of state specify density as a function of temperature and pressure, while phase diagrams specify melting curves, crystal structures, the phase separation of helium and hydrogen, and the metallization of hydrogen.

In the past, because of experimental difficulties, properties of helium and hydrogen at the conditions of planetary interiors almost entirely depended on theoretical calculations. Without the basis of experimental measurements, the validity of theoretical calculations were untested, and the choice of various theories were uncertain. With the development of the diamond-anvil high-pressure cell, pressures of 600 kilobars in helium and 1470 kilobars in hydrogen have been reached at the

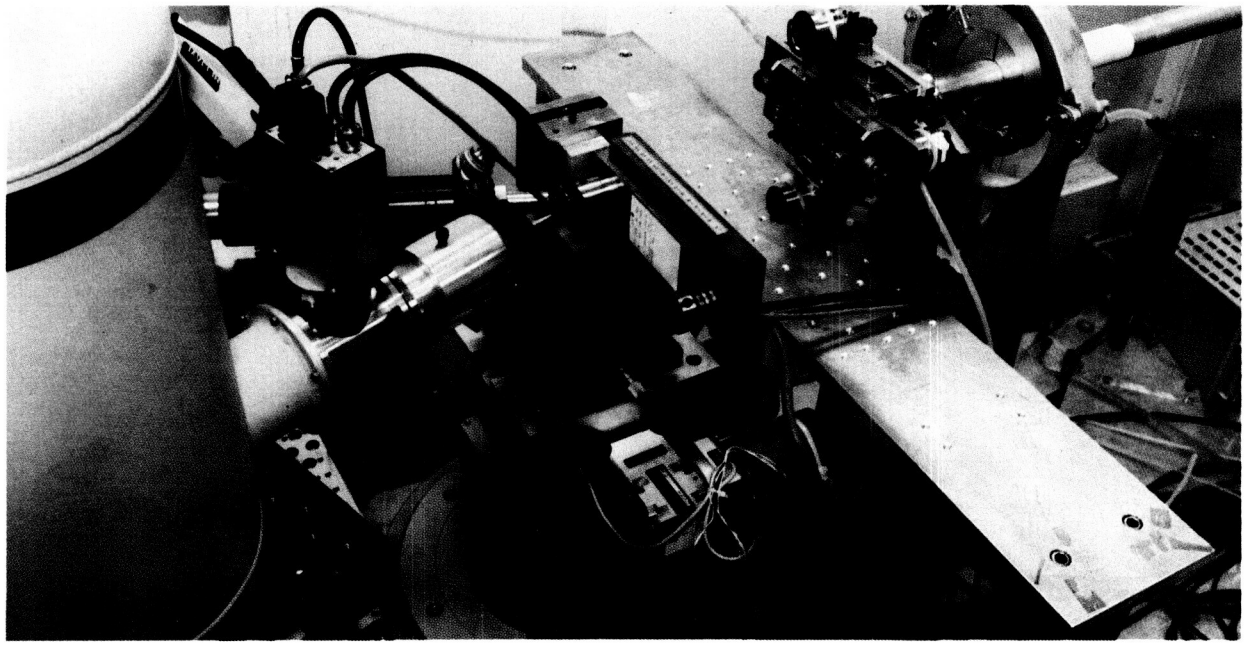

Fig. 28. Photograph showing the apparatus used for X-ray diffraction experiments with the diamond-anvil cell at beamline X7A of the National Synchrotron Light Source, Brookhaven National Laboratory. The large cylindrical tank (dewar) at left contains liquid nitrogen for cooling the germanium detector. The diamond-anvil cell is situated at center on top of a goniometer and can be positioned in the X-ray beam with motor drives (shown in blue). The incident X-ray beam from the synchrotron ring enters the enclosed experimental area from the right and is collimated by a remote-controlled slit system.

Geophysical Laboratory. However, these studies did not give a direct answer to crystal structure and density. X-ray diffraction is the most accurate and reliable method of determining these properties because it is possible to identify the phase directly at a specific pressure and temperature.

Even though high-pressure measurement techniques have continuously advanced, direct measurements of the crystal structure of solid helium have been limited to lower pressures (a few kilobars) because helium has both an extremely low scattering cross-section (atomic number $Z = 2$) and a high compressibility, which lead to small sample volumes at high pressures. Since the scattered X-ray intensity is proportional to the sample volume and the square of the atomic number, the signal of helium is exceedingly weak and is easily lost in background noise.

Recently, a new technique was developed at the Geophysical Laboratory for measuring X-ray diffraction from single crystals of low-Z materials in a diamond-anvil cell at high pressure. Such measurements are made possible by using high-intensity synchrotron radiation to obtain a strong signal from the sample, by narrowly collimating the incident and diffracting X-ray beams to reduce background noise and by using energy-dispersive diffraction techniques with polychromatic (white) radiation (fig. 28).

With the above technique, X-ray diffraction measurements on solid hydrogen to 265 kilobars were obtained. Similarly, X-ray diffraction was applied to determine the equation of state and phase diagram of solid helium at high pressures. Pressures were measured by ruby fluorescence excited by the X-ray beam. Excellent signal to noise ratio was observed. Diffraction patterns at four pressures from 156 to 233 kilobars at 300 K (80°F) were taken. Throughout this range, helium exhibited the hexagonal close-packed crystal structure, which is the same structure exhibited by hydrogen at these conditions. Interestingly, theoretical calculations had predicted that helium would exhibit a different crystal structure than that observed. The equation of state of helium was discovered to be surprisingly "soft," indicating that helium is highly compressible (fig. 29). From 156 to 232 kilobars helium exhibited a 15% change in density from 1.013 grams per cubic centimeters to 1.158 g/cm^3, (0.037 to 0.042 pounds per cubic inch), making it the most compressible known material in that pressure range.

These experiments have helped to resolve the controversy over the crystal structure and equation of state of helium. They have also pointed to the need for better theoretical calculations to predict the behavior of materials at high pressures. More accurate theories may be generated to reproduce the new data. Understanding the atomic-level basis for the properties of condensed helium (in electronic terms one of the simplest of atoms) will also provide an important foundation for moving on to more complicated materials. These improved theories will also facilitate the study of planetary interiors. As studies of hydrogen and helium move on to higher pressures, the diamond-anvil cell will act as a window through which we can probe the depths of the giant planets.

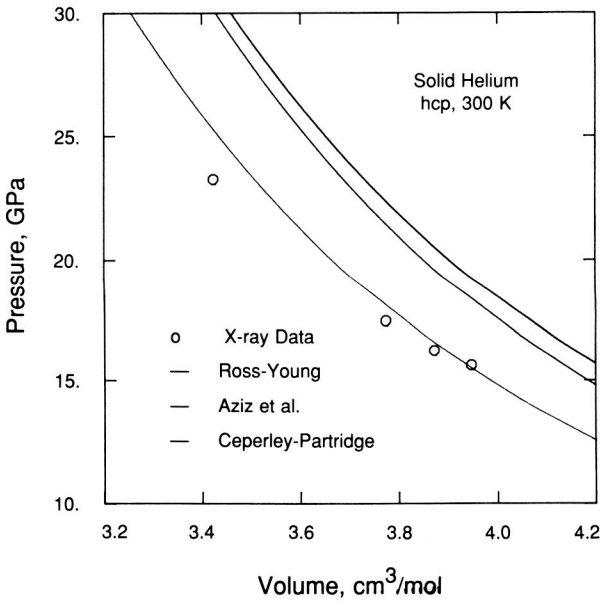

Fig. 29. Pressure-volume data for solid helium determined by synchrotron radiation methods to 233 kilobars. The solid curves are several theoretically predicted equations of state at room temperature based on different potentials.

Vacuum Weathering—A Newly Recognized Planetary Surface Process

Douglas B. Nash, Jet Propulsion Laboratory, Pasadena, CA 91101

A serendipitous discovery in the laboratory during studies of the effects of irradiation on sulfur has led to a new way of thinking about the effects of a vacuum environment on the surface properties of small Solar System bodies such as icy satellites and comets. The experiments were initially undertaken to study the surface properties of Jupiter's satellite, Io, which was shown to exhibit active sulfur volcanism during the Voyager flybys. During the experiments, it was discovered that the surface of freshly frozen sulfur is drastically modified by the effects of vacuum evaporation. These "vacuum weathering" effects are caused by differential sublimation of two different molecular phases that make up the solid material and that have very different sublimation rates. For sulfur, which is composed of ring and chain molecules that by exsolution form a distinct grain intergrowth structure, the ring sulfur has a much higher sublimation rate than the chain sulfur. As a result, under continuous vacuum pumping, the surface of sulfur gradually becomes depleted in ring sulfur, enriching the surface with a residual layer of chain (polymeric) sulfur. The chain sulfur forms a highly porous, extremely fine-grained fluffy material that reaches a thickness of about 1 millimeter at vacuum maturity.

This process produces major changes in the visible and ultraviolet (UV) reflectivity of the surface of sulfur: in the visible wavelengths (fig. 30), the surface brightens and the color changes from an original yellow, tan, or brown (depending on the maximum temperature and thermal history of the sulfur during its prefreeze molten state) to white—the color it takes on when the weathering process has gone to a "vacuum mature" stage. The corresponding spectral reflectance changes are shown in figure 31: the shoulder of the spectral absorption edge (that causes normal sulfur to appear yellow) shifts in wavelength from 0.52 to 0.46 micrometer;

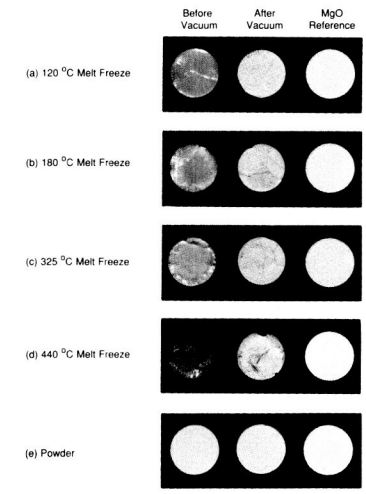

Fig. 30. Color of frozen sulfur samples before and after vacuum weathering in the laboratory. Each pair of samples is compared to fresh smoked MgO (which is pure white) for color reference.

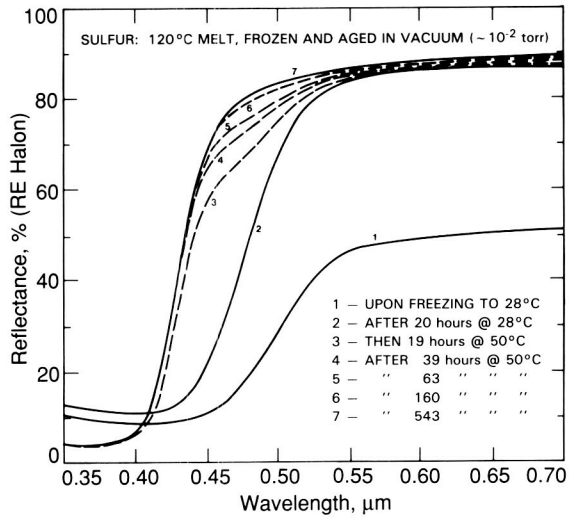

Fig. 31. Ultraviolet-visible reflectance spectra showing how the surface spectrum of solid sulfur varies progressively with time after freezing and during continuous vacuum pumping.

at the same time, the UV absorption trough shifts from near 0.45 to 0.39 micrometers, and the overall UV reflectivity near 0.35 micrometer decreases from about 12% to 3% or less.

The rate of this vacuum weathering process is highly dependent on the temperature of the surface because of the steep temperature dependence of the vapor pressure curve of volatile substances such as sulfur. For temperatures near 300 K (typical of volcanic hot spots on Io's surface), the sublimation rate is on the order of 10^{14} sulfur atoms per square centimeter per second, which is equivalent to an erosion rate of about 1 millimeter/year. The sublimation rate increases by an order of magnitude with a temperature increase of about 20 K.

At these rates, the changes in appearance of sulfur on Io's surface will be large on time scales of only tens to hundreds of hours. Because the corresponding spectral and textural changes that are possible in freshly emplaced sulfur lava deposits on Io are large, their detection by telescopic observation is possible and would signal that active volcanic resurfacing of Io may be occurring.

A thorough understanding of this newly recognized vacuum weathering process—as summarized in figure 32 for sulfur on Io's surface—may have application for deciphering the observed properties of other condensed volatile surfaces of planetary bodies. Examples of such bodies are the Galilean satellites Europa and Ganymede (which exhibit contaminated water-ice-rich surfaces), Neptune's satellite Triton (which may have a surface containing a solid mixture of methane and nitrogen) and comets that contain sulfur-laden ices. Continued laboratory experimentation and theoretical modeling of the vacuum weathering process may lead to further insight into the nature and mode of origin of the surface properties of condensed Solar System objects.

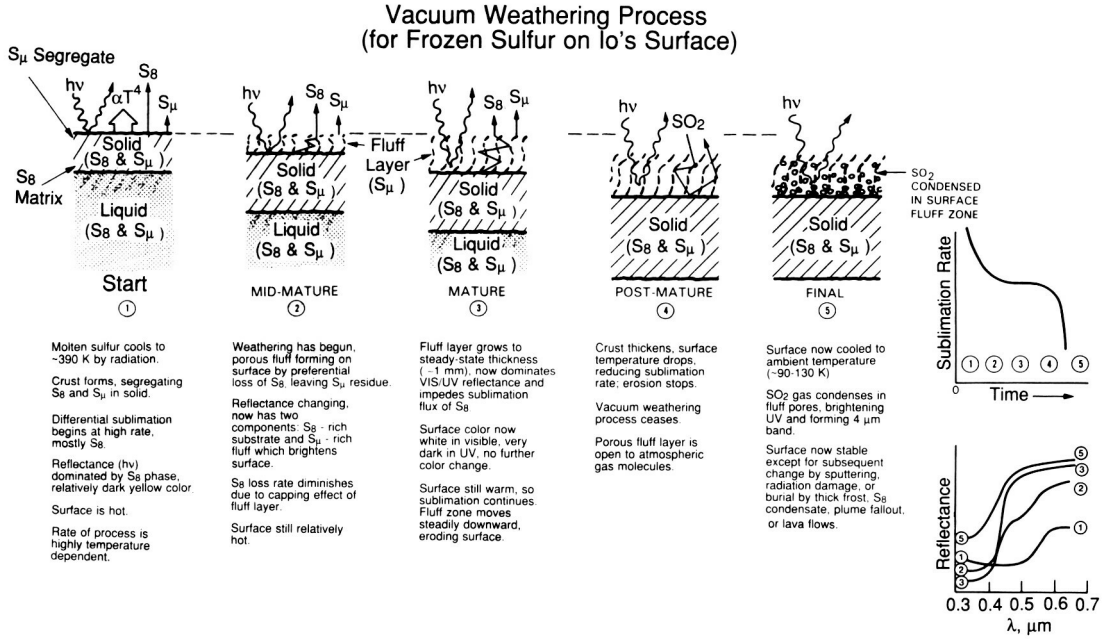

Fig. 32. Schematic representation of the postulated vacuum weathering process on the surface of frozen sulfur on Io. Process starts on the left; time progresses toward right from 1 to 5.

The Nature of the Interior of Uranus Based on Studies of Planetary Ices at High Dynamic Pressures

W. J. Nellis, D. C. Hamilton, N. C. Holmes, H. B. Radousky, F. H. Ree, and A. C. Mitchell, Physics Department and Institute of Geophysics and Planetary Physics, Lawrence Livermore National Laboratory, University of California, Livermore, CA 94550

M. Nicol, Department of Chemistry and Biochemistry, University of California, Los Angeles, CA 90024

The Voyager 2 spacecraft showed that Uranus has a strong and unusual magnetic field, which varies markedly around the surface of the planet. The maximum surface value is 1.1 gauss (G), twice the value of the Earth's field, while the minimum field is only 0.1 G. In addition, the axis of symmetry of the magnetic field is tilted 60° from the axis of rotation, in comparison with a tilt of about 20° for the Earth's field. This surprising Voyager 2 data stimulated our laboratory measurements for planetary materials at conditions in the interior to derive planetary models consistent with the observations.

Prior to Voyager 2, Uranus was thought to consist of three layers: an outer hydrogen-helium (H_2-He) gas layer; a middle layer composed mostly of water (H_2O), ammonia (NH_3), and methane (CH_4), collectively called the "ices"; and an inner rocky core. Because the temperatures inside Uranus are calculated to reach up to several 1000 K, the ices are actually in the fluid phase throughout much of the interior. The large surface magnetic field means that the field must be generated closer to the surface than was previously thought. The most likely source is the slow convective motion of ions formed from H_2O and NH_3, for example. Voyager 2 data also gave a better picture of the mass distribution inside Uranus. These data did not allow us to determine whether Uranus has an iron core but did indicate that if it has one, it is quite small, say, one-tenth the planetary radius or less. At this depth, any contribution from an iron core to the measured surface magnetic field would be negligibly small. Thus, the key to understanding the portion of the planet where the magnetic field is generated lies in studying the planetary ices.

Theoretical work by David J. Stevenson of California Institute of Technology, Pasadena, CA, indicates that the magnetic field is generated at depths near 0.7 of the radius (about 5000 miles or 8000 kilometers). The conditions at this depth range up to 0.5–1 megabars (500,000–1,000,000 atmospheres) and several 1000 K. For this reason we have measured electrical conductivities and equations of state of NH_3, CH_4, and a mixture we call "synthetic Uranus" up to 0.75 megabars and 5000 K (8540° F). Data for H_2O were measured previously. Both the conductivity and the equation of state data address the question of the chemical composition in the interior. The conductivity data are needed for magnetic field calculations, and the equation of state data are needed for calculations of mass distribution. At the high densities and temperatures of the interior, molecules decompose and react. For this reason, the synthetic Uranus mixture was studied to determine whether properties of a mixture of the ices differ significantly from the properties of the individual ices. Synthetic Uranus is hydrogen-rich because Uranus has an average density of only 1.2 g/cm^3 (0.043 pounds per cubic inch) and has near-cosmological abundance ratios of oxygen to carbon and oxygen to nitrogen. It is an H_2O-rich solution of H_2O, NH_3, and C_3H_8O. Because CH_4 is immiscible with H_2O and NH_3 at ambient pressure and temperature, while C_3H_8O is miscible, the latter was used to achieve the appropriate carbon composition.

High pressures and temperatures are achieved by the shock compression of liquid specimens. A strong shock wave is generated by the impact onto a liquid specimen holder of a metal plate at a

velocity as high as 7 kilometers per second (4.4 miles per second). The impact plate is accelerated to high velocity by a two-stage light-gas gun. In each experiment, the high shock pressures destroy the specimen holder, which is often cryogenic in nature because of the low-temperature boiling points of some of the liquid specimens.

The electrical conductivity of shock-compressed liquid NH_3, CH_4, and synthetic Uranus are plotted versus shock pressure in figure 33. Previous data for water are included for comparison. The temperature measurements show that conductivities are in the range of 1500–5000 K (2240–8540° F). The conductivities of synthetic Uranus, H_2O, and NH_3 all approach 20 $(ohm\text{-}cm)^{-1}$ above 0.4 megabars (400,000 atmospheres) providing an upper limit on the value of conductivity that can be used in magnetic field calculations. The small conductivity of CH_4 means that it probably does not contribute to the field. Although the detailed composition of Uranus remains uncertain, electrical conductivity is weakly sensitive to chemical composition at conditions that correspond to those where the magnetic field is generated—a good result for modeling the magnetic field. Dynamo theory for magnetic fields and our measured electrical conductivities indicate that the convective motions that cause the magnetic field are a factor of 10^6 smaller than the velocity of rotation.

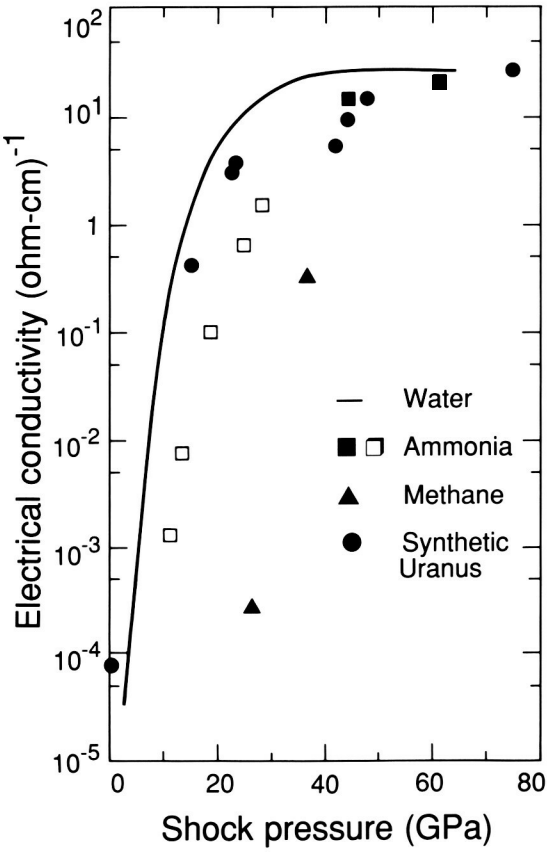

Fig. 33. Electrical conductivity versus shock pressure for planetary fluids. Solid symbols are present work. Solid curve is smooth curve through available water data. At 0.4 megabars (= 40 Giga pascals = 400,000 atmospheres), temperatures in these fluids are 2600 K (4220° F) in water, 2800 K (4580° F) in synthetic Uranus, 3100 K (5120° F) in ammonia, and 4100 K (6920° F) in methane.

These results, the results of previous shock compression experiments, and the results of theoretical analyses by others allow us to develop a physical picture of the deep interior of Uranus. The surface region is quite cold [60 K (−350° F)] and consists of fluid molecular hydrogen and

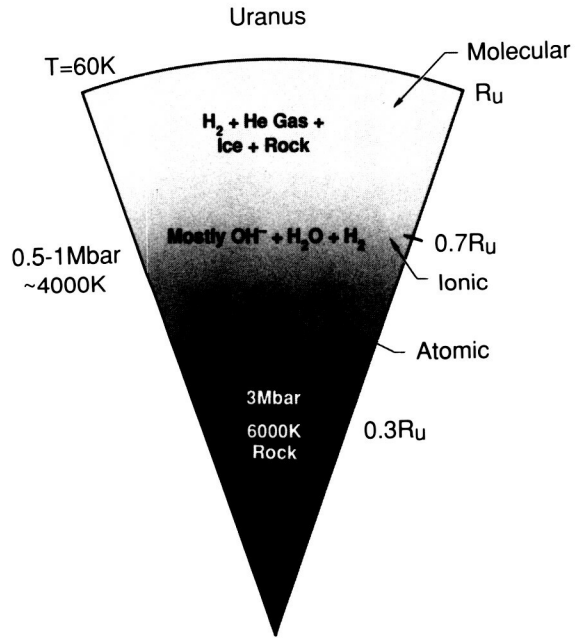

Fig. 34. Schematic illustration of interior of Uranus combining results of shock wave experiments and representative interior model of David J. Stevenson (California Institute of Technology, Pasadena, CA).

helium with frozen pieces of H_2O, NH_3, and CH_4 ices and rocks. As depth increases, the temperature rises and the ices melt but remain molecular. At still greater depths, pressures, and temperatures, molecules dissociate into electrically charged ions, such as OH^-, which generate the magnetic field by slow convective motions. The major contribution to the field comes from near 0.7 the planetary radius (a depth of 5000 miles or 8000 kilometers), where the pressures are 0.5–1 megabars (500,000–1,000,000 atmospheres), and the temperature is about 4000 K (6740° F). At still greater depths, pressures, and temperatures, all molecules and ions are expected to dissociate into monatomic species. These H–O–C–N species and rocks are extremely stiff and incompressible, indicating that the high interior pressures are not effective in compressing matter, which contributes somewhat to the large volume of Uranus. This physical picture and the planetary model of David Stevenson are illustrated in figure 34.

It is interesting to speculate on the nature of the stiff, monatomic H–O–C–N species. If the elements separate, then we expect the diamond phase of carbon to form, as well as hard, diamondlike phases of oxygen, nitrogen, and perhaps hydrogen. Other possibilities include novel chemical compounds and alloys or mixtures of hydrogen, oxygen, carbon, and nitrogen. Some of these phases might have high melting points and condense out of the solution of the fluid "ice" mixture. All of the materials are expected to be very light and stiff and, in this sense, diamondlike.

Ring Arcs of Neptune: Observations and Theoretical Models

Philip D. Nicholson, Department of Astronomy, Space Sciences Building, Cornell University, Ithaca NY 14853

Prior to 1977, Saturn was considered unique among the planets in possessing a ring system. As a subject of both observational and theoretical study since their discovery in 1610 by Galileo and their correct description by Huygens in 1655, the rings of Saturn have made major contributions to both astronomy and physics. Among the many possible examples of contributions, we may cite James Clerk Maxwell's prize essay on the orbital instability of solid rings presented at Cambridge University in 1857 and James Keeler's observation at Lick Observatory in 1895 of the differential Doppler shift across the rings, which confirmed Maxwell's concept of the rings as an ensemble of innumerable individual particles, each in orbit about Saturn in accord with Kepler's laws. Perhaps more important, however, has been the role that the rings play as a laboratory model in the study of other, more inaccessible astrophysical disk systems. These include spiral galaxies; the disks of extremely hot gas around neutron stars or black holes, which are inferred to fuel the intense bursts of X-rays and gamma-rays observed by orbiting telescopes; and the protosolar nebula, the gas and dust from which our own Solar System is believed to have formed 4.5 billion years ago.

By 1979, however, first Uranus and then Jupiter had joined the group of ringed planets: nine narrow, opaque rings were discovered about Uranus in 1977 by James Elliot (Massachusetts Institute of Technology, Cambridge, MA) and his colleagues during observations of a stellar occultation by that planet, while the broader, diffuse jovian ring system was first imaged by the Voyager 1 spacecraft and soon after by its sister probe Voyager 2. Although the ring systems of Jupiter, Saturn, and Uranus were found to be quite different in character, the question immediately arose of whether Neptune might also possess one or more rings. On the plus side of the argument were the considerable similarities shown by these four giant gas planets in many other respects (mass, density, atmospheric composition, etc.), while the only substantial negative argument was Neptune's rather odd satellite system. Whereas the other three jovian planets possess systems of a half-dozen or more regular, equatorial satellites (the inner two or three of which seem to be intimately related dynamically to the creation or maintenance of the ring systems), Neptune's only close satellite, Triton, is in a highly inclined, retrograde (reverse) orbit. (Nereid, the other neptunian satellite, is very small and located at a much greater distance from the planet.)

The first serious attempts to detect a neptunian ring system were made in May 1981, when three groups of observers set out to observe stellar occultations by Neptune from telescopes in Australia, Chile, and Arizona. Such events, which are comparatively rare astronomical phenomena, occur when the planet's orbital motion carries it in front of a star. The light from the star then provides an extremely high-resolution probe of the planet's atmosphere and of any material which may be in orbit around it. The advantages of this technique lie in its spatial resolution (about 1 kilometer at Neptune) and in the fact that a direct measurement of the optical depth of any ring material is made. (The term 'optical depth' refers to the fraction of starlight absorbed or scattered by the ring.) By virtue of its high resolution, a stellar occultation is capable of revealing rings far too narrow to be photographed directly, at least from Earth-bound telescopes. The compensating disadvantages lie in the very limited region of space around a planet probed during any one occultation and in the insensitivity of the techniques to diffuse material such as the tenuous dust discovered in Voyager images to envelope the narrower uranian rings.

The 1981 observations by James Elliot, Philip Nicholson, and their collaborators failed to pro-

vide any convincing evidence of neptunian rings, but Harold Reitsema and William Hubbard (both at University of Arizona, Tucson, AZ), observing another occultation in Arizona, reported the chance discovery of a new satellite of Neptune, designated 1981N1. Observations of a subsequent occultation in June 1983, coordinated at a far-flung network of telescopes around the Pacific Basin, also failed to yield any evidence of rings (or new satellites). In July 1984, however, William Hubbard and Andre Brahic (University of Paris), together with several colleagues, observed an occultation of a bright star from three telescopes in Chile, separated by up to 100 kilometers (63 miles). At all three stations, an unambiguous ringlike occultation was observed, with a width of ~ 15 kilometers (9 miles) and a normal optical depth $\tau \simeq 0.14$. The most puzzling feature of these observations, however, was that the 'ring' passed only once across the star; evidently, no ring material (or at least much less) existed at the point on the other side of the orbit where a circular ring should have again blocked the starlight. It was concluded that the event must have been the result of an arc of material, 15 kilometers wide but at least 100 kilometers long, in orbit around Neptune. This explanation can also account for the failure to detect such material during previous occultations and possibly for the supposed satellite, 1981N1.

To date, a total of 21 stellar occultations by Neptune have been observed at one or more sites on Earth, with campaigns having been organized in 1985 and 1987 at four to six telescopes for simultaneous worldwide observations. Observers from the United States, Canada, France, Australia, and South Africa have participated in an excellent example of international scientific coop-

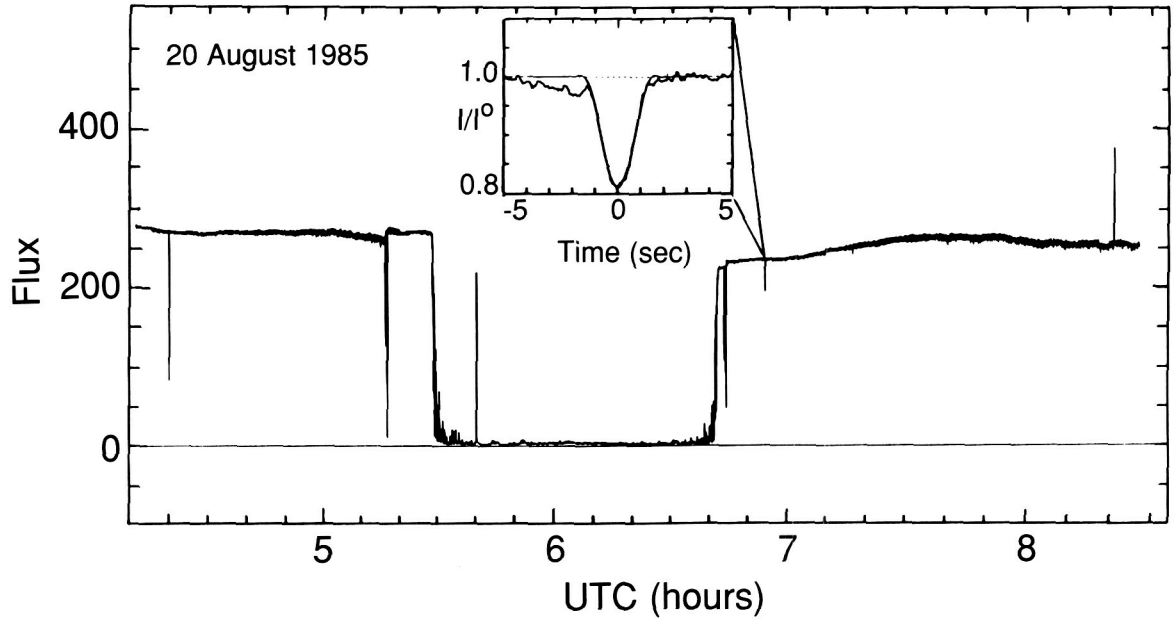

Fig. 35. Light curve obtained at the Infrared Telescope Facility during the stellar occultation by Neptune on August 20, 1985. The planet occulted the star from 5:28:18 to 6:41:17 Universal Time (UT), and shortly afterward a single arc occultation was observed at 6:53:49.3 UT. (All other features in the light curve are due to instrumental or timing checks, while the slow increase in signal after planetary emersion is due to obscuration of the telescope's field of view by the dome shutter.) The arc event is shown at a larger scale in the inset, where the data have been averaged to a resolution of 0.1 seconds corresponding to a radial distance of 1.6 kilometers (1 mile) in Neptune's equatorial plane. The smooth curve is a diffraction model fitted to the observations, with the arc parameters given in table 1 and an equivalent stellar diameter of 8.3 kilometers (5.2 miles), as projected at the distance of Neptune (4.4×10^9 kilometers or 2.75×109 miles).

eration. Our greatest success so far has been one more unambiguous arc occultation, shown in figure 35, and at least three more probable occultations. The latter refers to occultation events which were observed at only a single telescope (and thus could not be independently confirmed) or in one case to an event observed at two sites for which the match in time between the two telescopes was not exact. The occultation data shown in figure 35 were obtained at the Infrared Telescope Facility of the National Aeronautics and Space Administration in Hawaii, with an unusually bright star, and reveal an arc segment ~25 kilometers wide with a normal optical depth of ~0.075. The smooth curve superimposed on the light curve is a best-fit model that includes the effects of diffraction and the finite angular diameter of the star; the fit is excellent and compares favorably with that obtained for some of the uranian rings with data of similar quality. Note the curious "shoulder" at the inner edge of the arc, which is reminiscent of similar structures observed adjacent to the uranian δ and η rings in both Earth-based and Voyager occultation data.

Table 1 summarizes the properties of the neptunian arcs observed to date, giving their radial distances from the center of Neptune, their radial widths, and the inferred normal optical depths, τ. In figure 36, the apparent tracks of the stars relative to Neptune are shown, together with the locations of the arc occultations. In several cases, there are substantial uncertainties in the arc radius, much greater than the intrinsic astrometric precision of ~25 kilometers (16 miles). These are due, in most cases, to our rather poor knowledge of the orientation of Neptune's equatorial plane, where the arcs are assumed to lie. This situation should be rectified following the Voyager 2 encounter in 1989. Nevertheless, we see that the arcs lie at radii between 41,000 and 71,000 kilometers (25,625–44,375 miles) or 1.63 and 2.82 Neptune radii, and thus fall within the planet's Roche limit, as do the other planetary ring systems. (The Roche limit is the distance from a planet within which a satellite will be torn apart by differential gravitational forces.) With widths ranging from ≤4 kilometers (2.5 miles) to at least 25 kilometers (16 miles) and perhaps 80 kilometers (50 miles), the arcs are rather similar to the uranian rings, though generally less opaque. It is therefore not surprising that several attempts to obtain images of the arcs from Earth-based telescopes have been unsuccessful, even at near-infrared wavelengths where the scattered light from Neptune is minimized. We must probably await images from either Voyager 2 or the Hubble Space Telescope before we will know the complete spatial distribution of the arcs.

At the moment, there is little information concerning either the sizes or chemical compositions of the particles making up the arcs. The reso-

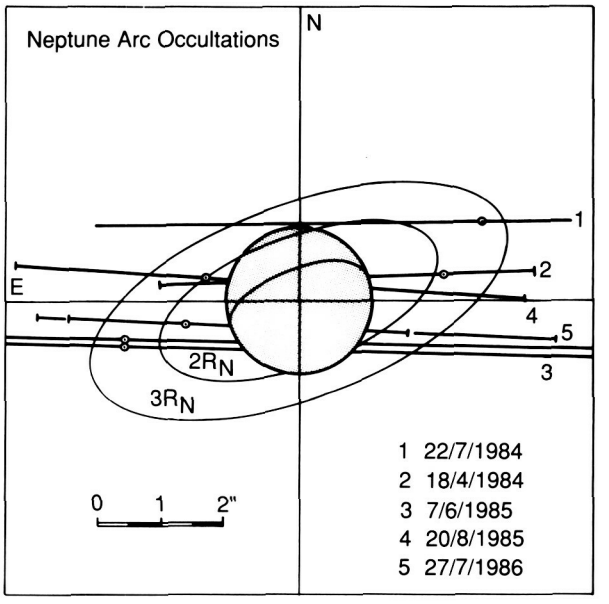

Fig. 36. A schematic diagram of Neptune, showing its orientation in 1984–1985 and the apparent tracks of the stellar occultations listed in table 1. (In reality, of course, the stars remain fixed and the planet moves; but it is more convenient to fix the planet in the diagram.) Each occultation track is shown by a heavy straight line, with the location of the arc occultation indicated by a small circle. The ellipses labeled $2R_N$ and $3R_N$ represent the projection of circular rings in Neptune's equatorial plane at distances of 2 and 3 planetary radii, respectively. In four of the five cases shown, a complete *circular ring in the equatorial plane would have occulted the star twice during the course of the observations, but this did not happen. The track of the May 24, 1981, occultation is not shown, but is to the south of the planet.*

nance model discussed below suggests that the typical particle size may be of order 10 centimeters (4 inches), comparable to the sizes of the particles in the uranian and saturnian rings, but this conclusion is entirely dependent on the validity of this particular model. Voyager and Hubble Space Telescope observations should tell us whether the arcs are made of bright, icy material (like the saturnian rings), or of dark, possibly carbon-bearing material (like the uranian rings).

The existence of partial rings, or arcs, of orbiting material around a planet raises profound theoretical difficulties. Even gentle collisions between the orbiting particles will soon give rise to small differences in orbital period, and the material should rapidly spread around the entire orbit to produce a complete ring. The time scale for this spreading is no longer than 10,000 years. Unless the arcs are extremely young, they must be actively confined, probably by external gravitational forces. Two theoretical models of arc confinement have been proposed. The first, by Jack Lissauer (State University of New York, Stony Brook, NY), illustrated in figure 37a, is based on the concept of a horseshoe orbit: the arc shares the orbit of a small satellite, labeled "Lagrange point moon" in the figure, whose perturbations force the arc material to oscillate back and forth along the orbit, without ever approaching the satellite closer than a certain limiting distance. This phenomenon is exemplified by the co-orbital satellites of Saturn, Janus and Epimetheus. The drawback of this model is that it also requires a second satellite (the "shep-

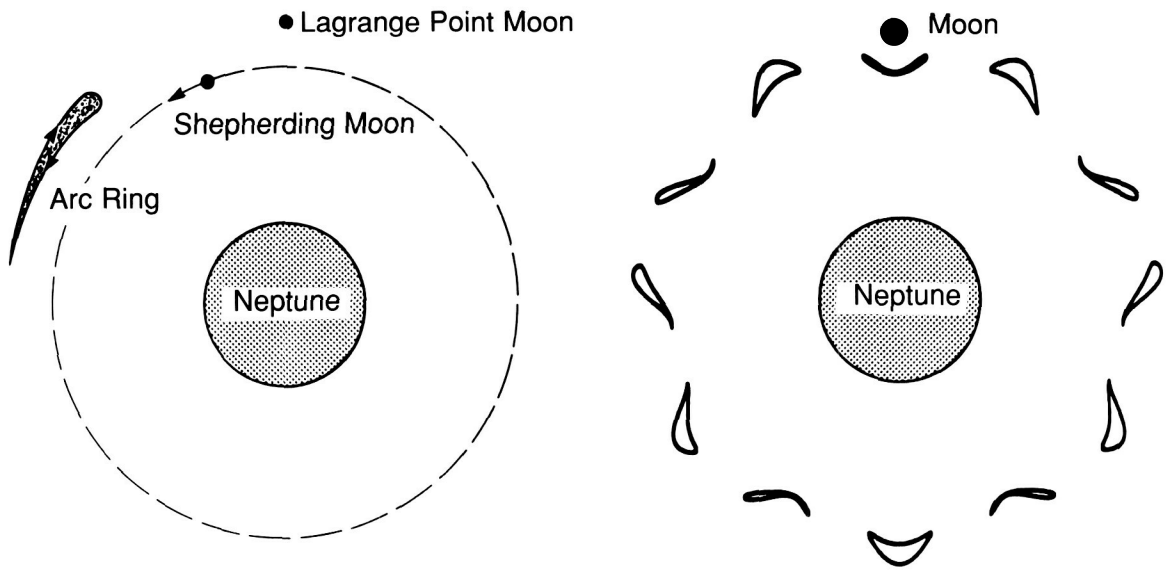

Fig. 37. Illustrations of two theoretical models proposed for maintaining narrow arc rings. The arcs are shown in a reference frame that rotates with the orbital motion of the satellite. Left, *the horseshoe orbit model of Lissauer, showing a single arc that shares the orbit of the Lagrange point moon and is prevented from spreading by the shepherding moon on a nearby orbit. The bodies that make up the arc circulate slowly in the direction indicated by the arrows.* Right, *the corotation resonance model of Peter Goldreich, Scott Tremaine (CITA), and Nicoles Borderies (Jet Propulsion Laboratory, Pasadena, CA). A single set of arcs located at the 5:6 resonance with a hypothetical satellite is shown. All 12 stable arc locations may not necessarily be populated with material, and arcs might also exist at other resonances (6:7, 7:8, etc.) with the same satellite. In both diagrams, the widths of the arcs are exaggerated to show their predicted shapes; in reality the widths are one-thousandth of the mean distance from Neptune. The hypothetical satellites are ~200 kilometers (125 miles) in diameter in both models.*

herding moon" in the figure) to overcome the effects of slow collisional spreading and, even worse, that it requires a separate pair of such satellites for every arc.

Peter Goldreich (California Institute of Technology, Pasadena, CA) and co-workers have proposed a second model, invoking only a single satellite, in which the gravitational perturbations of the satellite are capable of confining material in arcs at certain specific radii where the orbital period of the arc material is an exact fraction (two-thirds, five-sixths, etc.) of the satellite's period. This resonance model is attractive because it is possible to confine arcs at many different radii with only one satellite, whose diameter would be of order 200 kilometers (125 miles). It could thus easily be imaged by Voyager, providing an acid test of the theory. This theory also predicts the existence of several arcs at each resonant radius, as illustrated in figure 37b. Present calculations indicate that the observed arcs (see table 1) can indeed be fitted into the framework of the resonance model and that the putative satellite must orbit near Neptune's Roche limit at a radius of 65,000–70,000 kilometers (40,625–43,750 miles).

Table 1. Summary of Neptune Arc Parameters

Date	Station	Arc Radius (km)	Width (km)	τ
May 24, 1981	Catalina/Mt. Lemmon	60,000 ± 9000	80.0	≥0.7
April 18, 1984	Palomar	53,730 – 54,270 [a]	9.1	0.14
July 22, 1984	CTIO/ESO	67,000 ± 4000	15.0	0.14
June 7, 1985	SAAO	62,580 or 64,010 [b]	~8.0	0.12–0.34
Aug. 20, 1985	IRTF/CFHT	54,060 – 58,930 [a]	25	0.075
July 27, 1986	IRTF/Palomar	41,680 or 41,810 [b]	≤4	≥0.3

[a] Radial ranges correspond to uncertainty in Neptune's pole.
[b] Ambiguous astrometric solution.

Chaotic Dynamics of the Uranian Satellites

William C. Tittemore and Jack Wisdom, Department of Earth, Atmospheric and Planetary Sciences, Massachusetts Institute of Technology, Cambridge, MA 02139

Voyager 2 images of the uranian satellites indicate that some of the satellites, particularly Miranda (fig. 38) and Ariel, have had spectacular geologic histories. This finding was unexpected because the satellites are relatively small and cold. The energy source for this activity remains a mystery. After the successful prediction by Stan Peale (University of California, Santa Barbara), Pat Cassen (NASA/Ames Research Center), and Ray Reynolds (NASA/Ames Research Center) that there might be volcanoes on the jovian satellite Io, tidal heating associated with orbital resonance has been recognized as an important process in the thermal histories of natural satellites. The exotic appearance of the surfaces of the uranian satellites and unusual characteristics of their orbits suggest that similar processes may have occurred in the uranian system sometime in the past.

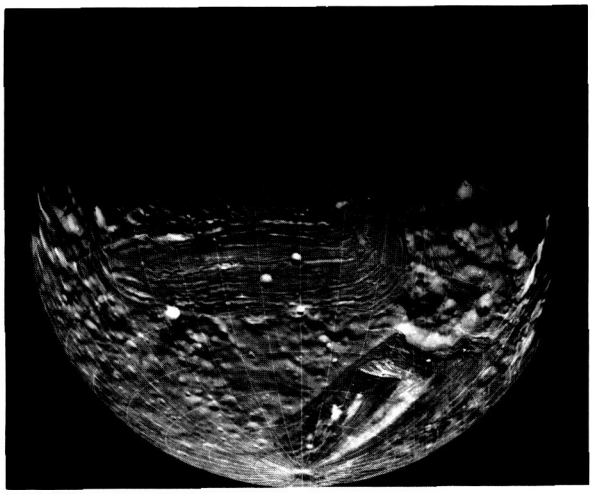

Fig. 38. Voyager 2 image of Miranda. Structural features on the surface (lineations near the center and lower right of image) occurred as a consequence of internal heating of Miranda that may have been induced by changes in the orbit of the satellite.

Tidal heating arises because planetary bodies are not rigid; that is, they deform in response to imposed forces. One such force is gravity. Because gravitation varies with inverse distance squared, parts of a planet or satellite that are at different distances from a gravitational source will feel different accelerations. These differential accelerations are referred to as tidal forces. When a planet deforms in response to tidal forces, energy is dissipated in the form of heat as a result of friction. It is this heating that may have caused the deformation at the surfaces of some of the uranian satellites.

Tidal forces can also produce changes in satellite orbits. For example, tidal friction is the cause of the slowly increasing distance between the Earth and the Moon. The rate at which the orbital changes occur depends on the rate at which tidal energy is dissipated within the planet. This is measured by the parameter Q; the higher Q, the less the dissipation. Gravitational attraction between some of the uranian satellites may have forced these bodies into orbits with higher eccentricities than they would have been in if they had not been disturbed by the others. (Eccentricity is a measure of the amount which an orbit deviates from circularity.) Tidal friction in satellites damps their orbital eccentricities, producing circular orbits. The changes in a satellite orbit with time due to tidal forces is referred to as tidal evolution.

Tidal evolution is believed to have established a number of the orbital resonances among the satellites of Jupiter and Saturn. In an orbital resonance, the periods of the satellites are nearly commensurate (i.e., the period of one is a rational fraction of the other). For the 2:1 Enceladus-Dione resonance, the period of Dione is twice the period of Enceladus. The rate at which tidal energy is dissipated in Uranus is unknown, but if it is comparable to that estimated for Jupiter and Saturn, a number of resonant configurations of the uranian satellites would have been encountered. Since resonances in the jovian and saturnian satellite system arise naturally as a result of tidal evolution, it is curious that there are currently no

resonances among the uranian satellites. Another oddity concerns the shape of the orbits. For the uranian satellites, the time scale to tidally damp the eccentricities is much shorter than the age of the Solar System, yet Miranda, Ariel, and Umbriel have somehow retained significant orbital eccentricities. Finally, the inclination of Miranda is near 4.2°, about a factor of 10 larger than the inclinations of the other uranian satellites. How did the anomalously large inclination arise?

The exotic surfaces of the uranian satellites, together with the existence of anomalies in their orbits, have led us to carry out a systematic study of the passage of the satellites through the principal resonance configurations to determine the consequences of each resonance passage. Only with a detailed understanding of the complicated resonance dynamics can we begin to unravel the mysteries presented by the uranian satellites.

The study of planetary dynamics has been significantly enhanced in recent years by discoveries in the area of nonlinear dynamics, in particular, the discovery that there are solutions to Newton's deterministic equations of motion that behave in a highly erratic manner. This irregular motion is termed "chaotic." The existence of chaotic behavior profoundly affects the way that we think about planetary motion and the methods that we use to study it. The methods of modern nonlinear dynamics allow us to understand the global nature of the solutions and to understand qualitative features of trajectories and their relationship to other possible trajectories of the system. We know much more about how that global structure changes as the system evolves. Nonlinear dynamics also provides us with new methods to study the time evolution of orbits that dramatically reduces the requirements for computer time, bringing many calculations that were previously unthinkable into the realm of possibility. Chaotic behavior plays an important role in numerous physical situations in the Solar System: the Kirkwood gaps in the asteroid belt are associated with chaotic zones, meteorites are transported to Earth from the asteroid belt along chaotic trajectories, the saturnian satellite Hyperion is tumbling chaotically, and many other irregularly shaped satellites in the Solar System tumbled chaotically in the past. Even the motion of Pluto appears to be chaotic.

We have found that the dynamics of the uranian satellites near resonance are significantly more complicated and interesting than the dynamics of the jovian and saturnian satellites. As a result of the relatively small oblateness of Uranus and the relatively large satellite masses, resonances among the uranian satellites are associated with large zones in which the orbital eccentricity arc inclination vary chaotically, and this may persist for up to 100 million years as the satellites pass through the resonance. Figure 39 shows a short 2000-year sample of the chaotic behavior of Ariel's eccentricity on passage through a resonance with Umbriel.

Another significant result of our study is that the anomalously large inclination of Miranda arises naturally on passage through 3:1 mean motion commensurability with Umbriel. There are several resonances associated with this commensurability. The dynamics of the passage through this suite of resonances are particularly interesting. Figure 40 shows a sample evolution of the inclination of Miranda. Initially, the Miranda-

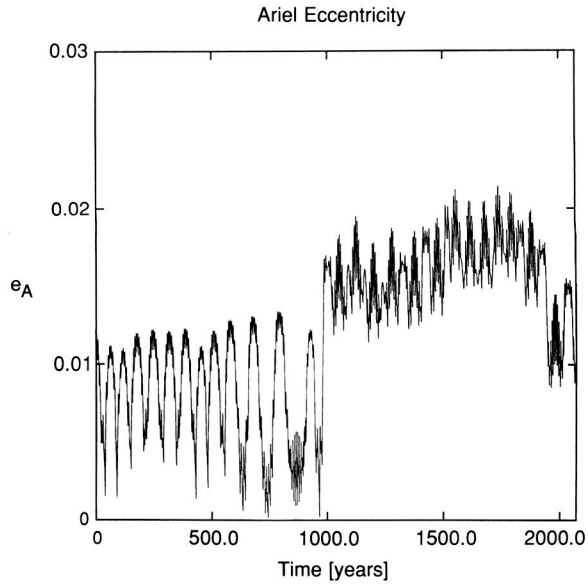

Fig. 39. Sample of the chaotic variation of the orbit of Ariel during passage through the 5:3 mean motion commensurability with Umbriel. The parameter e_A is eccentricity.

Umbriel pair are captured into a resonance that leads to a dramatic increase in the inclination of Miranda to values near that observed today. This phase of the evolution is not chaotic and can be analytically predicted. Escape from the resonance then occurs by a previously unidentified mechanism. The frequency of oscillation within the resonance becomes commensurate with other frequencies in the problem, and the structure of the resonance changes. The system is pulled out of the resonance into a relatively large chaotic zone, from which it may escape from the region where inclinations are strongly affected. The system then encounters a group of resonances that strongly affect the eccentricities. The system again becomes chaotic. During this chaotic phase, the eccentricity of Miranda may be driven to relatively high values, perhaps as high as 0.08. The system ultimately escapes from the resonance region altogether. It is possible that the increase in the eccentricity of Miranda resulted in significant tidal heating of Miranda, although further study is required to determine whether this tidal heating can account for any of the observed surface features.

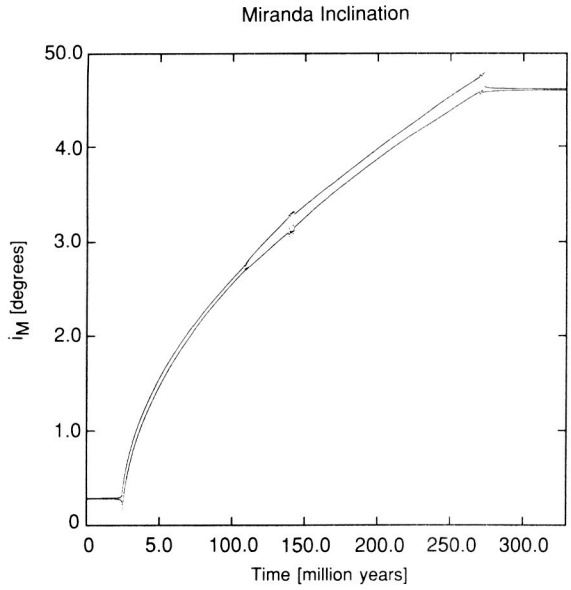

Fig. 40. Inclination (i_M) of Miranda rises dramatically during passage through the 3:1 mean motion commensurability with Umbriel to values comparable to the anomalously large present-day 4° inclination.

Our calculations indicate that the inclination of Miranda arises naturally on passage through the 3:1 commensurability with Umbriel. The requirement that the system has encountered this commensurability places a lower limit on the rate of internal tidal dissipation in Uranus, constraining the Q of Uranus to be less than 39,000.

Systematic examination of the most important resonances has also led to the identification of a dynamical barrier to the evolution. An extensive set of simulations has indicated that the passage through the 2:1 commensurability between Ariel and Umbriel is very unlikely. Thus, if the uranian satellites had encountered this resonance, they would have had very low probability of evolving to their current configuration. The requirement that they have never encountered this resonance constrains the Q of Uranus to be greater than 11,000. Thus, this study of the dynamical evolution of the uranian satellites has placed stringent bounds on the rate of internal dissipation in Uranus ($11{,}000 < Q < 39{,}000$).

Our results have shown that chaotic behavior plays an essential role in the dynamics of the uranian satellites. Our other recent studies have established the importance of chaotic behavior in many other physical problems in the Solar System. It is no longer possible to carry out studies of planetary dynamics without being conscious of the results of modern nonlinear dynamics.

Evolution of Comets to Asteroids

Paul Weissman, Earth and Space Sciences Division, Jet Propulsion Laboratory, Pasadena, CA 91109

The first objects to form in the solar nebula 4.5 billion years ago were planetesimals: rock and ice agglomerations of interstellar dust and gas ranging from 5 to 50 kilometers (3 to 30 miles) in diameter. Most of the planetesimals collided and accreted to form the major planets. Today, the comets and the asteroids are the remnants of that original primitive population of small bodies.

In the main asteroid belt, which lies between Mars and Jupiter, nature has preserved one of the most interesting parts of the compositional spectrum of those small bodies, the region where it changes from refractory (i.e., rocky) bodies to volatile, ice-rich bodies. In addition, the asteroids show evidence of a variety of planetary processes such as accretion, chemical differentiation, collisional disruption, and, most importantly, short-lived internal heating.

In contrast, the comets represent a more distant, and possibly more compositionally uniform, region of the solar nebula, the Uranus-Neptune zone and beyond. Until recently, it was widely believed that comets had experienced very little processing or modification from their original state and had been stored in distant, cold orbits far from the Sun in the Oort cloud. Although a number of modifying processes have now been recognized, the comets have still undergone far fewer changes than the asteroids have.

The question of whether comets can evolve to appear as asteroidal objects arises because of a desire to understand the source of the meteorites recovered on the Earth's surface. Meteorites are our main source of information on conditions in the early Solar System. The meteorites we collect must be fragments of objects already in Earth-crossing or Earth-approaching orbits, known as Apollo and Amor asteroids, respectively. But such objects have dynamical lifetimes in those orbits of only 30–100 million years, far less than the age of the Solar System. Either we must assume an immense original population of Earth-crossers, a concept that is physically unrealistic and not supported by cratering data, or there must be a replenishment source.

Historically, the identification of that source has been divided between observers, who believe that it must be asteroids, and celestial dynamicists, who believe that it must be comets. To the observers, the Earth-crossing asteroids show no evidence of cometary activity (i.e., observable coma) and have surface compositions as determined by reflectance spectroscopy, which mimic the range (though not the statistics) of surface compositions for the main belt asteroids and which generally have the aphelia (points farthest from the sun) of their orbits in the main belt. To the dynamicists, there were no known mechanisms for transferring the required flux of asteroids from the main belt into Earth-crossing orbits, whereas short-period comets are regularly thrown into Earth-crossing orbits by close encounters with Jupiter and are sufficiently numerous to provide the needed flux.

A number of recent discoveries have changed this situation. First, dynamicists reevaluated two crucial mechanisms for delivering asteroids into Earth-crossing orbits and found that they can supply on the order of 60% of the estimated population of 800 $\pm$ 300 Earth-crossers. These two mechanisms, called "secular resonances" and "orbital commensurabilities," each involve specific orbits in the asteroid belt that receive periodic gravitational tugs from Jupiter, the largest planet in the Solar System. Those periodic tugs can force the orbits to become chaotic and suddenly increase in eccentricity so that they become Earth-crossing. Thus, a significant fraction of the Apollo and Amor asteroids can be accounted for in this way.

On the other side, observers have now seen a number of peculiar features in some Earth-crossing asteroids that can not be easily explained. For example, the Pioneer Venus Orbiter noted disturbances in the solar wind when one particular asteroid, called 2201 Oljato (the number is its official catalog ordering), passed close to Venus, as if the asteroid or debris in its orbit was spewing out clouds of gas. Another observer looking at Oljato saw a spectral emission feature, again possibly indicative of gas emission. Dynamicists have noted that Oljato is in one of the most chaotic orbits of any of the Earth-crossing asteroids, another apparent indictor of a possible cometary origin. Finally, Oljato is in the same orbit as several faint meteor streams; most meteor streams are identified with and derived from active short-period comets.

One of the strongest pieces of evidence along these lines came in 1983 when the Infrared Astronomical Satellite (IRAS) discovered an asteroid in precisely the same orbit as the Geminid meteor stream, one of the two brightest annual meteor showers observed. Now officially designated 3200 Phaeton, that asteroid has been studied for signs of cometary activity but none has been observed.

A final piece of evidence that helped to convince many astronomers was the photographs of the nucleus of Comet Halley from the Vega and Giotto flyby spacecraft in 1986 (fig. 41). Those pictures showed that 70% of the surface of the icy cometary nucleus had been covered by an inactive crust, a lag deposit of rocky and carbonaceous material left behind as the more volatile ices sublimed. This demonstrated that comets could indeed transform themselves from active to inactive objects by slowly building up such a crust over their entire surfaces.

The emerging consensus is that some fraction of the Earth-crossing asteroids are likely extinct cometary nuclei. That fraction may be as low as 10% or as high as 50%. In the future, additional physical studies of Earth-crossers will be important in identifying just which ones are likely cometary candidates, while theoretical studies will continue to refine the expected delivery mechanisms for both asteroids and comets.

Fig. 41. The nucleus of Comet Halley as photographed by the Giotto spacecraft in March 1986. Over 70% of the nucleus surface appears to be covered by a dark, nonvolatile lag deposit that effectively prevents the ice below from sublimating. As this crust grows and cometary activity continues to diminish, the comet nucleus might evolve to an object very similar in appearance to a dark, carbonaceous asteriod. Photograph courtesy of H. U. Keller, Max Planck Institute for Aeronomy, Lindau, West Germany.

Lunar Samples

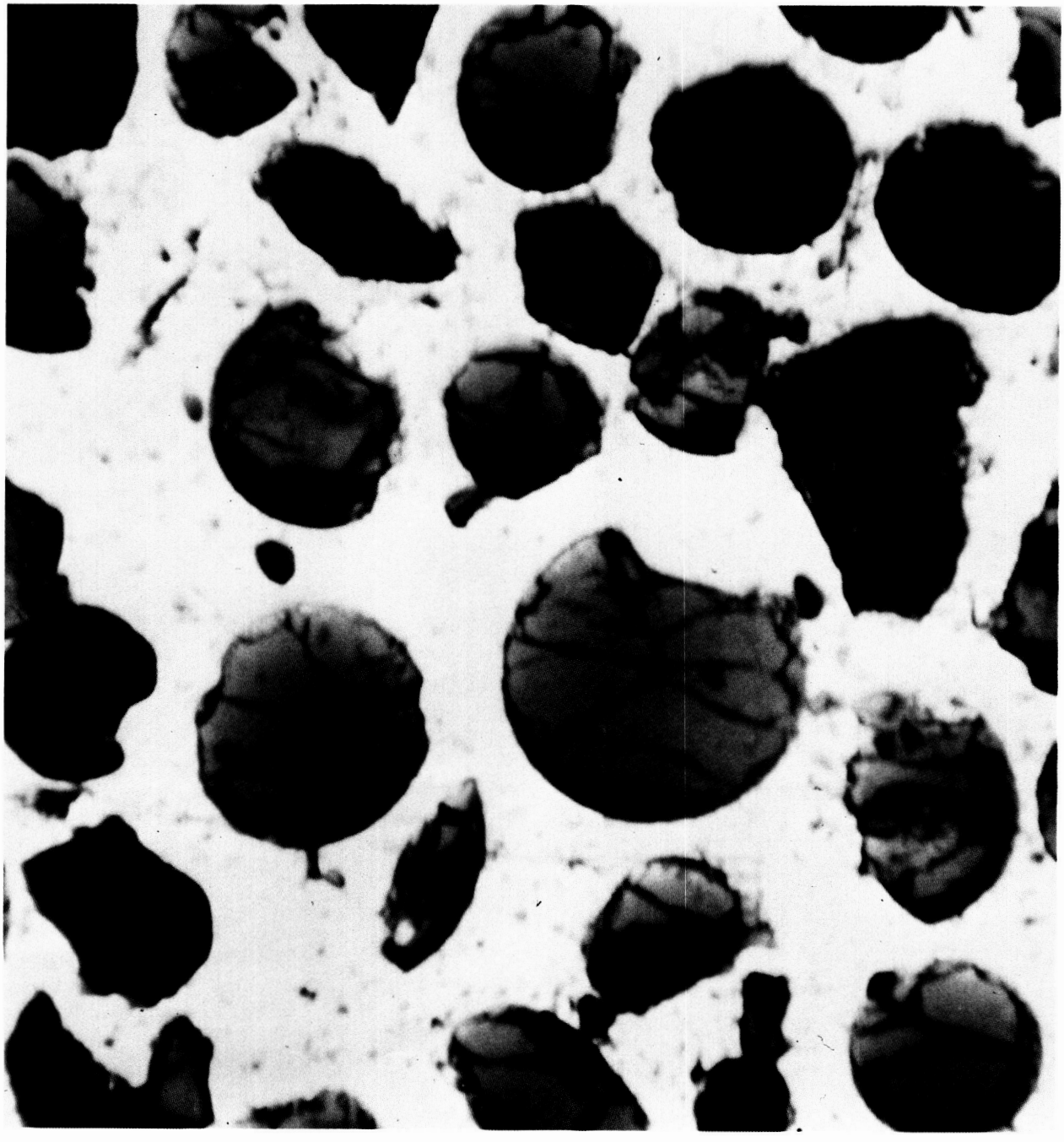

Densification of Mantle-Derived Liquids in the Earth's Moon: Implications for the Earth and Other Terrestrial Bodies

J. W. Delano, Dept. of Geological Sciences, State University of New York, Albany, NY 12222

The dark gray areas on the side of the Moon that faces the Earth are basaltic lava flows that were erupted onto the lunar surface mostly between 2.5 and 3.9 billion years ago. Four Apollo missions landed at widely separated, predetermined locations on these volcanic plains. Analysis of returned samples shows that these regions of the Moon consist of crystalline rocks and volcanic glass droplets that rose to the lunar surface as magmas from depths of about 400 kilometers (250 miles). The best-known example of lunar volcanic glass is the orange soil collected by Apollo 17 astronauts (fig. 42); this soil consists of tiny spherules of orange glass (fig. 43). Detailed chemical analysis of samples from all Apollo sites have identified 24 other varieties of volcanic glass whose compositions span a large range. These glasses were explosively erupted onto the lunar surface and provide lunar scientists with constraints on the chemistry, mineralogy, and processes in the lunar mantle.

Recent advances in our understanding of geochemical processes that operate inside the Earth have demonstrated that mantle-derived liquids can become denser than the solid crystals with which the melt is in chemical equilibrium during the partial melting, at pressures of 80,000 bars (80 kilobars, or about 79,000 atmospheres).

Fig. 42. Orange soil discovered by the Apollo 17 astronauts occurs in the foreground of this photograph. The orange soil is composed of orange glass spheres (see fig. 43) produced during explosive volcanism about 3.5 billion years ago. (For scale, the tripod is about 55 centimeters, or 2 feet tall.)

Fig. 43. Photomicrograph of the Apollo 17 orange soil showing that it is composed of glass spherules measuring about 100 microns (four-thousandths of an inch) in diameter.

The full implications of this new process in the Earth are still to be investigated but appear to be of profound geologic importance.

Spurred on by these insights, the author has solved a third-order Birch-Murnaghan equation of state for a plausible range of physical parameters in each of the 25 compositions of mantle-derived magmas represented by the lunar volcanic glasses. Because the maximum pressure in the center of the Moon is only about 47 kilobars (about 46,000 atmospheres), one's first impression based on the Earth would be that densification of the melt beyond that of its coexisting solids would not be likely. However, owing to (1) the enormous compositional variety of lunar magmas, (2) the high abundances of iron and titanium in some lunar magmas, and (3) the low oxidation state of lunar magmas, calculations suggest that melt densification may operate for the most titanium-rich lunar magma compositions at pressures as modest as 20 kilobars, equivalent to depths in the Moon of 400 kilometers (about 250 miles). This is a familiar depth because it corresponds to the experimentally inferred location of the original source regions of the lunar magmas mentioned earlier in this article.

Figure 44 illustrates the results of calculations performed on an Apollo 14 volcanic composition that contains 12.7 mol % TiO_2 (titanium dioxide). This volcanic glass has the highest abundance of titanium and iron observed in any magma yet sampled on the Moon. At its melting temperature at zero pressure of 1330°C, this melt has a density of about 3.13 grams per cubic centimeter, whereas the crystalline solid (magnesian olivine) in equilibrium with that melt has a density of about 3.30 grams/cm^3. Note that with increasing pressure (and depth in the Moon) the difference in densities between the melt and solid gradually diminishes until a crossover occurs at about 20 kilobars.

When liquids become denser than their coexisting solids, the melts will separate from those solid phases by sinking rather than rising. In this regard, figure 44 shows that the Apollo 14 black glass with 12.7 mol % TiO_2, which is the most chemically extreme composition of magma known to have been erupted onto the Moon's surface, appears to be a limiting case. Although the Moon may have generated magmas at depths of 400 kilometers with higher abundances of titanium than this, such magmas would have sunk deeper into the lunar interior and, therefore, never been erupted.

This process of liquid densification offers new insights into the redistribution of elements inside the Moon during its complex history that need to be explored further by geophysicists and

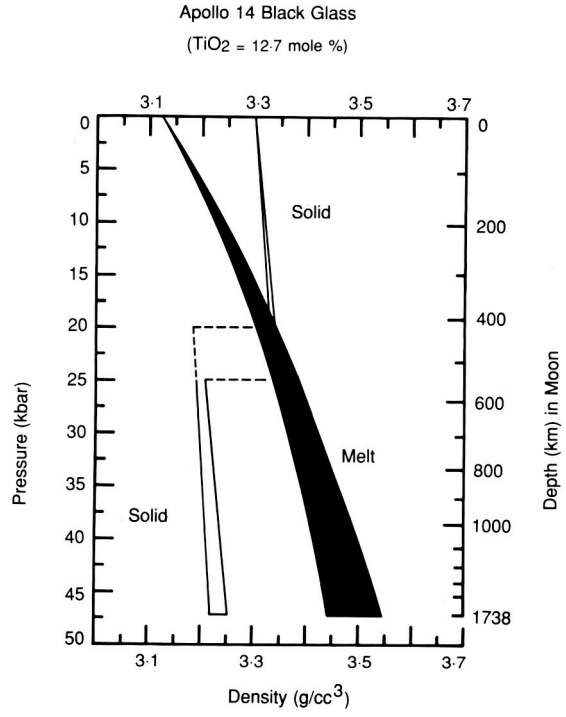

Fig. 44. Calculated range of melt density for the Apollo 14 black glass composition at its melting temperature as a function of pressure and depth inside the Moon. The density of the solid phase in chemical equilibrium with that magma is also shown. At pressures between 0 and 25 kilobars, the equilibrium solid is magnesian olivine, and at pressures greater than 25 kilobars the equilibrium solid is magnesian orthopyroxene. Note that this composition of mantle-derived magma becomes denser than its equilibrium solid at pressures of only 20–25 kilobars. Other experimental data indicate that this magma ascended to the surface from that pressure regime of the Moon.

geochemists. For example, dense high-titanium liquids that plummeted into the deepest regions of the Moon would not only have affected its density structure but also its thermal structure because these melts are known to have been enriched in the radioactive elements potassium, uranium, and thorium. It is tempting to speculate that the seismically defined "attenuating zone" at depths greater than 1000 kilometers (about 620 miles) in the present Moon is the location of dense high-titanium melts that have drained downward to form an intergranular fluid along crystal boundaries.

The occurrence of melt-solid density crossovers in a small planetary body (the Moon) with modest internal pressures implies that this process for redistributing elements within terrestrial bodies need not be restricted only to large planets, like the Earth, where high pressures exist. Indeed, the compositional range of magmas, the oxidation state of planetary interiors, and the abundances of volatiles in the magmas are major parameters that need to be evaluated, in addition to pressure, for assessing the potential of this process occurring in any terrestrial body.

In summary, detailed chemical analysis of volcanic glasses contained in samples collected by the Apollo astronauts has furnished new insights into a process of major importance for understanding not only the geochemistry of the Moon but also that of other terrestrial bodies. The existence of this process during the history of planets had, until recently, been unknown.

Trace-Element Constraints on the Lunar Magma Ocean

Larry A. Haskin and Randy L. Korotev,
Department of Earth and Planetary Sciences and
McDonnell Center for the Space Sciences,
Washington University, St. Louis, MO 63130

Did the lunar crust crystallize atop a deep, global ocean of molten rock? If so, what kinds of rocks formed that crust? Concentrations of trace elements in the rocks and soils of the Apollo and Luna collections and Antarctic lunar meteorites constrain the answers to these questions.

Some chemical elements were preferentially extracted into the lunar crust. The average surface concentration of aluminum is 13.5%, compared with 1.7–4% for the bulk Moon. Nearly all crustal aluminum is in the mineral plagioclase, which makes up 70% of the crust. Rock melt in equilibrium with the lunar interior would only yield about 55% plagioclase as it crystallized. Therefore, the crust contains some 15% excess plagioclase.

Rare rocks among the lunar samples called ferroan anorthosites consist almost entirely of plagioclase. This observation led to the suggestion that the outer half of the Moon (by mass) was once a global ocean of molten rock (magma). As it cooled, this magma first crystallized the dense minerals olivine and pyroxene, which accumulated on its floor. Eventually, plagioclase crystallized; it was less dense than its parental magma, so it floated to form the crust. In a simple magma ocean model, the outer Moon is zoned. Its upper 50–60 kilometers (31–37 miles) are plagioclase, underlain by 250 kilometers (about 150 miles) of olivine and pyroxene. Between these shells is a thin layer of the last dregs of the magma.

This picture is too simple; the 30% of the lunar crust that is not plagioclase is mainly olivine and pyroxene. How were these minerals incorporated into the crust? Perhaps crater-forming impacts stirred residual magma into the crust. Perhaps later melting in the lower shell or beneath it produced magma that entered the crust. Either of these mechanisms would reduce the proportion of surface plagioclase from nearly 100% to a lower value. Alternatively, the crust may have formed from magmas that merely lost olivine and pyroxene, so the plagioclase and residual liquid remained together. If this was the case, there may not have been a global magma ocean.

When plagioclase crystallizes, the "incompatible trace elements" mainly remain in the magma. The geochemical behavior of a subset of these elements, the rare-earth elements (REE), is well known. One REE, europium, partially separates from the rest under chemically reducing lunar conditions and concentrates into plagioclase. A crust with 15% excess plagioclase would have a low ratio of REE to europium (e.g., of samarium to europium). Alternatively, if the magma did not float excess plagioclase but merely lost olivine and pyroxene because they sank when they crystallized, the crustal ratio of samarium to europium would be normal.

Rocks of the early lunar crust (highlands rocks) have a wide range of ratios of samarium to europium. We need the average value. Figure 45 shows the samarium to europium ratios versus concentrations of another incompatible element, thorium, for polymict samples. All lunar soils and most lunar rocks are polymict (i.e., mixtures of two or more rock types formed by cratering impacts). They contain many rock types, but the original identities of those rocks have been obliterated. Sampling of the lunar surface is sparse and biased; the sample average may not be the crustal average. Thorium concentrations were sensed remotely from orbit over about 10% of the surface, however, by means of thorium gamma rays. The vertical line represents the resulting average thorium concentration; the horizontal line represents the normal ratio of samarium to europium. The lines cross within the band of data. On the average, the lunar surface has a normal ratio of samarium to europium. These data provide no evidence that on a global scale a shell of anorthosite floated above the residue of its parent magma. Locally, however, blocks of anorthosite may have floated.

Magma oceanographers suggest that ferroan anorthosite is primordial crustal material. It has a very low ratio of samarium to europium (points at the left-hand edge of fig. 45). They suggest that mixtures of ferroan anorthosite, KREEP, and magnesian norite and troctolite make up most polymict highlands materials. KREEP, which is enriched in all incompatible trace elements and whose name is an acronym for lunar rocks rich in potassium (K), REE, and phosphorus (P), is generally thought to represent the last dregs of the magma ocean. It has very high ratios of samarium to europium. Magnesian norites and troctolites (rocks that contain abundant pyroxene or olivine as well as plagioclase) are generally thought to have crystallized from magmas that formed later than the magma ocean.

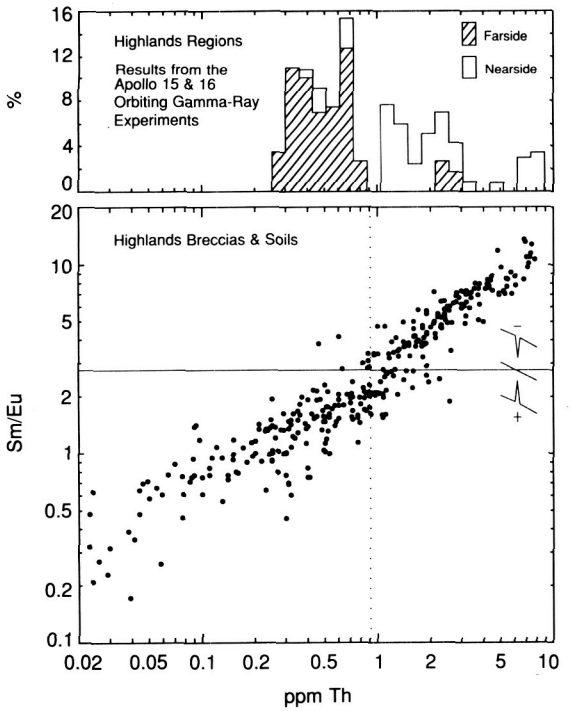

Fig. 45. Variation of the samarium to europium (Sm/Eu) concentration ratio with thorium (Th) concentration in polymict samples from the lunar highlands. The horizontal line represents the Sm/Eu ratio of the bulk Moon; the vertical dotted line represents the mean Th concentration of the surface crust. The lines intersect within the trend of the data, indicating that plagioclase is not, on the average, enriched or depleted in the crust with respect to the liquid from which it crystallized.

Trace-element considerations suggest that these four rock types cannot have been the only major components of the early crust. If they were, the rock type KREEP and the anorthosite would contain nearly all the europium present in the highlands crust. The average thorium concentration of highlands material limits the proportion of KREEP to about 4%, which can provide only a small fraction of the europium. The aluminum concentration indicates that about 70% of the crust is plagioclase, which must thus contain most of the europium. Average highlands material contains too much europium, however, for most of this plagioclase to be like that in ferroan anorthosite; not more than about 40% of the plagioclase in the crust could be of that type. At least half of the plagioclase must be substantially richer in europium. The plagioclase in some magnesian norites and troctolites has suitably high europium concentrations, but the proportions of those rocks needed to supply the necessary amount of europium to the polymict material would bring along too high a ratio of magnesium to iron. Thus, there must be major rock types contributing to the polymict materials that we have not yet identified in sample collections.

We are evaluating the following hypotheses for formation of the primordial crust. Trace-element constraints suggest that the crust formed from magmas whose compositions were those expected for partial melts from the lunar interior. These magmas crystallized plagioclase, pyroxene, and olivine but somehow lost an average of about 12% of their olivine and pyroxene. Perhaps the olivine and pyroxene sank in the proposed magma ocean and lie deep within the lunar interior. We note, however, that polymict samples cover a substantial range of compositions, and remote sensing data indicate the presence of broad crustal regions with variable proportions of plagioclase and iron-magnesium minerals, so perhaps the crust formed from separate pools of magma. The largest of these may have accumulated high proportions of plagioclase at their surfaces. Individual pools may have lost less than or more than the average of 12% of their pyroxene and olivine, thus producing a variety of rock types.

Determining the Ages of Rocks of the Ancient Lunar Crust

Charles Meyer, NASA Johnson Space Center, Houston, TX 77058

The author and William Compston and Ian Williams (Research School of Earth Sciences of the Australian National University, Canberra, Australia) have determined the ages of numerous samples of lunar rocks by the uranium-lead ion microprobe method. The method requires that zircon grains be located within rocks in which the interrelations of the minerals indicate that they crystallized from a silicate liquid (igneous rocks). Zircon is a mineral found in low concentrations in lunar rocks. It contains trace amounts of uranium (U) and thorium (Th), which are radioactive elements that decay to lead (Pb) at a known rate. The time when the zircon crystallized from its parent liquid can be accurately measured by determining the ratios of the isotopes of these elements using the very sensitive, high-resolution ion microprobe mass analyzer (SHRIMP) developed by Compston and Williams at the Australian National University. Using this technique, the ages of grains of zircon smaller than 100 microns (4/1000 inch) across can be determined, so that ages can be measured for rock fragments that are much too small for age determination by other, more conventional techniques.

The earliest period of lunar history, between 3.9 billion years ago and the time the Moon formed about 4.55 billion years ago, is one from which we have very few lunar igneous rocks large enough for age determinations by conventional techniques. The SHRIMP studies are proving invaluable in identifying rocks formed during this interval and in helping to outline the chronology of the evolution of the lunar crust. Figure 46 is a histogram of $^{207}Pb/^{206}Pb$ ages obtained on lunar zircons by the SHRIMP. These data more than double the number of high-quality age determinations for lunar rocks from the earliest period of lunar history.

An important result of this work has been to show that at least some lunar granite formed very early in lunar history. (Lunar granite is a rock that consists almost entirely of a silica mineral, usually quartz, and the potassium-aluminum silicate mineral potassium feldspar. On the Moon, granite forms only at the very end stages of crystallization of silicate liquids.) So far, five fragments of lunar granite have been found to have ages of about 4.3 billion years, indicating that they formed within the first 250 million years following the origin of the Moon. Apparently, there was enough melting and generation of magmas (silicate liquids) very early in lunar history that the magmas could evolve extensively and produce granites. Other techniques have previously shown that some lunar granites are younger, and this finding is also confirmed by SHRIMP analysis of uranium-rich zircons from lunar breccias (rocks that represent aggregates of fragments from many different sources).

Ages measured by the SHRIMP on numerous fragments of igneous rocks other than granites range from 4.3 to 4 billion years. The younger ages could be artifacts, due to the loss of lead

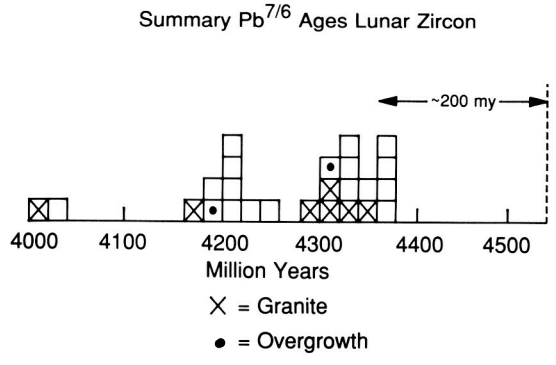

Fig. 46. Summary of $^{207}Pb/^{206}Pb$ ages of lunar zircons determined by the very sensitive high-resolution ion microprobe mass analyzer (SHRIMP) at the Australian National University.

from the zircon, or they could be real crystallization ages. Further work is needed to clarify the interpretation of these data. Also, one unusual patch of broken zircon grains was found in which the zircon clearly formed by a two-stage process (the grains have distinct cores and rims). Using the SHRIMP, the rims were found to have formed 120 million years later than the cores, indicating lunar metamorphism (processes that modify rocks after they are formed).

While searching for zircon-containing rock fragments, the author found several minute (200 micron, or 8/1000 inch) grains of tungsten-bearing yttrobetafite in a small fragment of lunar granite. This unusual mineral contains large amounts of niobium, yttrium, rare-earth elements, uranium, thorium, and lead, along with significant amounts of tungsten (0.3 wt %). These elements are generally found only in trace amounts in lunar rocks and minerals, and this is the first occurrence of tungsten in measurable concentration in any lunar mineral. The structural formula of the yttrobetafite indicates that at least one-third of the iron it contains is ferric (trivalent). Iron this oxidized has never before been reported in a lunar mineral. Most lunar iron is ferrous (divalent) or occurs as native metal. Finding a mineral with so much ferric iron is evidence that some late-stage lunar magmas may have become naturally more oxidized, as high-valence state ions were concentrated in the latest liquid.

Lunar KREEP Volcanism Triggered by Basin-Scale Impact

Graham Ryder, Lunar and Planetary Institute, Houston, TX 77058

Volcanic rocks tell us about the internal chemistry and thermal history of a planet. We want to know what part of the planetary interior melted to produce the lavas, what the source rocks were made of, and why they melted at that particular time. On the Moon, the older highlands rocks have been less tractable for interpretation than mare basalts, even in establishing which might be volcanic, but highlands volcanic rocks are intrinsically at least as important as mare basalts. (The lunar highlands are the light-colored, densely cratered areas of the lunar surface; they formed mostly more than 3.9 billion years ago. The lunar mare areas are the dark-colored, smoother areas of the lunar surface; they are floods of basaltic lavas, most of which erupted more recently than 3.9 billion years ago.)

Some of the basalts collected at the Apollo 15 landing site, at the edge of Mare Imbrium, have highlands rather than mare affinities. They crystallized much before most of the mare basalts collected at the same site, and they are more aluminous and much richer in incompatible trace elements (elements such as rare earths, barium, uranium, and thorium) than mare basalts are. These rocks are known as KREEP basalts. KREEP is an acronym used to designate lunar rocks that are unusually rich in potassium (K), rare-earth elements (REE), and phosphorus (P) and that have distinctive ratios of certain trace elements. Trace-element data indicate that many highlands soils and breccias contain small amounts of rock having the trace-element characteristics of KREEP. (Breccias are rocks that consist of aggregates of fragments of many different rocks.)

Although the Apollo 15 KREEP basalts were not distinguished by the Apollo 15 astronauts (because the fragments are all so small), they are an important component of the soils all over the site. Their volcanic origin has been claimed by many workers but disputed by others, some even suggesting that they represent the melt produced by the giant impact that formed the Imbrium Basin. One of the reasons that this dispute has not been resolved is that the small particles have been studied in varied uncoordinated surveys. Syntheses have, in particular, lacked a good chemical data base on which to form conclusions, as most of the analyses have been incomplete.

The author has almost completed a study of Apollo 15 KREEP basalt samples that includes a dozen new analyses of individual fragments for major and trace elements as well as detailed petrographic and electron microprobe work, on both these and other particles. This study is specifically aimed at understanding the origin of the rocks rather than simply describing them. With data obtained recently by others and the results of published and unpublished older studies, the chemical and petrographic data base is now probably as good for these KREEP basalts as for most other types of lunar basalt.

The textures of the KREEP basalts (the shapes and interrelations of the mineral grains and glassy areas in the rocks) show that they are volcanic; that is, they crystallized from lavas formed by melting of the planetary interior as a result of internal heating. Experimental data on the crystallization of silicate liquids indicate that textures such as those shown in figures 47 and 48 only develop with two-stage cooling, unlikely in a silicate liquid produced by melting during a meteorite impact but common in volcanic environments.

Several KREEP basalt fragments contain a yellow glass filling in the spaces between mineral grains (fig. 49). This glass represents a quenched liquid, and its presence demonstrates two-stage cooling. All such samples show the effects of disruption, usually minor, in which fractured crystals were penetrated by the liquid that was then quenched to

yellow glass (fig. 50). A few fragments are totally disrupted, with shattered crystals in a yellow glass. Although other interpretations are possible, it appears that the lava flow from which these basalts came was hit by a meteor, and splashes of the lava were thrown out and quenched before the lava finished crystallizing.

The chemical analyses of the KREEP basalt fragments show a range in compositions that is regular and consistent with igneous crystallization in which 30–40% of the liquid crystallized and crystals were subsequently removed (perhaps by gravity-induced settling). The compositions of the samples lie extremely close to the compositions at which pyroxene (an iron-magnesium silicate mineral) and plagioclase (a calcium-aluminum silicate mineral) crystallize simultaneously. Compositions such as these are commonly generated by crystallization of lavas but are not usually produced during melting by meteorite impacts and subsequent crystallization of the melts.

Fig. 47. Photomicrograph of KREEP basalt 15243,19; plane-polarized transmitted light. Longest dimension of photograph is 2 millimeters (8/100 inch). The rock consists of elongate crystals of plagioclase (white) that were produced by an early stage of slow crystallization enclosed by an intergrowth of very small mineral grains (dark areas) produced by a late stage of very rapid crystallization.

The bulk chemistry of the KREEP basalts (particularly their enrichment in aluminum relative to mare basalts) suggests that their parent magmas formed by partial melting of rocks of the lunar crust rather than the mantle. Alternatively, parental magmas formed in the mantle may have melted crustal rocks as they rose to the surface and then incorporated the crustal melts, changing their compositions.

Age determinations made on the few KREEP basalt samples that are large enough for isotopic study indicate that these rocks formed 3.85 billion years ago. This age is indistinguishable from the age we infer for the Imbrium Basin impact. The

Fig. 48. Photomicrograph of KREEP basalt 15404,19; plane-polarized transmitted light. Longest dimension of photograph is 2 millimeters (8/100 inch). The rock consists of clots of coarsely intergrown crystals of plagioclase and pyroxene (top of photograph) enclosed by an intergrowth of much smaller crystals of the same minerals. The clots of larger crystals were formed in an early stage of slow crystallization, and the areas of smaller crystals were formed in a later stage of more rapid crystallization.

limited isotopic data suggest that more than one set of flows is represented. The chemistry is identical with that of the Apennine Bench formation (determined by remote-sensing studies). The Apennine Bench formation is a plains unit near the landing site that formed immediately after the Imbrium impact but before the Imbrium Basin was flooded by mare basalt lavas. Remote-sensing studies also indicate that material of similar composition underlies the mare lavas in the western Imbrium region, on the other side of the basin from the landing site. Thus, the Apollo 15 KREEP basalts probably make up the Apennine Bench formation and were extruded immediately following (geologically speaking) the Imbrium impact, flooding the basin. The disrupted samples show that the KREEP basalts were extruded during a period of heavy meteorite bombardment, which is consistent with their being immediately post-Imbrium.

That KREEP volcanism occurred immediately after the Imbrium impact, in the Imbrium Basin, yet did not occur anywhere at any later time (as far as we know), suggests a very close relationship between the basalts and the impact. The observations very clearly point to some combination of pressure changes and release, fracture conduit formation, crustal removal, and heat input being directly responsible for the formation of the Apollo 15 KREEP basalts and the lava flooding that produced the Apennine Bench formation. KREEP volcanism demonstrates that internal and external processes were very closely related on the early Moon.

Fig. 49. Photomicrograph of KREEP basalt from breccia 15358,16; plane-polarized transmitted light. Longest dimension of photograph is 750 microns (about 3/100 inch). Elongate crystals of plagioclase (white) and stubby crystals of pyroxene (tan) formed by slow early crystallization are enclosed by a glass (orange) formed by late quenching of the remaining silicate liquid.

Fig. 50. Photomicrograph of KREEP basalt 15434,111; plane-polarized transmitted light. Longest dimension of photograph is 750 microns (about 3/100 inch). Broken grains of plagioclase (white) are enclosed by orange glass.

Lunar Sample Studies: The Many Stones Left Unturned

Paul H. Warren, Institute of Geophysics and Planetary Physics, University of California, Los Angeles, CA 90024

The Apollo lunar missions took place nearly two decades ago, and most of the largest rock samples were characterized fairly well during the first few years of intense study. However, the Apollo samples still offer important scientific opportunities. The basic reason that the Apollo collection still commands attention is that for every large rock fragment in the inventory, there are many more fragments of slightly smaller size; and for some purposes, a small rock serves nearly as well as a giant boulder. Studies of these small but important lunar samples are contributing greatly to our understanding of the lunar crust, especially its ancient highlands portion. The younger, mare portion of the crust is also the subject of ongoing studies, but in comparison with the complex, impact-bashed highlands, the mare crust is already relatively well understood.

Crust is a layer of geochemically differentiated matter near the surface of a planet. Most of geoscience concerns the nature and history of crust. Despite being only 27% as large as the Earth in radius, our Moon is endowed with a crust about three times thicker than the average crust of the Earth. In other words, crust accounts for about 10% of the Moon's volume, versus only 1% of the Earth's volume. Even so, lunar crustal evolution was virtually complete before the very oldest known crust formed on Earth (3.8 billion years ago). By 4.0 billion years ago (0.5 billion years after the origin of the Solar System), the Moon was already geologically comatose. Most of the mare crust had yet to form, but the mare crust accounts for only about 0.1–1% of the total crustal volume. Although the Moon's crust is not closely analogous to the modern Earth's crust, lunar rocks are valuable as products of an important, formative era that unfortunately seems to have left no trace on Earth. In fact, the bulk of the lunar crust is so ancient, rocks from its accessible top generally owe their final origins not to intrinsically lunar processes but to meteoritic impact processes. Meteorites are essentially stragglers, tardy participants in the process of planetary accretion, which occurred at an exponentially decaying rate starting 4.5 billion years ago. Despite rapid decline of the meteoritic flux, lunar rocks indicate that violent collisions between large meteorites and planets were still frequent as recently as 3.8 billion years ago. The most common type of rock found at the lunar surface is a welded melange of fragments of older rocks, called a polymict breccia. Textures, ages, and trace-element analyses indicate that lunar polymict breccias are products of violent crushing and heating associated with meteoritic impacts.

This polymict nature of the upper lunar crust is a true mixed blessing. The disadvantage is that almost nothing can now be found in its original place. Except at gross, near-global scales, geological relationships among all but the youngest lunar rocks have been essentially randomized by the cumulative effects of innumerable violent impacts. This disadvantage is offset by several benefits, however. One is that the Moon, even with only limited data, is extremely useful in studying the nature, and especially the rate through time, of a process of profound importance in the evolution of the planets: meteoritic cratering. A second benefit stems from the limited nature of lunar exploration. The Apollo landings were magnificent, but the samples obtained were limited in amount (the average was 64 kilograms, or about 140 pounds, per mission) and confined to tiny areas within a few kilometers of the landing points (1 kilometer = 0.62 miles). By a generous estimate, the six Apollo landings combined sampled 200 square kilometers of the lunar surface (about 0.0005% of the total). Fortunately, this limitation is partially offset by recent discoveries of lunar meteorites (see report by Marilyn M. Lindstrom, this volume) and by the mixed, polymict character of many Apollo samples. For scientific purposes, a single polymict breccia may be regarded as a naturally produced random collection of smaller samples, gathered from

many scattered places into one small package that an astronaut may conveniently grab and transport to Earth. Actually, the same might be said of any lunar soil because lunar soils also form by meteoritic mixing, except that the individual particles within soils include many that are large enough to be regarded, for some types of study, as tiny rocks.

By studying individual fragments within polymict breccias and coarse particles sieved from soils, we can, in effect, greatly enhance our clearly inadequate sampling of the lunar crust. A fairly typical lunar polymict breccia (in this case a small lunar meteorite) is shown in figure 51. The number of discrete multi-millimeter fragments seen here only hints at the diversity of isolable rock fragments in such a sample. Actually, the larger fragments within lunar polymict breccias are mostly polymict (mixtures) themselves. Polymict samples, including polymict fragments within breccias, owe their bulk compositions to meteoritic mixing, not to intrinsically lunar processes. Only unmixed, monomict fragments of igneous rocks, which are relatively rare in the ancient, impact-battered highlands portion of the crust, preserve direct constraints on early lunar evolution. Monomict fragments can be recognized from details of their textures (unfortunately, a simple macroscopic view is seldom sufficient; generally a thin section must also be studied) and their trace-element compositions. The compositional range of monomict rock fragments found in a single polymict breccia can be remarkable. For example, known fragments in one Apollo breccia (sample 14321) range all the way from primitive magnesian olivine-plagioclase cumulates to highly evolved potassium-feldspar granite.

Through careful searching, about 5–10 new monomict highlands fragments are found each year. Thus far, roughly 100 have been studied. Results have been intriguing. Among the older sorts of lunar rocks, at least two distinct groups seem to be present. One group, called ferroan anorthosites, stands apart from all the rest on many geochemical diagrams. (Fig. 52 shows one example.) Ferroan anorthosites also differ from virtually all other lunar rocks by containing much more of the mineral feldspar, which is the most common mineral in lunar soils and polymict breccias (and thus by implication in the crust as a whole) and also has by far the lowest density of any common lunar mineral. Currently, the favored explanation for the anomalous chemistry of the ferroan anorthosites is that they originated by flotation of feldspar over a primordial global magma ocean, produced by melting associated with the origin of the Moon. According to this model, the other old lunar rocks formed in various smaller magmatic bodies, slightly after the magma ocean epoch. This hypothesis implies that the Moon formed at an extremely high temperature, but not so hot that it was entirely molten, because the abundance of rocks other than ferroan anorthosite implies that melting occurred in stages. Last year, the first reliable age data were reported for one of the ferroan anorthosites (the unusual compositions of these rocks make isotopic dating very difficult); these studies were done by B. B. Hanan and George Tilton (University of

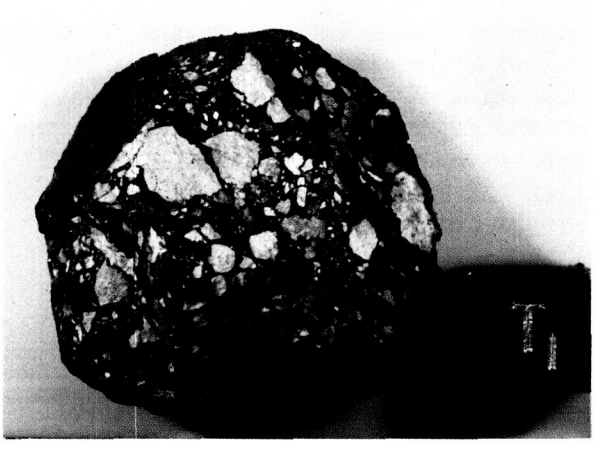

Fig. 51. Photograph of lunar meteorite Allan Hills 81005, showing abundance of discrete rock fragments that have been brought together by the natural process of repeated meteorite impacts. The cube at the right is 1 centimeter, or about 4/10 inch, on a side. Lunar rocks are seldom colorful because their cations are nearly always in low oxidation states. A comparatively recent impact, about 200,000 years ago, fortuitously transported this breccia from the Moon to Antarctica, where it was found in 1981. Five additional lunar meteorites have been found since. At 31 grams (about 1 ounce), this one is relatively small. Apollo breccias are as massive as 11.7 kilograms (about 26 pounds).

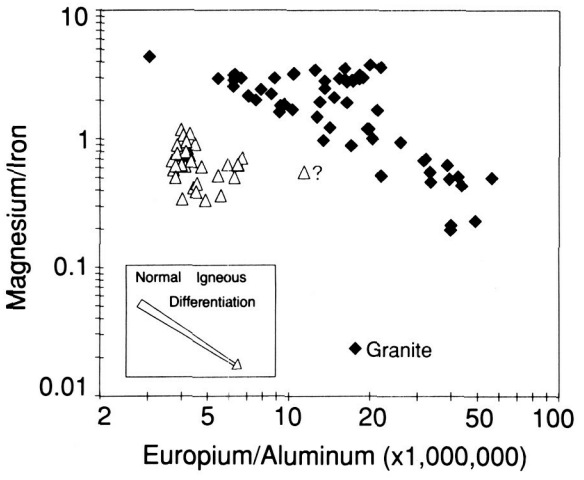

Fig. 52. Geochemical ratio diagram (weight ratio for the rare-earth element europium over aluminum versus weight ratio of magnesium over iron, using logarithmic scales) for monomict fragments of lunar highland rocks, illustrating anomalous compositions of ferroan anorthosites (triangles) in comparison with all other monomict rocks (filled diamonds). This diagram does not include data for the youngest sorts of lunar monomict rock, the distinctive mare basalts.

California at Santa Barbara) and by Rick Carlson (Carnegie Institution of Washington, Washington D.C.) and Guenter Lugmair (University of California at San Diego). These new data are consistent with the magma ocean hypothesis, albeit they have not yet confirmed it. A test of the magma ocean hypothesis will require further studies of Apollo samples as well as lunar meteorites, especially the isolation and study of additional monomict fragments. Only this year, traces of two exotic new minerals were found among lunar rocks (by Charles Meyer, NASA Johnson Space Center, Houston, and by David Vaniman, DOE Los Alamos National Laboratory, and his co-workers). Also, for the first time, the common terrestrial mineral cordierite was found in a monomict lunar fragment (by Ursula Marvin, Smithsonian Astrophysical Observatory, Cambridge, and her co-workers). Preliminary data for the cordierite-bearing fragment and others from the same polymict breccia appear to blur the distinction between ferroan anorthosites and other lunar rocks. If ferroan anorthosite proves to be just another lunar rock type, the magma ocean hypothesis, and with it many current models for the earliest development of the planets, and the Earth-Moon system in particular, would require serious revision.

Meteorites and Cosmic Dust

Platinum-Group Element Alloys in Meteorites

Joel D. Blum, Division of Geological and Planetary Sciences, California Institute of Technology, Pasadena, CA 91125

The platinum-group elements (platinum, iridium, osmium, palladium, rhodium, and ruthenium) are exceedingly rare in the Earth, Moon, and most meteorites. However, in some tiny clusters of grains within primitive meteorites, they are enriched to levels higher than in most valuable platinum ore deposits on Earth. The platinum-group elements are observed as submicroscopic nuggets of one or more metal compositions, which in turn occur clustered together with more common nickel-iron metal and sulfide and oxide minerals as small spheroidal grains called "opaque assemblages" (fig. 53). The meteorites that contain opaque assemblages are aggregates of particles that are believed to have formed by direct condensation from the solar nebula—the cloud of gas out of which the Sun and planets of our Solar System ultimately formed. Opaque assemblages have overall proportions of platinum-group elements close to what one would predict (from fundamental chemical principles) to have condensed as the first solid material from a hot part of the solar nebula as it began to cool. What is puzzling, however, is the occurrence of a wide variety of discrete metal compositions within individual opaque assemblages; in particular, each metallic phase contains only a few of the platinum-group elements rather than all of them. One possibility that has been proposed is that the various metals and sulfide and oxide minerals in opaque assemblages each formed by condensation under highly variable conditions in different source regions of the solar nebula and were later aggregated to form the opaque assemblages. This scenario, however, faces the difficult question of why the wide variety of metals and other minerals that form opaque assemblages are almost always mixed in proportions that yield overall platinum-group elemental proportions equal to those predicted for condensation of one mixture of the elements.

To understand better the origin of opaque assemblages in meteorites, the author conducted experiments in which the chemical compositions and textures of the platinum-group element alloys and sulfide and oxide minerals in opaque assemblages were reproduced by subjecting mixtures of metals to a variety of temperatures and gas atmospheres in the laboratory. The experiments demonstrate that the diverse metallic phases and other minerals could not have condensed separately and later aggregated to form opaque assemblages. Instead, opaque assemblages probably originated as homogeneous alloys of nickel and iron with the platinum-group elements dissolved within them, early in the history of the Solar System (when the dominant element in the nebular gas was hydrogen). Later in the history of the Solar System, when the nebula began to cool and small planets formed, more sulfur and oxygen were present as gases. The homogeneous alloys were unstable in the presence of these gases and

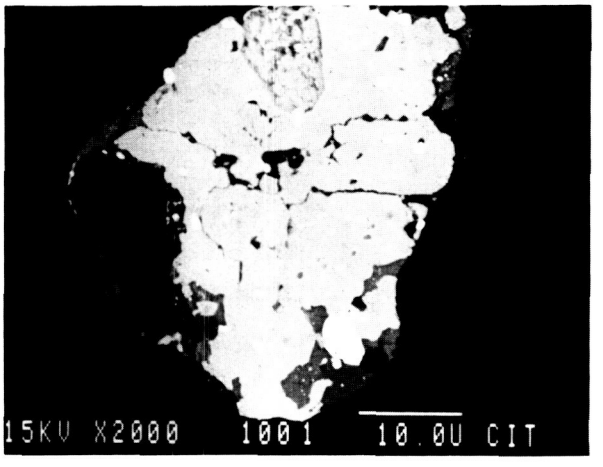

Fig. 53. Scanning electron microscope image of a meteoritic opaque assemblage rich in platinum-group elements; the scale bar is 10 micrometers (1/2500 of an inch) long. The white regions are alloys of nearly pure platinum-group elements, the light gray regions are nickel-iron alloys with lesser amounts of dissolved platinum-group elements, the gray mottled region at the top center is molybdenum sulfide, and the dark gray regions are nickel-iron sulfide and iron oxide.

reacted with them in a process similar to the rusting of steel. This caused the precipitation of the distinct platinum-group element-rich metallic phases and the sulfide and oxide minerals. Therefore, the alloys and sulfide and oxide minerals that form opaque assemblages reflect low-temperature conditions in the solar nebula and possibly the early planets, whereas the overall platinum-group element proportions in opaque assemblages reflect the early high-temperature condensation of matter from the solar nebula.

In summary, these laboratory experiments demonstrate that low-temperature reactions are capable of producing virtually all of the metals and sulfide and oxide minerals observed in opaque assemblages in meteorites. Nuggets rich in precious platinum-group elements that occur in meteorites are, therefore, not the oldest solid materials in the Solar System as was once thought; rather, they formed during the rusting of nickel-iron metal at low temperatures in the solar nebula or on early formed planets.

Basaltic Meteorites: Guides to Asteroidal Melting

Roger H. Hewins, Geological Sciences, Rutgers University, New Brunswick, NJ 08903

The eucritic meteorites are basaltic rocks (fig. 54) similar to basalts found on the Earth and Moon and apparently throughout the inner Solar System. (Basalt is one of the most common types of lava rock on Earth; it makes up most of the Earth's ocean floor, and in a few areas it forms broad plains on the continents.) Together with related igneous rocks found in diogenite and howardite meteorites, the eucrites form the howardite-eucrite-diogenite (HED) suite. These rocks are known to have formed about 4.55 billion years ago at low pressures on a small body.

The study of relationships between HED igneous rocks is important in understanding asteroidal composition, asteroidal heating, and the nature of the early Solar System in general. Remote sensing has shown that one asteroid, Vesta, has surface mineralogy very similar to HED suite rocks. Other asteroids at the inner edge of the main asteroid belt were probably also heated and partly melted to form basaltic lavas, but remote-sensing results suggest that they were subsequently stripped of their basaltic crusts by impacts. Because only the asteroids closest to the Sun experienced melting, a heating mechanism such as electromagnetic induction caused by an early strong solar wind (during what is referred to as an early "T-Tauri" stage of the Sun) was probably important. In addition, heating caused by the decay of short-lived radioisotopes like ^{26}Al (aluminum) was probably also important.

Fig. 54. Eucrite basalt seen under the polarizing microscope. Elongate crystals of plagioclase feldspar (gray-white) are enclosed by pyroxene (yellow).

Edward Stolper (California Institute of Technology, Pasadena), established, by melting and crystallization experiments performed at Edinburgh University, Scotland, that most of the eucrites could have been erupted as primary (compositionally unmodified) magmas derived by partial melting of a peridotite source region like the mantles of the Earth and Moon but more iron rich. (Peridotites are rocks composed mostly of silicates of iron and magnesium.) The most common type of eucrites (asterisks in fig. 55) could possibly have formed by fractional crystallization of such primary magmas; that is, they are solidified examples of liquids produced at varied stages of crystallization of a more magnesian basaltic magma, after extraction of the previously formed crystals. This process could have operated only if the pressure dropped by about 1 kilobar (about 990 atmospheres) as the magma rose from the deep interior of the asteroid and crystallized.

It is hard to explain the whole range of basaltic compositions found in the HED suite by a single, simple process, however. Eucritic basalts having a much wider range of compositions than common eucrites have been found as fragments in howardites. Different levels of trace elements measured by Monty Smith (then at Oregon State University, Corvallis) in such rocks suggest that there are several different suites of HED basalts that formed from different parent magmas. These parent magmas do not appear to have come from the same

source region because they lie on different partial melting lines (fig. 55). This observation suggests that eucrite source areas had previously gone through an episode of differentiation before they were again melted to form the magmas that subsequently crystallized as the eucrites. That is, the eucrite parent body went through a period in which its rocks were partly melted and the melt or melts were extracted, rose toward the surface, and crystallized, at which time magma composition was modified by loss or accumulation of crystals. The diverse rocks produced by this early differentiation episode were later partly melted to form the eucrite parent magmas. Petrologic and geochemical studies of new HED meteorites collected in Antarctica (fig. 56) are eagerly awaited because it is hoped that they will clarify the complex volcanic relationships.

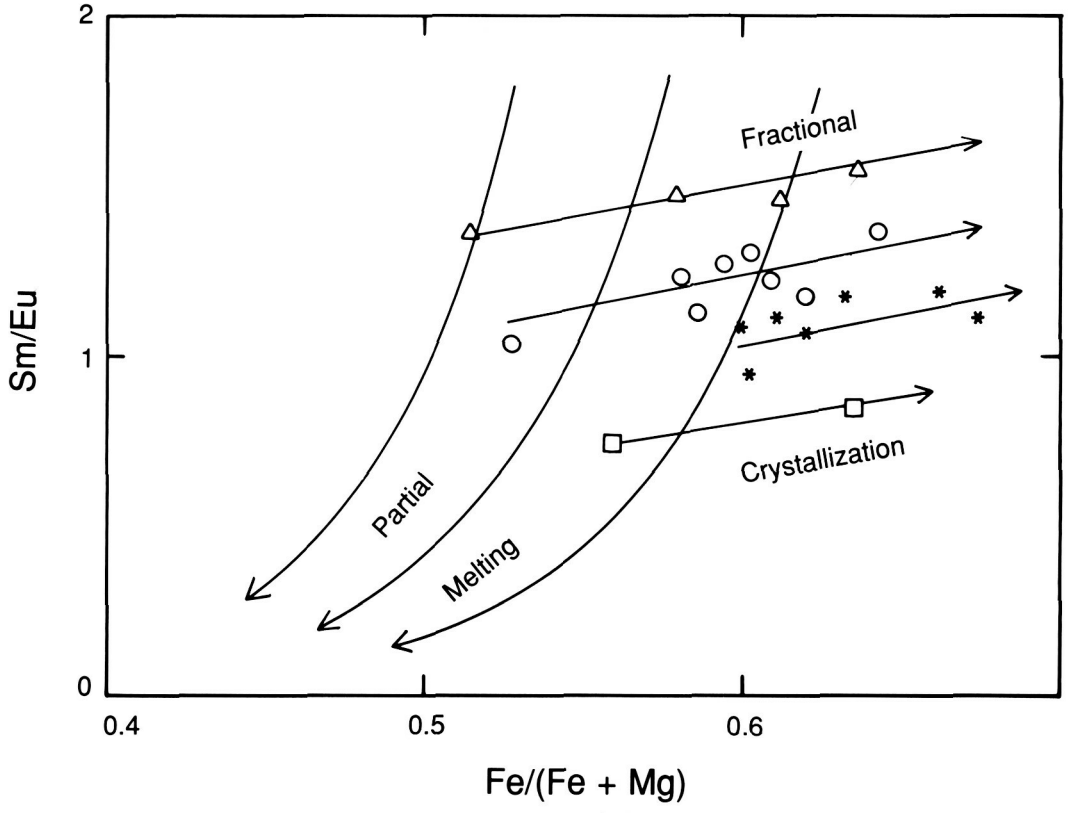

Fig. 55. Ratios of trace elements (samarium/europium, or Sm/Eu) and major elements (iron/iron plus magnesium, or Fe/Fe+Mg) of basaltic melts vary in a different way for partial melting (steep descending curved arrows) and crystallization accompanied by loss of crystals, or fractional crystallization (straight arrows trending to right). With increased partial melting, liquid compositions move down the curved arrows toward the origin of the graph; with increased fractional crystallization, liquid compositions move along the straight arrows toward the right of the graph. Four suites of eucritic basalts show variations attributable to fractional crystallization. The four suites are as follows: triangles, trace-element rich eucrites including Stannern; circles, fragments in Allan Hills 77302 polymict eucrite; asterisks, common eucrites, including Sioux County and Nuevo Laredo; and squares, depleted fragments in Kapoeta howardite. The compositions of the parent magmas of three of these suites are fairly well defined (symbols at the left end of each arrow). Since the parental magmas to the four suites appear to lie on different partial melting tracks, their source regions must have had different compositions.

The trace elements that concentrate in metallic iron are depleted in eucrites relative to undifferentiated Solar System material (chondritic meteorites). This observation suggests that a core rich in metallic iron formed on the parent body, extracting trace elements. The detailed variation of such trace elements (e.g., tungsten and molybdenum) suggested to Herbert Palme and Horton Newsom (Max Planck Institute, Mainz, West Germany), that the core formed before the melting event that formed the eucrite magmas.

In conclusion, many aspects of the geochemistry of the HED basalts are difficult to explain if their parent bodies were heated, melted, and differentiated only once but can be explained if portions of asteroidal crust and mantle that formed in an early differentiation event were remelted. Thus, the study of eucrites suggests that some asteroids experienced at least two episodes of heating and melting. Perhaps the heat source for the first episode was decay of short-lived isotopes, and the heat source for the second episode was electromagnetic induction that occurred during an early period of the evolution of the Sun in which there was an enhanced solar wind.

Fig. 56. A brecciated meteorite from Lewis Cliff, Antarctica, containing many fragments of eucritic basalt, many of which are as much as a centimeter across.

The Discovery of ^{26}Al in Ancient Planetary Material—The Quest for a Heat Source

Ian D. Hutcheon, Division of Geological and Planetary Sciences, California Institute of Technology, Pasadena, CA 91125

A long-standing problem in deciphering the early history of the Solar System is identifying the source of heat for melting in small planets. Some meteorites are igneous (once molten) rocks that clearly are the result of melting on a small planet, yet the decay of long-lived radioactive isotopes such as uranium, thorium, and potassium could not have provided nearly enough heat to initiate melting 4.5 billion years ago even on bodies as large as 1000 kilometers (just over 620 miles) in diameter. This problem was addressed by Harold C. Urey of the University of Chicago in 1955, who recognized that the presence of *short*-lived (and now extinct) radioactive isotopes in the early Solar System could have provided an adequate heat source if they were sufficiently abundant. In particular, an isotope of the abundant element aluminum—known as ^{26}Al (with a half life of approximately 720,000 years)—is a major candidate. Because any ^{26}Al initially present in the Solar System would have decayed completely after only a few tens of millions of years, the only way to test Urey's hypothesis was to find evidence for an excess abundance of the daughter product of ^{26}Al, namely ^{26}Mg.

Early attempts to find evidence of extinct ^{26}Al were unsuccessful, and it was concluded that this isotope was not an important heat source for early planetary melting. During the mid-1970's, however, Typhoon Lee, Dimitri Papanastassiou, and Gerald J. Wasserburg of the California Institute of Technology (T. Lee now at Academia Sinica in Taipei, Taiwan) found small excesses of ^{26}Mg in material from the Allende carbonaceous chondrite meteorite. Calculating backwards to 4.5 billion years ago, they estimated the initial abundance of ^{26}Al to be about 50 parts per million of the total aluminum, more than sufficient to melt planetary bodies more than a few kilometers in size *providing that these samples are representative of the entire Solar System.*

Since that time, the presence of ^{26}Al has been confirmed in nine additional chondrite meteorites. However, two facts have prevented a firm assessment of the Solar System-wide distribution of ^{26}Al derived from these data: (1) the occurrence of radiogenic ^{26}Mg (*i.e.*, derived from the decay of ^{26}Al) is restricted to rare, aluminum-rich inclusions that comprise only a minor fraction of normal meteoritic material; and (2) the initial abundance of ^{26}Al inferred from the data is not constant, and many samples show little or no evidence for its having ever been present. In particular, no evidence for ^{26}Al has ever been found in igneous meteorites—the very meteorites for which the heat source is being sought. These observations have led most scientists to conclude that ^{26}Al was heterogeneously distributed in the solar nebula.

If ^{26}Al was a major heat source on small planets, some evidence should be preserved in "old" igneous rocks that cooled on a time scale comparable to the half-life of ^{26}Al. The preservation of isotopic effects is strongly affected by the extent of thermal and chemical reprocessing experienced by a meteorite since its formation. Therefore, the search for evidence of ^{26}Al has focused on those meteorites that show the least evidence of such reprocessing, referred to as "unequilibrated" chondrites; in particular, a chondrite known as Semarkona is one of the least reprocessed of all chondrites.

Recently, Robert Hutchison (British Museum), Colin Alexander (formerly at the University of Essex; now at the Open University, Milton Keynes) and David Barber (University of Essex) found a fragment of an igneous rock in Semarkona that contains the calcium-aluminum feldspar known as anorthite. This 1-millimeter diameter fragment (roughly, 1/25 of an inch) of

what was once a larger rock is named CC-1, and has properties in common with some lunar rocks and some igneous meteorites. Anorthitic feldspar is relatively abundant in reprocessed (equilibrated) chondrites, but is thought to be a product of that reprocessing. The anorthite in the Semarkona fragment differs from that in the equilibrated chondrites in containing no detectable sodium, indicating that the fragment formed at much higher temperatures than the feldspar in the equilibrated chondrites.

The fragment CC-1 (see Fig. 57) was found in a 10-micron thick polished section of Semarkona, so its isotopic composition could not be analyzed by conventional mass spectrometric techniques. The magnesium isotopic composition was therefore analyzed using an ion microprobe, which uses a finely-focused beam of oxygen ions to sputter material from an area of only a few micrometers (1 micrometer is approximately 1/25,000 of an inch) in diameter on the surface of the sample; the sputtered ions are then directed to a mass spectrometer where the isotopic composition can be determined.

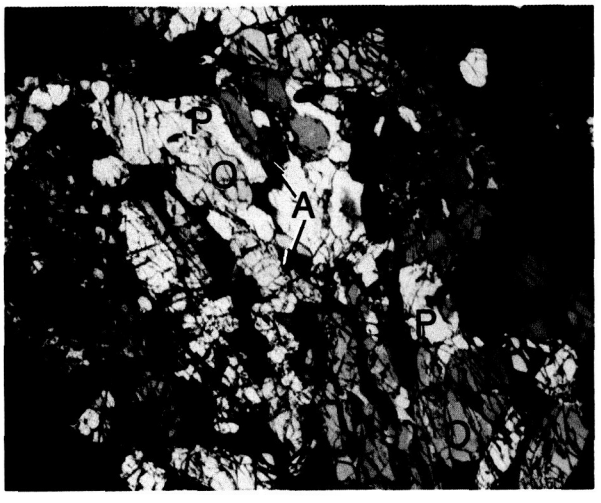

Fig. 57. Photomicrograph of the Semarkona fragment CC-1, taken with an optical microscope. Polarized light was used for illumination, so different minerals are revealed by different colors. The elongate yellow crystals are olivine (O), while the white or gray crystals are pyroxene (P). The anorthite (A) containing excess ^{26}Mg can be seen in the center of the fragment as the small crystal that appears half light and half dark. The small spot in the center of the anorthite is the hole produced by the ion microprobe beam. The entire fragment is approximately 1 millimeter (1/25 of an inch) across.

The isotopic data from CC-1 show small but clear excesses of radiogenic ^{26}Mg that can be attributed to the former presence of ^{26}Al. These data indicate that ^{26}Al was relatively abundant when CC-1 formed, approximately 8 parts per million of the total aluminum. The Semarkona fragment is the first object with a normal "planetary" composition to exhibit evidence for live ^{26}Al when it formed, as opposed to the aluminum-rich inclusions in carbonaceous chondrites that are thought to have formed in the solar nebular cloud long before planetary bodies accreted. The chemistry and mineralogy of CC-1 show that it formed by melting on a small planet, and could not easily have formed in the solar nebula. Thus, the presence of excess radiogenic ^{26}Mg in Semarkona fragment CC-1 indicates that small planets accreted early enough to have incorporated a substantial amount of ^{26}Al. Accordingly, the time scale for accretion and differentiation (melting) of small planets must have been comparable to the half life of ^{26}Al, ~1 million years. These data are the first direct evidence that asteroidal-sized bodies formed and began to melt within a few million years after the origin of the Solar System. Because the Semarkona fragment is more representative of normal Solar System material than are the aluminum-rich inclusions in carbonaceous chondrites, the isotopic data for CC-1 provide evidence the ^{26}Al was reasonably widespread in the early Solar System. If ^{26}Al was present in the nebula at the levels found in CC-1 (8 parts per million), it would have been the dominant heat source in all planetary bodies that formed very early. Such an abundance would heat the center of a 100 kilometer diameter body to a temperature in excess of 1250°C, causing incipient melting.

It should be remembered that the inferred ^{26}Al content for CC-1 refers to the abundance of ^{26}Al when CC-1 solidified. If planets formed earlier,

when less ^{26}Al had decayed, melting would have been more widespread. For smaller bodies, heat loss due to conduction would have been significant, resulting in a lower maximum temperature. For a 40 kilometer diameter body, 1 ppm of ^{26}Al would have heated the interior to temperatures in excess of 600°C, not high enough to produce melting but more than sufficient to cause widespread recrystallization. Thus, even if widespread melting did not occur, the Semarkona data demonstrate that ^{26}Al played a major role in thermal reprocessing on small planets.

Presolar Interstellar Diamonds in Meteorites

Roy S. Lewis, Enrico Fermi Institute and the Department of Chemistry, University of Chicago, Chicago, IL 60637

Scientists have come to realize in the last 18 years that primitive meteorites (called chondrites) contain small amounts of exotic material from outside the Solar System. This material can be recognized by its anomalous isotopic composition. One such component—known as xenon-HL—has isotopic ratios differing up to twofold from solar values. As xenon is a gas, it must be contained in a solid "carrier", which obviously must itself be exotic. This carrier, constituting less than 0.03% of the meteorite, is some form of carbon. It also contains anomalous nitrogen, further proof of an exotic origin.

Recently, the carrier of this anomalous xenon has been separated from the rest of the meteorite, including most of the carbon, in sufficient purity to allow its identification (fig. 58). It consists of very small (26 Ångstroms; approximately 1/10,000,000 of an inch) diamonds along with some kind of amorphous carbon. The final stage of separation is quite dramatic, as the black suspended sample suddenly turns white when the last traces of ordinary carbon are removed. The diamonds have been identified in several ways, including analytical electron microscopy, electron diffraction, X-ray diffraction, chemical resistance, and visual appearance.

It was a complete surprise that diamonds are the carrier of the anomalous xenon. Diamonds of

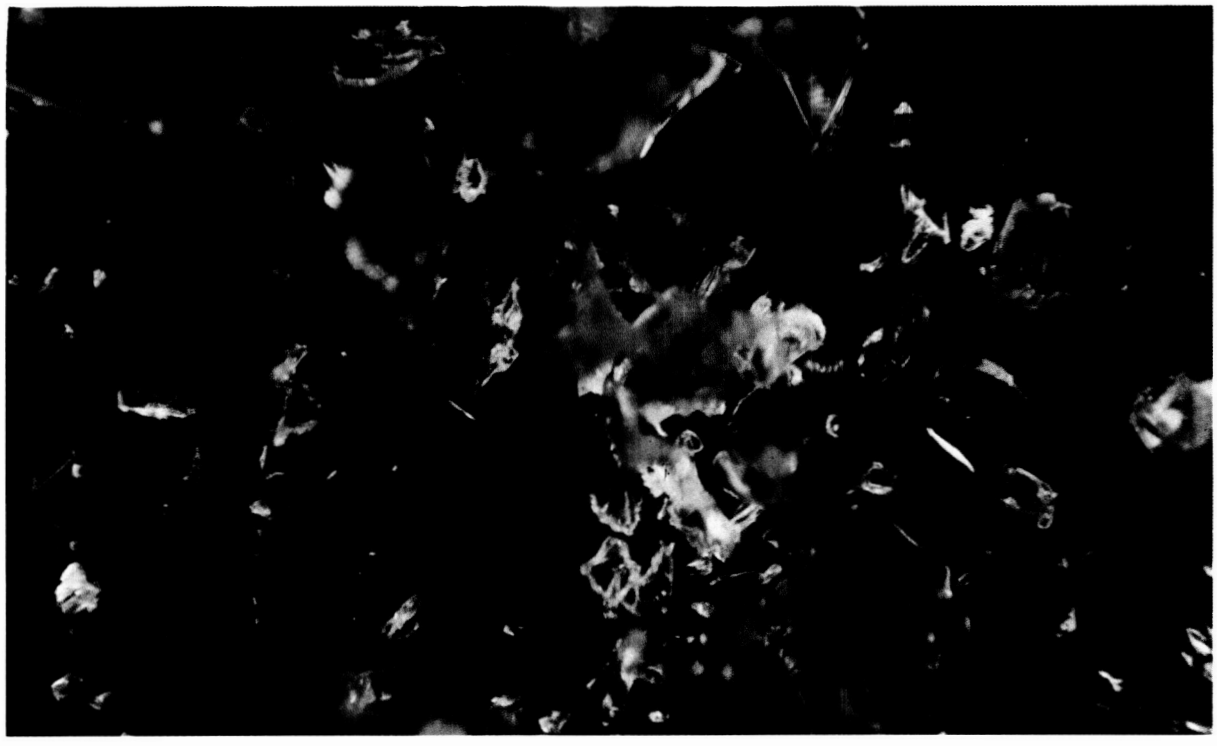

Fig. 58. Purified presolar diamonds, dried and crushed. The field of view is 1 millimeter wide (roughly 1/25 of an inch). These are all aggregates, the individual 26 Ångstrom (1/10,000,000 of an inch) crystals being much too small to be resolved by an optical microscope. The dark yellow-brown color, going to black in thicker pieces, is almost certainly due to the absorption of light by the extrasolar nitrogen trapped within the diamonds. At a few thousand parts per million, the nitrogen is the next most abundant element in the diamonds after carbon.

another kind had previously been found in some rare and very different meteorites from the ones studied in our work. Those diamonds were made in high-speed collisions (either in space or on Earth) when shock pressures briefly reached greater than 100,000 atmospheres converting some graphite into diamond. In contrast, the meteorites that contain anomalous xenon were never involved in such violent collisions. Moreover, the diamonds inside these meteorites could not have formed like the diamonds on Earth at high static pressures inside a large planet. Some new mode of formation must be involved.

As the isotopic evidence for a presolar origin seems compelling, these diamonds most likely formed in the gas shell ejected by a star when the gas had cooled enough for carbon vapor to condense into solid grains. On first thought, such an origin for diamonds seems unlikely. Pressures in such a gas shell are many millions of times lower than those needed to make diamonds in the Earth's mantle and in conventional laboratory synthesis. Recently, however, Russian and Japanese workers have synthesized diamonds by metastable growth at low pressures in conditions similar to those in gas shells expelled by stars. Evidently, what man can accomplish, nature has done before.

These diamonds may be the oldest solid objects we have, predating the earth and every other thing formed in the Solar System. Astronomers have long known that old stars (red giants) shed gas shells, which on cooling yield dust grains. The present work suggests that at least in some cases the dust includes diamonds. Later, when the star explodes as a supernova, atoms of *e.g.* xenon-HL are ejected at high speed and are buried within the dust grains when they overtake them. There is evidence that a massive supernova exploded near the forming Solar System and contributed material to it. Perhaps the diamonds came in large part from the same supernova. Now we can directly analyze such stardust, which must carry as a record of its formation the whole periodic table of the elements. While such analysis may be exceedingly difficult, with many elements too low in abundance to be measured, surviving presolar grains offer a unique opportunity to analyze in detail the actual material of other stars.

Methods for purifying and for examining this exotic material have continued to improve and have now shown that neither the diamonds nor the xenon are completely uniform: there may be several varieties. The challenge for the future will be to understand the origin of all of these varieties and what their survival implies regarding the formation of the Solar System.

Antarctic Meteorites: Down to Earth Search for Extraterrestrial Materials

Marilyn M. Lindstrom, NASA Johnson Space Center, Houston, TX 77058

Meteorites are fragments of various Solar System bodies, including asteroids, comets, the Moon, and other planets, which have survived transit through the atmosphere and collision with the Earth. Most meteorites are ancient rocks that have ages very close to the age of the Solar System (about 4.5 billion years old). They therefore provide a record of early Solar System history. Some meteorites (called chondrites) are very primitive rocks formed, in the solar nebula or cores of comets, before the planets accreted. Others (meteorites called achondrites, irons, and stony irons, or, collectively, differentiated meteorites) formed by processes that took place on asteroids or planets, after these bodies accreted from the solar nebula.

The discovery in 1969 of a concentration of meteorites on Antarctic ice led to extensive Antarctic meteorite collection programs by both the United States and Japan. Between 1973 and 1986, approximately 8800 meteorite specimens were recovered from Antarctica (see fig. 59), more than tripling the number of known meteorites on Earth. The U.S. Antarctic collection includes about 3400 meteorites, 700 of which were collected during the most recent field season, in 1987–1988.

The U.S. Antarctic Meteorite Program is a collaboration between the National Science Foundation (NSF), the National Aeronautics and Space Administration (NASA), and the Smithsonian Institution (SI), in which NSF is responsible for collecting specimens and NASA and SI are responsible for curating them. The goal of this program is to provide a continuous supply of new meteorite specimens for scientific research on the evolution of the Solar System.

A current and controversial topic in meteorite research concerns whether the nature of meteorites arriving on Earth has changed with time. To investigate this question, the Antarctic meteorites whose terrestrial ages are between 10,000 and 700,000 years (those that arrived on Earth between 10,000 and 700,000 years ago) are being compared to meteorites that arrived more recently (those that were observed to fall in historic times and were collected shortly after they fell). The proportions of differentiated meteorites and various types of primitive chondrites differ between Antarctic meteorites and more recent arrivals. Noting these differences, Michael E. Lipschutz (Purdue University, in West Lafayette, Indiana) and his co-workers have analyzed a large suite of achondrites and chondrites collected from Antarctica and from elsewhere on Earth. They have found that contents of half the elements analyzed are different in Antarctic meteorites than they are in non-Antarctic meteorites. Whether these differences indicate that the nature of the meteorites arriving on the Earth has changed with time is now being debated on the basis of considerations of statistics and orbital dynamics.

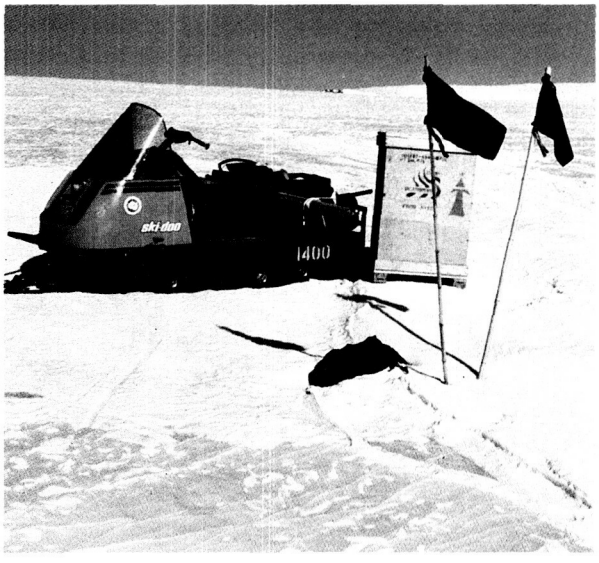

Fig. 59. Collection of 110-kilogram (about 240 pounds) chondrite Lewis Cliff 85320 in Antarctica.

Meteorite research often focuses on the unusual specimens because such samples commonly contain unique clues to the processes that formed meteorites. During the past year, two small unique meteorites have been the subject of considerable attention. One is a 12-gram (about 4/10 ounce) primitive chondrite, Allan Hills 85085, which has characteristics intermediate between several different meteorite classes. The other is a 7-gram (about 1/4 ounce) achondrite, Lewis Cliff 86010. In this rock, the interrelations of the mineral grains indicate that it crystallized from a silicate liquid (probably on an asteroidal body), but its bulk composition is similar to that of primitive chondrites. Both meteorites are discussed in more detail in other sections of this volume (see articles by Edward R. D. Scott and Gordon A. McKay).

In 1982, a meteorite that clearly came from the Moon was found among the Antarctic meteorites (fig. 60). This discovery has been of considerable importance to both meteoritics and lunar science. Before 1982, theories on the formation of meteorite impact craters had argued that rocks ejected at their escape velocities from planetary bodies as large as the Moon could not survive intact. Finding meteorites from the Moon on the Earth forced modifications to those theories and lent credence to the proposal that certain meteorites, shergottites, nakhlites, and chassignites (SNCs), are rocks from Mars. The SNCs are discussed in more detail in another section of this volume (see article by John Longhi).

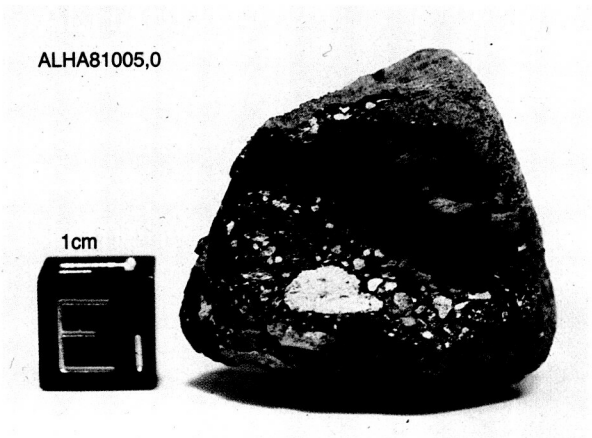

Fig. 60. Lunar meteorite Allan Hills 81005 is a complex breccia containing fragments of anorthosite (a rock consisting almost entirely of the mineral plagioclase feldspar). The meteorite has a thin fusion crust, formed as its surface melted during transit through Earth's atmosphere. The cube at the left is 1 centimeter, or about 4/10 inch, on a side.

In the last 5 years, five additional lunar rocks have been identified in the Japanese collection of Antarctic meteorites. It is important to know how many impacts these meteorites represent. The meteorites have been studied by a number of geochemical and petrologic techniques. The meteorites are all complex breccias; that is, they are mixtures of fragments of various rock types. They have similar bulk compositions and contain similar assemblages of fragments, but they are not identical. Studies by Kuni Nishiizumi and coworkers (University of California at San Diego) of isotopes created by exposure to solar radiation (on the lunar surface and in space but not on Earth because of the protective effect of the atmosphere) have shown that the meteorites have different terrestrial ages. It is therefore likely that the analyzed lunar meteorites were blasted off the surface of the Moon by at least two different impacts.

In conclusion, during the last 15 years, the Antarctic meteorite collection programs have provided a continuous supply of new extraterrestrial materials. These materials have yielded information on the origin and evolution of the Solar System. Continued collection of these fascinating rocks is expected to yield further valuable insights into the history of the Solar System.

The Parent Magmas of the SNC Meteorites

John Longhi, Lamont-Doherty Geological Observatory, Palisades, NY 10964

For many years, there were two good reasons why most planetary scientists believed that all meteorites came from the asteroid belt. First, most meteorites have formation ages close to the age of the Solar System (4.55 billion years). Therefore, the presumption was that old meteorites come from planetary parent bodies that cooled off quickly enough to preserve their ancient rocky crusts and mantles. The asteroids, which have radii of a few tens to a few hundreds of kilometers, are ideal sources because their small sizes would have allowed any accretional heat to escape rapidly and would have prevented heat generated by radioactive decay from building up. In contrast, the Moon, with a radius of 1740 kilometers (or 1080 miles), was geologically active for at least 2 billion years and the Earth, which is larger still, is of course still active. Second, the larger the planetary body, the stronger its gravitational field and consequently the more difficult it is for an incoming meteorite to strike a planet and accelerate fragments of the planet beyond its escape velocity. Until 1982, the absence of known meteorites from the Moon provided a calibration point: planetary objects smaller than the Moon were acceptable sources for the Earth's meteorites, whereas larger objects (e.g., planets such as Mars or Venus) were unacceptable.

The conventional wisdom began to be contradicted about 10 years ago when new radiometric dating by Larry Nyquist and co-workers (NASA Johnson Space Center, Houston) showed that a disparate group of meteorites, the shergottites, nakhlites, and chassignites (SNCs), apparently had crystallization ages of 1.3 billion years or less—2 billion years younger than the youngest lunar rock returned by the Apollo missions. It seemed that these meteorites (fig. 61) must have come from a very large, planet-sized, parent body. Subsequently, Richard Becker and Robert Pepin (University of Minnesota, Minneapolis), and Donald Bogard and co-workers (NASA Johnson Space Center, Houston), found that one shergottite contains what seems to be trapped gases from the atmosphere of Mars—nitrogen and argon isotopic ratios in glass are very similar to ratios of these isotopes measured in the martian atmosphere by the Viking mission. The recent discovery of lunar rocks among the meteorites collected in Antarctica demonstrates that samples of one planetary body can indeed be blasted off that body by impacts and arrive relatively intact on the surface of another planet. Although some healthy skepticism remains, most planetary scientists now regard the SNCs as the meteorites from Mars.

What are the SNCs? They are igneous rocks, crystallized from magmas (silicate liquids), and they consist of plagioclase feldspar (calcium-, sodium-, and aluminum-rich silicate minerals) and pyroxenes and olivine (iron-, magnesium-, and calcium-rich silicate minerals). Although oxygen isotope ratios measured by Robert Clayton and Toshiko Mayeda (University of Chicago, Chicago) clearly show that the SNCs are not from the Earth, the SNCs have several chemical features (the presence of water, ferric iron, and alkali feldspar) that are more like terrestrial igneous

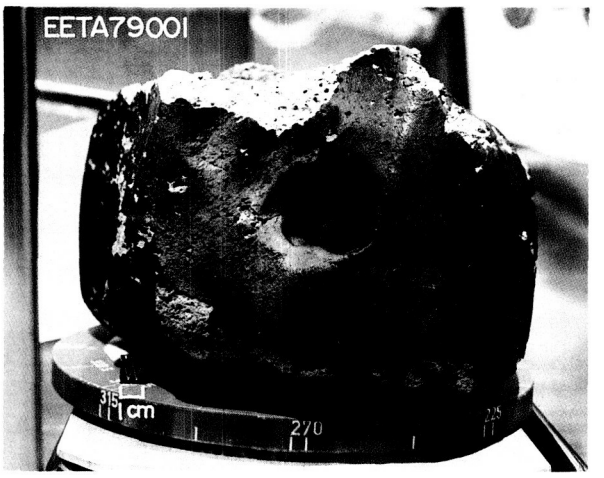

Fig. 61. Possible martian meteorite Elephant Moraine A79001 is a basalt with some vesicles and a dark fusion crust.

rocks than other groups of meteorites or lunar rocks.

Despite intensive efforts by several research groups to extract as much petrogenetic information as possible from the SNCs, with measurements of mineral compositions, trace-element concentrations, and isotopic ratios, scientists have had only a vague idea about the major-element compositions (i.e., concentrations of oxygen, silicon, aluminum, calcium, iron, and magnesium) of the magmas from which the SNCs crystallized. Most of the SNCs are not lava rocks that solidified quickly, preserving the compositions of their parent magmas; rather, they represent more slowly cooled mixtures of crystals and liquid. Because of probable migration and chemical alteration of liquid during slow cooling, determining the original liquid composition is not always straightforward. A new iterative technique developed by the author that combines data derived from melting experiments with computergraphic representations of those data makes it possible to reconstruct the composition of the parent magma from the mineral compositions.

The following scenario emerges from the constraints imposed on melting and source region composition by the combination of major-element, trace-element, and isotopic data: the shergottites that have been found in Antarctica (samples referred to as Elephant Moraine A79001 and Allan Hills A77005) crystallized from high-temperature magmas (1300°C) that were generated by remelting of a source rock that was low in aluminum, depleted in light rare-earth elements (lanthanum, cerium, neodymium, etc.), and had been strongly differentiated more than 4 billion years ago (by melting followed by extraction of the liquid or by melting followed by accumulation of pyroxene in the liquid). The nakhlites and chassignites crystallized from parent magmas that also came from a previously differentiated source region, but the parent magmas of these meteorites have markedly elevated concentrations of the light rare-earth elements as shown by Monty Smith and co-workers (Oregon State University, Corvallis), which suggests that melting was a two-stage (or more) process. The first stage of melting may have produced a carbon dioxide-rich magma. The classic shergottites, Shergotty and Zagami, crystallized from magmas that initially were similar to those that produced the Antarctic shergottites, but as these magmas rose to the surface they apparently assimilated ancient rock enriched in potassium and the light rare-earth elements. This assimilated rock resembles terrestrial continental crust more closely than it does any other lunar or meteoritic material.

What do the SNCs tell us about Mars? Primarily, they tell us that Mars has had a complex geological history, that its interior is extensively differentiated by episodes of melting, and that beneath the extensive lava flows visible on the surface there may be an ancient crust compositionally like the Earth's continents. It follows that any single sample-return mission to Mars is bound to be geologically incomplete.

Lewis Cliff 86010—A Unique Antarctic Meteorite: Possible New Clues to the Early History of the Solar System

Gordon A. McKay, NASA Johnson Space Center, Houston, TX 77058

A fundamental goal in planetary science is to learn more about the earliest history of the Solar System. Most of our information about this period comes from detailed studies of meteorites. Meteorites are thought to have formed on various parent bodies, which are believed to have formed through accretion of dust that condensed from the hot gas cloud, or solar nebula, from which the Sun was formed. The ultimate physical, chemical, and isotopic characteristics of a meteorite are the combined result of (1) nebular processes such as condensation, transportation, and mixing of dust grains and (2) planetary processes such as chemical and thermal processing of initially primitive material within the parent body of the meteorite. The goals of studying any meteorite include (1) understanding the planetary processes that gave rise to that meteorite on its parent body and (2) trying to look back through those processes to understand the nebular processes that gave the parent body its fundamental chemical and isotopic characteristics.

The meteorite Angra dos Reis (ADOR) is particularly informative regarding the nature and chronology of events in the early Solar System. First, its ratio of radiogenic ^{87}Sr (strontium) to nonradiogenic ^{86}Sr is among the lowest ever observed, implying that strontium in ADOR was isolated from the radioactive parent element, rubidium, very early in Solar System history, before that in almost all other meteorites. Moreover, ADOR has a very old crystallization age, 4.54 billion years, indicating that its isotopic and chemical characteristics have been undisturbed since very early times. Finally, the abundances of a number of key elements in ADOR are highly fractionated, indicating that its precursor material underwent extensive nebular or planetary processing.

Several questions arise regarding how ADOR acquired its unusual characteristics. To what extent are those characteristics the result of nebular rather than planetary processes? Did the separation of strontium from rubidium occur in the solar nebula prior to the accretion of the parent body of ADOR? Was the separation a result of volatility differences or igneous differentiation early in the history of the parent body? Is ADOR from the same parent body as another group of old differentiated meteorites called basaltic achondrites, with differences in intensity and timing of planetary processing being responsible for the differences in chemical and isotopic characteristics? Or, are they from separate parent bodies that acquired different chemical and isotopic characteristics as a result of nebular processes? Can the effects of planetary processes be unraveled to reveal the composition of the parent body of ADOR, to understand the nebular processes which produced that composition?

Answering these questions has been difficult because the nature of the planetary processes involved in the formation of ADOR are not well understood. Additional meteorites related to ADOR might shed light on these processes. Unfortunately, until recently no other meteorites were known to be related to ADOR. Therein lies the significance of Lewis Cliff 86010 (LEW 86010), a unique meteorite (fig. 62) recently collected from an ice field near Lewis Cliff in Antarctica. Preliminary examination of this sample by Brian Mason (Smithsonian National Museum of Natural History, Washington, D.C.) suggested a number of chemical and mineralogical similarities to ADOR. Several research groups including Martin Prinz and co-workers (American Museum of Natural History, New York), Jerry Delaney and Steve Sutton (Rutgers University in New Brunswick, N.J., and the Brookhaven National Laboratory in Upton, N.Y., respectively), the author and coworkers (NASA Johnson Space Center, Houston)

and Cyrena Goodrich (University of Arizona, Tucson) performed detailed petrographic investigations of this sample, which confirmed and elaborated on Mason's findings. The similarities include unusual enrichments or depletions in a number of elements. For example, in both meteorites, the mineral pyroxene is unusually enriched in aluminum and titanium and depleted in sodium. Moreover, olivine, another common meteoritic mineral, is unusually enriched in calcium in both samples. In addition, ion microprobe analyses of the rare-earth elements, a particularly diagnostic group of trace elements, by Ghislaine Crozaz and co-workers (Washington University in St. Louis, Missouri) also revealed strong similarities between the two meteorites. On the basis of the observed similarities, it appears likely that these samples are from the same parent body.

These studies also revealed significant differences between LEW 86010 and ADOR, which might provide important clues to differentiation processes on their parent body. The mineral grains in ADOR are highly equilibrated, as if the sample were recrystallized by a long heating episode after initial solidification. Thus, it appears

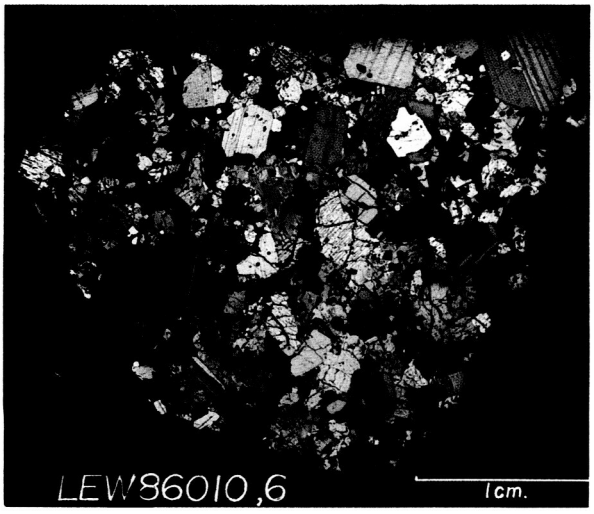

Fig. 62. Photomicrograph of a thin section of Lewis Cliff 86010 (LEW 86010) in partly polarized light. The gray striped grains are plagioclase, the yellow-gray grains with a highly fractured appearance are pyroxene, and the brightly colored grains are olivine. The shapes of the grains and their relationship to one another clearly indicate crystallization from a melt.

that the record of melt composition typically contained in igneous minerals has largely been erased from ADOR. Minerals in LEW 86010, on the other hand, still contain a record of melt evolution (fig. 62). For example, pyroxene grains show typical igneous variations in iron, magnesium, titanium, aluminum, chromium, and rare-earth elements from core to rim, in contrast to the homogeneous ADOR pyroxenes. Furthermore, crystallization experiments performed on synthetic LEW 86010 analogs by the author and co-workers produced minerals having the same unusual compositional characteristics as those in the meteorite (fig. 63). Thus, evidence supporting an igneous origin for LEW 86010, with much less recrystallization than ADOR, is unequivocal.

To understand the origin of the melt from which LEW 86010 crystallized, it is desirable to know the composition of that melt. If LEW 86010 crystallized as a closed system without differential enrichment in one or more minerals, then the composition of the melt is simply the bulk composition of the meteorite. The crystallization experiments of the author and co-workers indicated that when LEW 86010 cools below its liquidus temperature, olivine, pyroxene, and plagioclase begin to crystallize nearly simultaneously (fig. 64). This behavior makes it likely that LEW 86010 represents a crystallized melt, without differential enrichment by crystal accumulation.

One important unanswered question is the nature and origin of the volatile-depleted material that was partially or wholly melted to form LEW 86010. One possibility proposed by Prinz and co-workers is that the sample was formed by melting of a mixture of ordinary chondritic meteorite material and material similar to certain primitive highly refractory white fragments in the meteorite Allende. Future melting experiments are planned to test this hypothesis and to investigate the nature of the source region where the LEW 86010 melt may have formed. For example, with additional study, it might be possible to compute the degree of chemical fractionation which such a melting episode produced, thus allowing an estimate of what proportion of the observed chemical fractionation occurred on the parent body and what proportion occurred via nebular processes.

In summary, LEW 86010 is an extremely interesting meteorite of clear igneous origin, is probably closely related to ADOR, and most likely crystallized from a melt of its own composition. Consortia of investigators have been formed to study in greater detail the chronology, chemical and isotopic characteristics, cooling rate, and many other aspects of LEW 86010. All of these studies will be performed on a tiny sample, which is smaller than a marble (it weighs only 7 grams, or about 1/4 ounce), but which contains important clues to events that occurred during the birth of our Solar System.

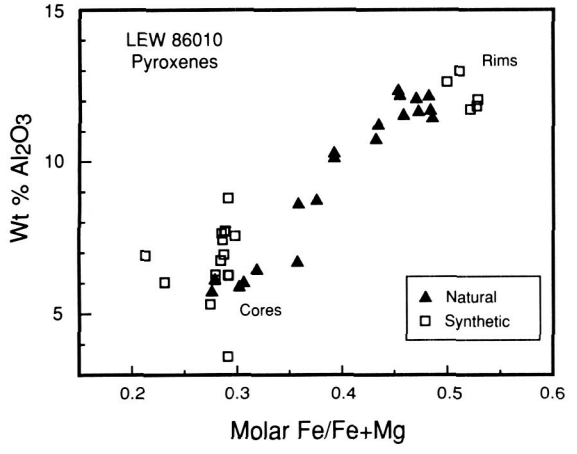

Fig. 63. Concentrations of aluminum oxide versus the ratio of iron to iron plus magnesium for pyroxenes from Lewis Cliff 86010 (LEW 86010) and a synthetic analog. The analog was prepared by melting material similar in bulk composition to LEW 86010 and then cooling it slowly and allowing it to crystallize. The unusually high aluminum content of natural LEW 86010 pyroxenes is reproduced in the synthetic sample, suggesting that the high aluminum content of the melt, rather than unusual crystallization processes, is responsible for aluminum enrichment in the pyroxenes. Pyroxenes in both the natural and synthetic samples have higher aluminum content at the rims of the crystals than at the cores, reflecting changes in the aluminum content of the melt during crystallization.

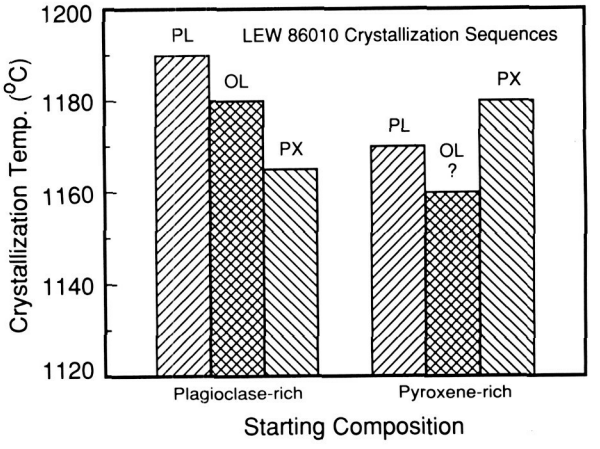

Fig. 64. Crystallization temperatures of the major minerals plagioclase (PL), olivine (OL), and pyroxene (PX) formed during cooling experiments on two synthetic Lewis Cliff 86010 (LEW 86010) analog melts. The bulk compositions of the synthetic analogs have different plagioclase to pyroxene ratios, corresponding to the range in bulk composition of LEW 86010 observed from one thin section to another. The average bulk composition of LEW 86010 probably lies somewhere between these extremes and hence would begin to crystallize all three minerals at very nearly the same temperature. This behavior suggests that LEW 86010 crystallized from a melt of its own composition. (The question mark indicates uncertainty in the crystallization temperature of olivine for the pyroxene-rich composition.)

Ureilites: Enigmatic Meteorites That Reluctantly Yield Their Secrets

David W. Mittlefehldt, Lockheed Engineering and Science Co., 2400 NASA Road 1, Houston, TX 77058

Ureilites are one of the most enigmatic groups of meteorites. These stones show a curious mixture of primitive and evolved characteristics that makes interpretation of their genesis difficult. Ureilites are composed primarily of the minerals olivine and pyroxene (silicates of magnesium, iron, and calcium) (fig. 65). Their similarity to rocks on Earth that are found as fragments of the upper mantle has led many researchers to conclude that ureilites are similarly deep-seated samples of their parent body. Ureilites are, however, rich in planetary-type noble gases (neon, argon, krypton, and xenon) and carbon. These elements are normally abundant in those meteorites that are thought to be the most primitive samples of the Solar System, the carbonaceous chondrites (meteorites unaffected by melting processes that occurred in planetary or asteroidal bodies). The ureilites have suffered extreme shock damage from one or more impacts that have obscured the original textures of the rocks. It is perhaps not surprising that models for the genesis of ureilites run the gamut from interpreting these rocks to be primitive materials formed in the solar nebula and not greatly modified by later processes to interpreting them to be samples of planetary bodies, perhaps even Venus. In spite of the conflicting signals that ureilites present, most meteoriticists currently believe that the ureilites are differentiated meteorites and are products of crystallization from magma on a planetary or asteroidal body. (Differentiated meteorites are rocks whose bulk compositions are the result of magmatic processes occurring on planetary or asteroidal bodies.)

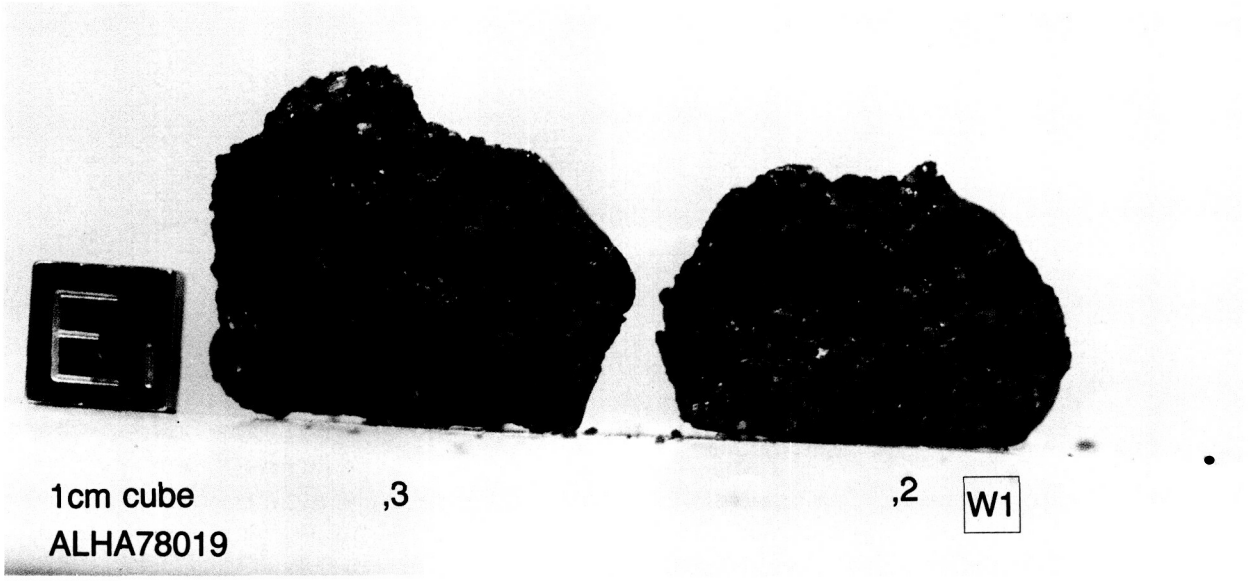

Fig. 65. The interior surfaces of Allan Hills A78019 (ALHA 78019) show the typical coarse-grained texture of ureilites. This small meteorite (30 grams weight, or just over 1 ounce) has played a key role in deciphering the history of ureilites. ALHA 78019 has not suffered the extreme shock damage common to ureilites and therefore provides unique information about textures and compositions of this meteorite group.

Until recently, one longstanding obstacle to understanding the genesis of ureilites has been the lack of high-quality chemical and isotopic data for these rocks. The ureilites are exceedingly poor in many elements, such as the rare-earth elements, that are highly diagnostic of geochemical processes. In recent years, however, much new information on the geochemistry of ureilites has been obtained, and efforts to interpret their textures have been redoubled.

Undoubtedly, the most significant and exciting new work on ureilites has been the oxygen isotope studies by Robert Clayton and Toshiko Mayeda (University of Chicago, Chicago). They discovered that, unlike all other differentiated meteorite groups and lunar and terrestrial samples, the data points for ureilites on a plot of $\delta^{17}O$ versus $\delta^{18}O$ (fig. 66) are arrayed along a line with a slope of 1. In fact, the ureilites plot along the same line that is defined by inclusions in the primitive, carbonaceous, chondritic meteorite Allende. Clayton and co-workers had previously shown that the dispersion of points along this Allende mixing line is attributable to isotopic heterogeneities in the solar nebula. (Normal chemical fractionations, in processes that occur on planetary bodies, disperse samples along lines with slopes of one-half on such a plot; this type of dispersion is what is observed for all terrestrial

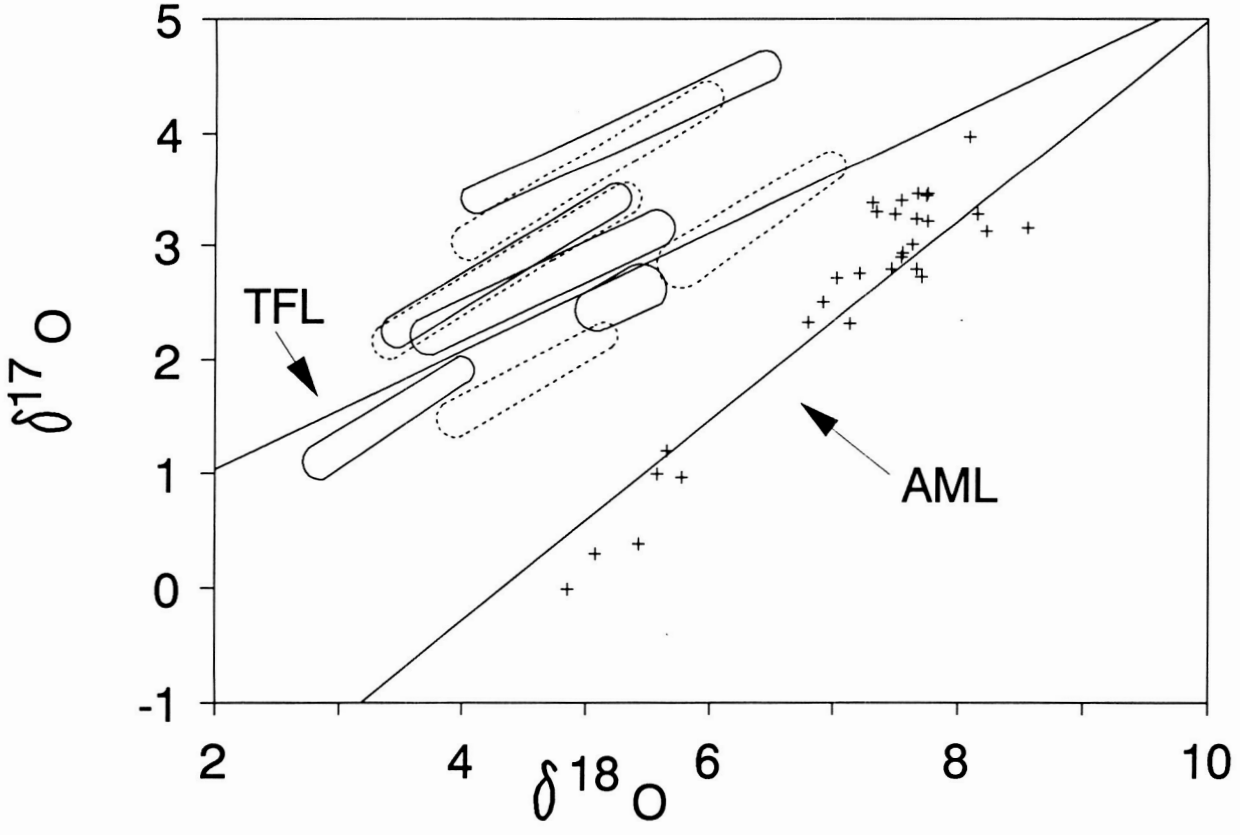

Fig. 66. A plot of $\delta^{18}O$ versus $\delta^{17}O$ for ureilites shows the anomalous oxygen isotope characteristics of these meteorites. $\delta^{17}O$ equals 1000 times ($^{17}O/^{16}O$ in the sample minus $^{17}O/^{16}O$ in a reference standard) divided by $^{17}O/^{16}O$ in the reference standard; $\delta^{18}O$ is similarly defined. AML is the Allende mixing line (slope of 1), and TFL is the terrestrial fractionation line (slope of 0.5). Solid ellipses are fields for different differentiated meteorite groups, dashed ellipses are the fields for primitive meteorite groups, and pluses are analyses of ureilites. The ureilites follow a trend with a slope of 1 that results from addition of pure ^{16}O. Most other meteorite groups follow a trend with a slope of one-half. All data are from Robert Clayton's laboratory at the University of Chicago.

and lunar samples and most other meteoritic samples.) Clayton and Mayeda conclude that models in which the ureilites were produced in a single magma cannot be correct and that the oxygen isotope data suggest that ureilites were formed from at least two separate magmas on an isotopically heterogeneous parent body. No other group of differentiated meteorites exhibits this heterogeneous oxygen isotope composition. Clayton and Mayeda have also shown that the oxygen isotope compositions may correlate with several other compositional parameters of ureilites, including bulk mineral compositions and some trace-element concentrations, implying that some of the bulk elemental and isotopic properties of the ureilites were acquired in the solar nebula and not as a result of the igneous processes that affected these meteorites during their later evolution in a planetary or asteroidal body.

The abundance of planetary-type noble gases in ureilites, sited primarily in the carbon phases, has led many researchers to suggest that the carbon and noble gases were injected into the ureilites by the meteoroid impact event(s) that produced diamonds and damaged the silicate minerals. A petrographic study by John Berkley (State University of New York at Fredonia) and John Jones (now at NASA Johnson Space Center; work done at the University of Arizona, Tucson) of the textures of the least shocked ureilite Allan Hills A78019 (ALHA 78019), recovered from the Allan Hills region of Antarctica, showed that the graphite form of carbon in this rock was not injected in an impact event but instead formed when the parent magma of the rock crystallized. This was the first conclusive evidence that at least some of the carbon was not a late addition to the rocks but was present during their igneous history. These authors went on to calculate that under moderate pressure, the noble gases could be retained in graphite, even at high magmatic temperatures. John Wacker (University of Chicago) has followed up this lead by studying the noble gases in ALHA 78019. He has shown that the noble gases are sited in a fine-grained carbon fraction and that the gases are tightly held by this carbon. Wacker interprets his results to indicate that the noble gas abundances in the carbon were established in the solar nebula and were somehow retained through the melting and crystallization that occurred in the meteorite parent body.

An important constraint on the genesis of ureilites is knowledge of the timing of the various events that produced these stones. Recently, Cyrena Goodrich, Jonathan Patchett, and Michael Drake (University of Arizona, Tucson) began performing the difficult isotopic measurements needed to set age limits on the evolutionary events of the genesis of ureilites. The preliminary results suggest that the ureilites may have been affected by one or more relatively recent events that might have occurred less than 3 billion years ago, perhaps even within the past few hundred million years.

A good, widely accepted model for the formation of the ureilites still does not exist, but recent, precise, and meticulous measurements have greatly expanded the information that we have on these enigmatic objects. The oxygen isotope results of Clayton and Mayeda will surely unleash a flurry of geochemical and petrologic studies of the ureilites. The near future will bring the genesis of these meteorites into sharper focus, with the revelation of new, exciting information on the origin of the Solar System.

Laboratory Analogs to Circumstellar, Interstellar, and Interplanetary Dust Particles

Joseph A. Nuth and Bertram D. Donn, Code 691, NASA Goddard Space Flight Center, Greenbelt, MD 20771

Robert N. Nelson, Chemistry Department, Georgia Southern College, Statesboro, GA 30460

The Earth is composed of matter that was once finely dispersed between the stars. Indeed, most of the atoms in the Earth were made in the fiery interiors of stars and expelled into the interstellar medium—sometimes quietly as part of a relatively gentle circumstellar wind and sometimes violently as part of a nova or supernova explosion. A large fraction of the ejected material was either hydrogen or helium gas, but a small amount consisted of heavier elements such as silicon, magnesium, or iron, which condensed to form tiny dust grains less than a thousand angstroms in diameter. Although these grains comprise only 1% of the mass of the galaxy, their influence is profound. They are the major source of interstellar light extinction (the scattering and absorption of starlight) and the catalyst for many of the most important chemical reactions that occur in the interstellar medium. Grains acted as a thermal blanket during the formation of the Solar System, and their specific properties determined the temperature structure of the solar nebula. The aggregation of grains in the solar nebula was the first step in the formation of the planets—had small grains been less "sticky", the planets may not have formed. To understand the formation and the evolution of the Solar System, it is important to understand the properties and history of interstellar grains.

For the last several years, we have studied the physical, morphological, and spectral properties of simple smokes, condensed at high temperatures from vapors of magnesium and silicon monoxide in hydrogen gas, as analogs to more complex materials that condense in the outflowing shells of stars. The presence of several broad features seen in these smokes in the spectral wavelength range between about 9 and 25 micrometers should be detectable in the spectra of certain stellar sources, provided that high-resolution observations are obtained. As an example, figure 68a shows the spectral changes induced in an amorphous magnesium silicate smoke produced in our laboratory as a function of the time that individual samples were heated in a vacuum at 1000 K. Samples A–G were annealed for 0, 1, 2, 4, 8, 16.5, and 30 hours, respectively. This can be compared to two spectra of the circumstellar material surrounding the irregularly varying star OH 26.5 + 0.6 shown in figure 68b. Weak features present in laboratory samples at wavelengths of 9.2, 11.5, 12.5, 18, 20, and 22 micrometers might be present in the circumstellar source; however, higher-resolution observational data will be needed to confirm this prediction. In addition to the spectral similarity between natural materials and our laboratory-produced analogs, the morphology of a typical magnesium silicate condensate, heated in a vacuum for 4 hours at

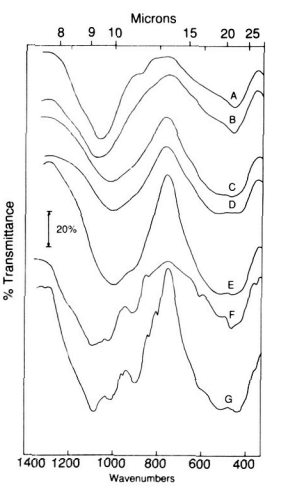

Fig. 67a. Infrared spectra of amorphous magnesium silicate smokes, heated in vacuum for O (sample A), 1 (sample B), 2 (sample C), 4 (sample D), 8 (sample E), 16.5 (sample F), and 30 (sample G) hours at 1000 K.

1000 K (shown in fig. 68a) is similar to that of a cosmic dust particle collected in the stratosphere (fig. 68b).

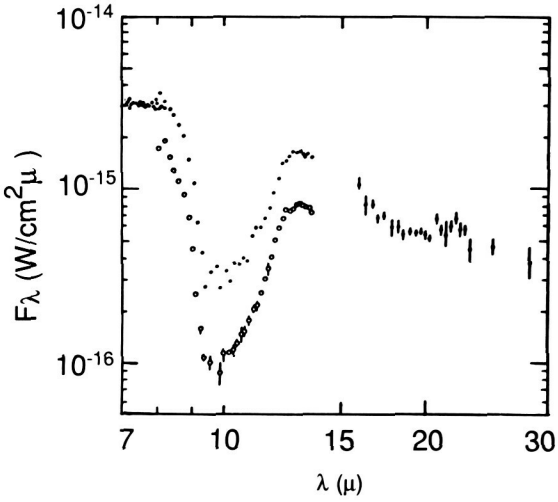

Fig. 67b. Infrared spectra of the material in the circumstellar shell around the irregularly varying star OH 26.5+0.6 at two times, approximately 2 years apart. The spectra are in units of the energy received at the earth per unit area per unit wavelength versus wavelength.

Fig. 68a. Scanning electron microscope image of an amorphous magnesium silicate smoke produced in the Goddard Space Flight Center laboratory and heated in vacuo for 4 hours at 1000 K. Scale bar is 1 micrometer long, the arrows indicate a series of hexagonal, silicon-rich plates formed during heating.

Because natural processes such as intense heating or reaction with liquid water or water vapor might change the properties of interstellar materials, it is important to understand how fast such changes occur in order to better understand the properties of the grains that exist in each type of astrophysical environment. We have measured the rate at which vacuum heating changes the spectral properties of amorphous silica smokes as a function of temperature and the rate at which amorphous magnesium silicate smokes undergo hydration in ice, liquid water, and water vapor. These simple analog studies allow us to make limited predictions about the composition and structure of refractory particulates as they are transported from the circumstellar regions in which they formed, through the interstellar medium, and into the solar nebula (the dust and gas from which the Solar System formed). It is possible that a few of these grains survived such transport with very limited processing. This is especially true of grains that have been trapped and frozen in comets and that fall into the Earth's atmosphere after having been released from the deep freeze of space by the passage of the comet through the inner Solar System. We expect that thermal annealing and hydration studies of smokes containing iron, aluminum, magnesium, silicon, titanium, oxygen, sulfur, and carbon (which we have begun to produce in our laboratory) will produce even more realistic analogs of such natural particles.

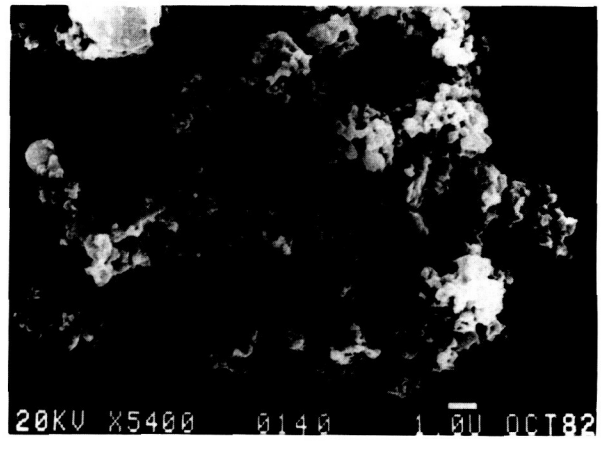

Fig. 68b. Scanning electron microscope image of an interplanetary dust particle collected in the stratosphere. Scale bar is 1 micrometer long.

The Discovery of a New Kind of Primitive Meteorite: The Unique Chondrite, Allan Hills 85085

Edward R. D. Scott, Institute of Meteoritics, Department of Geology, University of New Mexico, Albuquerque, NM 87131

During the past 5 months, excited researchers at five institutions have discovered that a 12 g meteorite found in the Allan Hills region of Antarctica is one of the most unusual primitive meteorites ever recovered. Primitive meteorites, which are called chondrites, are aggregates of diverse particles that are the oldest objects to be formed in the Solar System. Our best clues to the origin of the inner planets are contained in these rocks and the asteroids from which they are derived.

The discovery of the small Antarctic meteorite, called Allan Hills (ALH) 85085, is important for many reasons. Its constituent particles are remarkably different in size and composition from those in all other chondrites, and the rock itself comes from a previously unsampled part of the asteroid belt. The heating and aqueous alteration processes in asteroids that modified primitive particles and obscured their origins were milder for ALH 85085 than for almost all other chondrites. Finally, the chondrite is very fresh and suffered very little weathering in Antarctica. This chondrite therefore offers a new window for the study of how and why infalling interstellar dust and gas around an infant star were converted into planets, asteroids, and people.

Chondrites are mixtures of a wide variety of ingredients that formed in different environments: silicate spheroids called chondrules, which were once molten; refractory inclusions, which also formed at high temperatures and are largely composed of minerals rich in aluminum, calcium, and titanium and poor in silicon; porous, fine-grained (submicrometer to 10 micrometer; 1 micrometer is roughly 1/25,000 of an inch) mineral aggregates called matrix material; and grains of metallic iron-nickel and iron sulfide. The chondrules, refractory inclusions and metal grains are all typically about a millimeter in size. ALH 85085 (Figure 69) is remarkable in that its ingredients are 10–50 times smaller in size than, and the proportions of the various ingredients are unlike, those previously observed in other chondrites. Little is known about the cause of the brief, localized energetic events that produced chondrules and refractory inclusions in the solar nebula, the disk of dust and gas that surrounded the infant Sun. However, the diversity of particles in ALH 85085 offers many clues to the nature of these processes.

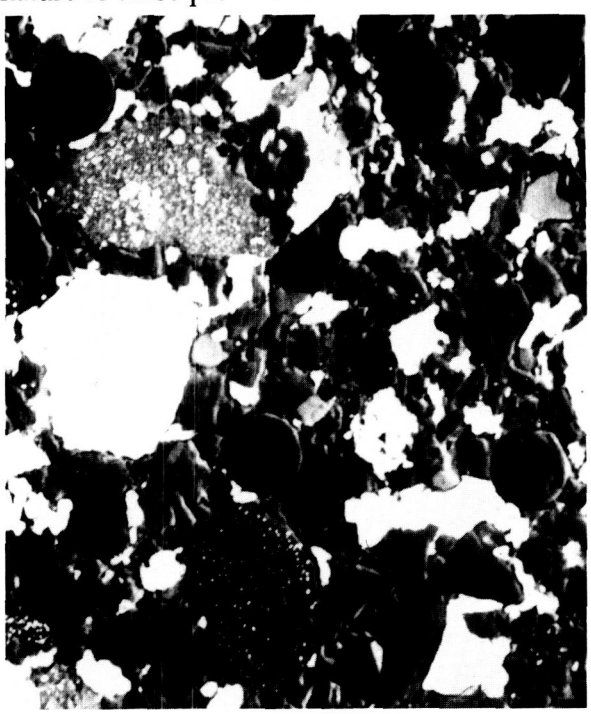

Fig. 69. Scanning electron photomicrograph of the primitive chondrite, Allan Hills 85085. This typical region, which is 150 micrometers wide (about 3/500 of an inch), contains three prominent spherical chondrules 15–20 micrometers in diameter, and numerous silicate fragments (gray) and grains of metallic iron-nickel (white), all less than 50 micrometers in size. This chondrite is unique in having such tiny ingredients, so much metal, so little iron sulfide and such low abundances of volatile elements.

Despite the unusual properties of ALH 85085 and its ingredients, nearly all researchers conclude that it is one of the most primitive chondrites ever discovered and that its ingredients formed in the solar nebula. Jeffrey Grossman (U.S. Geological Survey), Alan Rubin (University of California at Los Angeles), Glenn MacPherson (Smithsonian Institution), Michael Weisberg, Martin Prinz, Cherukapali Nehru (all at the American Museum of Natural History), and Edward Scott (University of New Mexico) all find certain mineralogical similarities between some of the ingredients in ALH 85085 and ingredients in other rare primitive chondrites. However, John Wasson (University of California at Los Angeles) believes that the differences between ALH 85085 and the other known chondrite classes are so great that ALH 85085 could not have formed in the solar nebula. In addition to the small sizes of its ingredients, ALH 85085 is remarkable in having fewer chondrules, more metallic iron-nickel, more lithic and mineral fragments, and lower abundances of iron sulfide and volatile elements such as sodium than any of the chondrite classes. Wasson therefore argues that ALH 85085 is a product of impacts on the surface of a chondritic asteroid that created tiny chondrules and metal grains. Other researchers disagree vigorously with this proposal.

During the last 10 years, isotopic measurements of chondritic ingredients have produced an impressive array of evidence to challenge the previously widespread belief that the inner Solar System was once so hot that all the interstellar dust was vaporized. All workers now accept that some fraction was not vaporized, but there is considerable controversy over whether chondrules, refractory inclusions, and matrix material were derived directly from heated interstellar dust or from grains that condensed in the solar nebula after vaporization of interstellar dust. Studies of ALH 85085 have not yet contributed toward a resolution of this question, but the volatile-poor nature of this chondrite suggests that further studies to identify clearly the reason for the low volatile content will be helpful. Grossman, Rubin, and MacPherson believe that the ingredients in ALH 85085 agglomerated in a region of the nebula that was so hot that sodium and sulfur had not condensed, whereas Scott, Weisberg, Prinz, and Nehru argue that volatiles may have been lost during chondrule formation. Whether volatiles were lost or failed to condense, the existence of ALH 85085 suggests that volatile-poor planetesimals accreted in the inner Solar System. The existence of such volatile-poor planetesimals has been invoked by several workers to explain the composition of the Earth and certain volatile-poor asteroids that melted.

A major aim of research on primitive meteorites is to deduce the place in the Solar System where each kind of chondrite and its ingredients formed and the location of the asteroid from which each is derived. Only then will it be possible to draw strong inferences about the nature of the planetesimals that accreted to form planets. The large differences between ALH 85085, another unique primitive chondrite with remarkable properties called Kakangari (which fell in India in 1890), and the various chondrite classes suggest that our sample of primitive material from which the asteroid belt was formed is remarkably incomplete. This in turn suggests that the most commonly represented class of chondrites, called ordinary chondrites, may not be so abundant in the asteroid belt and may be unrelated to any commonly observed class of asteroid.

The only samples of ALH 85085 that have been studied so far are thin sections, which have been subjected to non-destructive optical and scanning electron microscopy and electron microprobe analysis. When samples are released from the Johnson Space Center for isotopic and chemical analysis, it is likely that other exciting discoveries will be made. The recovery of ALH 85085 suggests that Antarctic meteorite recovery and studies of primitive chondrites will be fruitful endeavors for many years.

Chondrules as Recorders of Conditions in the Primordial Solar Nebula

John A. Wood, Harvard-Smithsonian Center for Astrophysics, Cambridge, MA 02138

Chondrites, the most abundant class of meteorites, are aggregations of tiny chondrules, refractory inclusions, and dust grains, that formed 4 1/2 billion years ago at high temperatures as dispersed objects in the primordial *solar nebula*—the cloud of gas and dust out of which the Sun and planets ultimately formed. The minerals in these objects contain information about the chemical and physical conditions under which they formed. To try to decode this information, we employ the condensation sequence, a table (such as that calculated by Lawrence Grossman in 1972 while at Yale University; now at the University of Chicago) which lists the minerals that would be stable in the solar nebula at any given temperature, given certain assumptions about gas composition (see below) and pressure (very low, usually assumed to be about 1/1000 atmosphere or lower).

There is a striking correspondence between the minerals in refractory inclusions and those predicted to form at high temperatures out of the solar nebula, but the mineral assemblages in *chondrules* (which are much more abundant in chondrites than are refractory inclusions) do not agree with the assemblages predicted at any temperature in the condensation sequence. For example, chondrules clearly were once molten ("igneous"), but the condensation sequence predicts their minerals would vaporize at a lower temperature than their melting range. In addition, many chondrules contain crystals of iron-rich olivine, yet the condensation sequence predicts that this mineral would be stable only at temperatures less than 500 K (approximately 440 °F), far beneath the temperatures at which the olivine must have formed.

The calculation and use of the condensation sequence rests on two principal assumptions: first, that the minerals are in thermodynamic equilibrium with one another; and second, that one can specify the bulk chemical composition of the system that produced the minerals. Grossman logically assumed that the "system" was the solar nebula, and that it therefore had the composition of cosmic or solar matter. The lack of correspondence between the minerals observed in chondrules and those predicted by the condensation sequence traditionally has been ascribed to a breakdown of the first of these two assumptions, namely a failure of the chondrules to achieve equilibrium. Chondrules are thought to have been produced by the melting of some precursor material rich in iron oxide; presumably they were molten for too short a time to vaporize away in the very low pressure environment, or for their iron to be reduced to metal and hence excluded from the crystallizing olivine.

Akihiko Hashimoto (Harvard-Smithsonian Center for Astrophysics) and I decided to test the second assumption underlying the condensation sequence, by recalculating the latter for various system compositions that differ in a more or less rational way from the cosmic abundance pattern. We have discovered that there are physical and chemical conditions under which the chondrules would be at equilibrium. Here I describe what these conditions would be for the chondrules in two important types of primitive chondrite.

A chondrule representative of those in *unequilibrated ordinary chondrites* is shown in Fig. 70. Such a chondrule would be stable at igneous temperatures if the system consisted only of the involatile (metal) elements in the cosmic mix, and enough oxygen to combine with them; in other words, all the hydrogen and most of the carbon and oxygen that made up 99.9% of the atoms in the solar nebula were missing. The chondrule would also be stable if all the cosmic oxygen and some hydrogen were present in the form of water vapor, and if the minerals formed under several atmospheres of confining pressure.

Chondrules containing iron-poor olivine and iron in the form of magnetite (Fe_3O_4), such as occur in the intensely-studied *carbonaceous chondrite* Allende (Fig. 71), would be stable at igneous temperatures in a system consisting of the involatile elements plus water vapor greatly concentrated (perhaps a thousand times) above the cosmic abundance of oxygen, again at several atmospheres of pressure.

These are bizarre requirements, greatly at odds with the conditions universally pictured for the solar nebula. To implement them, one would have to invoke settings of a very different sort. Such a setting might consist of a time and place in the nebula where temperatures were very low (less than 200 K), and water ice (snow) crystallized and clumped into icy planetesimals. The planetesimals also incorporated silicate dust, but sometimes in less than cosmic proportions. Gravity perturbations (by Jupiter?) disturbed the orbits of the planetesimals, and high energy collisions between them heated their substance to high temperatures, vaporizing the ice. As the steam and mineral matter from such collisions expanded and cooled, it could have passed through the temperature-pressure-composition regimes suggested above.

Maybe the failure of equilibrium discussed earlier is a more comfortable way to understand the properties of chondrules. However, exploration of the effect of non-cosmic compositions on equilibrium mineralogies provides interesting food for thought.

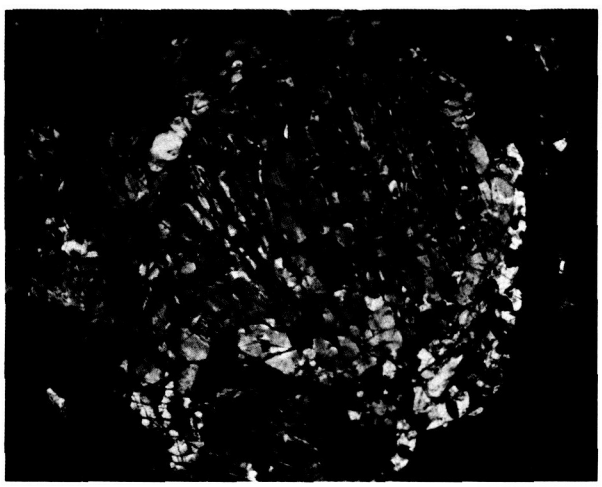

Fig. 70. Thin section of a chondrule in the unequilibrated ordinary chondrite Chainpur, illuminated by polarized transmitted light. The field is 2.6 millimeters (about 1/10 inch) wide. Brightly colored crystals are mostly iron-rich olivine (the colors are induced by the polarized illumination). Narrow spaces between the crystals contain glass, a residue from the previously molten state of the chondrule. Dark areas in the chondrule are opaque grains of nickel-iron metal and iron sulfide (troilite). In the chondrite, chondrules like this one are embedded in a matrix of fine, opaque, aggregated dust grains (the dark area surrounding the chondrule in this photograph).

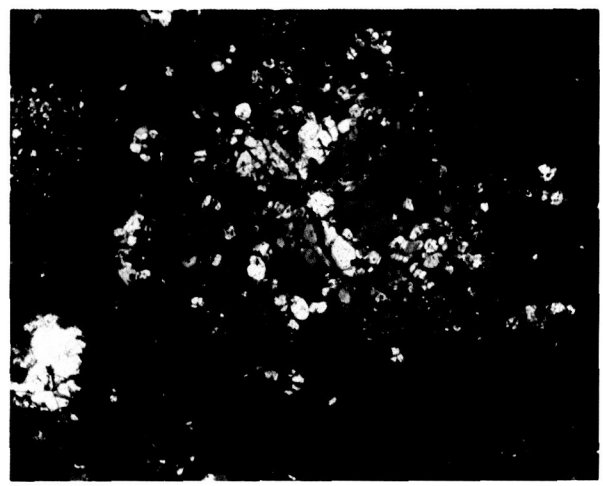

Fig. 71. Thin section of a chondrule in the carbonaceous chondrite Allende, photographed under the same conditions as Figure 70. Again, brightly-colored crystals are mostly olivine but, in this case, they are of a different morphology and are iron-poor in composition. Dark areas in the chondrule are opaque grains of magnetite, nickel-iron metal, and iron sulfide. This mineralogy would be stable in a much more oxidizing environment than is appropriate for the Chainpur chondrules. Portions of other chondrules as well as opaque matrix material can be seen surrounding the central chondrule.

Hibonites: A Glimpse at Presolar Processes Through Microscopic Grains From Primitive Meteorites

Ernst Zinner, Physics Department, McDonnell Center for the Space Sciences, Washington University, St. Louis, MO 63130

Newly developed analytical techniques have been used to study tiny mineral grains from primitive meteorites. These studies have provided information on the stellar sources that contributed material to the Solar System at its birth.

Stars form from clouds of gas and dust within galaxies. These clouds, in turn, contain material recycled both from dying stars and from newly formed ones, because both processes involve the ejection of gaseous matter. Our sun is roughly half as old as our galaxy; therefore, many different stars must have contributed to the gas and dust cloud that collapsed to form our sun and its planets. It was formerly believed that the dust contained within that cloud was completely vaporized during the collapse of the cloud. However, that idea changed dramatically about 15 years ago with the discovery of isotopic heterogeneities in primitive meteorites known as carbonaceous chondrites.

These meteorites are aggregates of the first solid particles to form in our Solar System and predate the sun and planets as we now know them; their study gives information on events that occurred during the formation of the Solar System. The discovery of isotopic heterogeneity within these meteorites demonstrated that the protosolar cloud was probably not completely vaporized, that the gas itself was not well mixed, and that interstellar grains and chemical components have been partially preserved for study. In fact, since the isotopes of all elements heavier than boron are formed by nuclear processes inside stars, the presence of isotopic variations in meteoritic samples offers the opportunity to obtain information on element formation processes in stars.

In recent years, the ion microprobe has played an increasingly important role in this endeavor. This instrument uses a highly focused beam of ions to analyze the isotopic and elemental composition of solid samples on a scale of a few micrometers (one micrometer is approximately 1/25,000 of an inch). An important example of its use is the study of individual grains of a rare mineral known as hibonite (calcium hexaluminate, $CaAL_{12}O_{19}$). Found inside carbonaceous chondrites, hibonite is believed to represent one of the very first solid substances to have formed (at extremely high temperatures) in the solar nebular cloud. Therefore, this mineral is most likely to preserve any isotopic heterogeneities that existed in the nebular cloud. Ion microprobe measurements have revealed isotopic anomalies (deviations from average solar system compositions) in the elements oxygen (O), magnesium (Mg), calcium (Ca), and titanium (Ti) within many grains of hibonite as small as 20 micrometers in size and weighing less than 10^{-7} grams (about 1/250,000,000 of an ounce).

The anomalies observed for calcium and titanium are 10–100 times larger than any found previously by analytical techniques with less spatial resolution. Two isotopes in particular, ^{48}Ca and ^{50}Ti, show departures from their "normal" Solar System values of -5.6% to $+10.5\%$ and -7.2% to $+27.3\%$, respectively. Moreover, the effects are correlated: an excess or deficiency of one isotope is accompanied by an excess or deficiency in the other. Both isotopes are known to be produced by nuclear reactions that occur during supernova explosions; their measurement in meteoritic hibonites provides us with a link to one of the most important and fascinating types of stellar phenomena.

However, measurements of the isotopic compositions of oxygen and magnesium in the same hibonite grains demonstrate that these *grains* were not themselves produced during a supernova

explosion—only some of their constituent elements. All grains measured so far with the ion microprobe contain an excess of the isotope ^{16}O relative to the other two isotopes of oxygen. Since these same grains can have either excesses or depletions of the isotopes of calcium and titanium noted above, there is no correlation between the oxygen and calcium-titanium systems. In addition, some grains of hibonite have excesses of the isotope ^{26}Mg that can be attributed to the radioactive decay of a short half-life (approximately 700,000 years) isotope of aluminum, ^{26}Al; what is most puzzling is that hibonites showing such evidence for the former presence of ^{26}Al on average do not show anomalies in calcium and titanium—the two effects are anticorrelated. Even though ^{26}AL and ^{48}Ca-^{50}Ti are produced by different types of nuclear reactions and in different stellar environments, such an anticorrelation is not expected. One clue that may lead to a resolution of this puzzle is that hibonites having calcium-titanium anomalies and no evidence for ^{26}Al appear to have formed in a relatively simple condensation or evaporation process in the solar nebula, while those without calcium-titanium anomalies but showing evidence for the former presence of ^{26}Al seem to have formed by a very complex sequence of events. Evidence for this conclusion comes from the analysis by ion microprobe of trace elements (*i.e.*, elements present at only the parts-per-million level) in the same hibonite grains.

In summary, ion microprobe analysis of the isotopic and trace element compositions of the tiny hibonite grains found in carbonaceous chondrites has revealed important information about the sources of matter from which our Solar System was formed and about the complex nuclear processes by which that matter was made. Our Solar System was formed from matter originating in a variety of stellar sources, and it was heterogeneous over a wide range of spatial scales.

A Review of Laboratory Studies of Interplanetary Dust

Michael E. Zolensky, Planetary Science Branch, NASA Johnson Space Center, Houston, TX 77058

Interplanetary dust particles (IDPs) are tiny (typically less than 100 micrometers, or roughly 4/1000 of an inch) grains that exist in space within the confines of our Solar System. They have been available for laboratory study for about one decade, during which analytical techniques have evolved to the point where we can now study the isotopic, trace element, light element, spectroscopic, and mineralogic properties of single particles through consortium studies. This kind of detailed analysis is facilitated by the fact that, although IDPs are collected and stored in only a few locations, they are widely distributed through the main curation facility at NASA Johnson Space Center. Consequently, a large number of scientists have participated in studying these particles using the diverse techniques noted above. Nanogram for nanogram, IDPs may be the most painstakingly studied of all Solar System material.

The importance of IDPs can be appreciated from examination of Figure 72. "Chondritic" IDPs include samples of dust from the primitive solar nebula, preserved from destruction during evolution of the Solar System by their residence in comets or protoplanets. Other recently discovered IDPs have cores believed to consist of interstellar dust grains that constituted part of the matter from which the Solar System was originally formed. Thus, some IDPs provide a window back through the entire history of the Solar System.

A recent important series of studies compared analyses of chondritic IDPs with those of dust particles made during the encounters of the Vega and Giotto spacecraft with Halley's comet. These studies showed that IDPs are much richer in volatile elements such as carbon than any other known extraterrestrial material, and are very similar to the dust from Halley's comet. This work thus verifies that at least some chondritic IDPs are probably of cometary origin, making their study

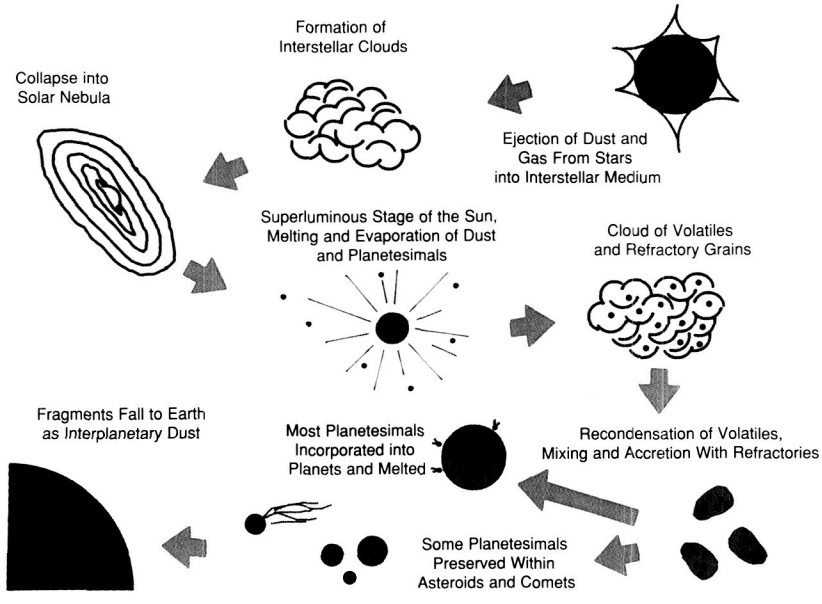

Fig. 72. The evolution of interplanetary dust particles from the original condensation of interstellar dust, through processing in the solar nebula, destruction of all but the most refractory material during the superluminous stage of the sun, recondensation of dust and incorporation into planets, asteroids, and comets, to, finally, collection on the earth.

the closest we will come in this century to the laboratory analysis of actual cometary material.

Until recently, the small sizes and friable nature of IDPs made detailed electron microscopic examination very difficult. Newly discovered techniques now make it possible, however, to slice individual particles into 1000 Ångstrom-thick (about 4/1,000,000 of an inch) sections that allow far more detailed characterization of their constituents and histories. A photomicrograph of one such sectioned IDP is shown in Figure 73. In addition to revealing details about the early history of the Solar System, the ability to make ultrathin sections of IDPs represents an important step in preparing for future analyses of actual returned cometary samples.

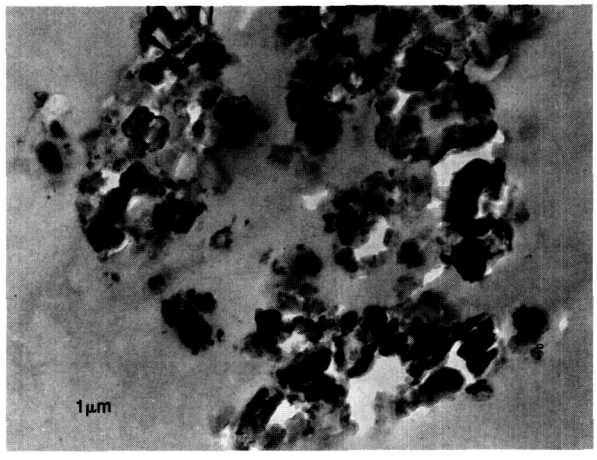

Fig. 73. A 1000 Å-thick slice of a chondritic interplanetary dust particle. Medium grey material is the enclosing epoxy. Note the extremely high porosity of this probable cometary particle. The scale bar measures 1 micrometer (about 4/100,000 of an inch). Photo courtesy of Wolfgang Klock (Johnson Space Center).

A few researchers have begun to search for IDPs that were deposited on Earth in ages past, and are now preserved in polar ices. Among other goals, this work will aid in refining estimates for the deposition rate of IDPs through time. The author and co-workers have recently discovered IDPs from ancient Antarctic ice that contain cores of the compound titanium carbide, not known as a naturally formed mineral on Earth but thought to form in the relatively cool dusty shells surrounding red giant stars. If that is indeed where these grains formed, they are true samples of interstellar dust that have great significance for the understanding of the properties of remote stars as well as for the evolution of our own Solar System. Isotopic studies that can test this idea are currently underway on these grains.

A long-term goal is the controlled orbital collection of IDPs, allowing the determination of their velocities and trajectory information. To this end considerable thought and development is going into the proposed Space Station Cosmic Dust Collection Facility.

Index

PRECEDING PAGE BLANK-NOT FILMED